COMPARING HIGH-THROUGHPUT METHODS TO MEASURE ANTIBODY DEPENDENT CELLULAR CYTOTOXICITY DURING HIV-INFECTION

By IYALOO MBODO

MBDIYA001

A dissertation submitted in fulfillment of the requirements for the degree of MSc (Med) in Virology

Supervisor: Associate Professor Jo-Ann Passmore
Co-supervisor: Hoyam Galmieldien

Department of Clinical Laboratory Sciences
Division of Medical Virology
Faculty of Health Sciences

University of Cape Town

PLAGIARISM DECLARATION

I, Iyaloo Mbodo, hereby declare that the work on which this dissertation is based on my original work (except where acknowledgements indicate otherwise) and that neither the whole work nor any part of it has been, is being, or is to be submitted for another degree in this or any other university.

I empower the university to reproduce for the purpose of research either the whole or any portion of the contents in any manner whatsoever.

SIGNATURE:

_____

DATE: 29th September 2014

ACKNOWLEDGEMENTS

Firstly, I would like to thank God for giving me the opportunity of doing this project in good health.

I would like to thank my supervisor, Associate Professor Jo-Ann Passmore, whose strong guidance, mentorship, training and support made this body of work possible. Thank you for being enthusiastic and always encouraging with your positive energy. You are a role model, especially for us women scientists.

To my Co-supervisor Hoyam, for training me in the lab going sometimes beyond your normal working hours. Such a sacrifice will forever be treasured.
To Smritee, Jean-Mari ,Ramla, Shameem and Anna for comments and inputs in writing this thesis. To Kathy for being so encouraging and making sure I have all the reagents needed for this project. To all my colleagues from the mucosal Immunology lab for the homely and conducive environment.

To my darling parents Loide and Jason Mbodo, for making it possible for me to further my studies, for all your prayers,phone calls and unwavering support. My siblings, I hope this thesis will inspire you to study further and know that everything is possible. My aunt Theodor and cousin Elise for taking care of my babies ensuring that I write my thesis.

To my loving husband Abisai, for your unfailing love, encouragement and support and for being my punching bag in the course of writing this thesis. To my babies (Etuhole and Etugama), for your unconditional love which got me through each and every day of writing this thesis knowing that you believe in me.

To friends and family members who have lost their lives to HIV, this one is for you.

Lastly, I would like to acknowledge my funder, SA-India. Thank you for making this project a reality.

TABLE OF CONTENTS

LIST OF FIGURES

LIST OF TABLES

ABSTRACT

The prevalence of HIV-1 is highest in Sub-Saharan Africa. Protective immune responses directed against HIV are complex and involve both cellular and humoral immunity. Based on the recent finding that the best correlate of protection against the first protective prophylactic RV144 vaccine were HIV-specific antibody responses, including those mediating natural killer (NK) cell antibody-dependent cellular cytotoxicity (ADCC), there has been considerable interest in measuring alternative roles for HIV-specific binding antibodies. The aim of this MSc dissertation was to optimise and compare two high-throughput flow cytometry based approaches - the GranToxilux and PanToxilux assays - to measure HIV-specific ADCC responses. To do this, NK cells from a panel of healthy HIV-negative individuals were screened for their ability to directly kill the tumour cell line K562, as a measure of direct NK cell cytotoxicity. The individual with the highest granzyme B and caspase activity against K562 cells was chosen as the universal NK cell donor for this study. For the ADCC assay optimisation, plasma from a panel of HIV-1 seropositive individuals was screened for binding antibody titres against HIV subtype C gp120 by ELISA, and confirmed by western blot. Plasma from a panel of HIV seronegative individuals was included as negative controls. The ADCC assay was optimised to include subtype C gp120-coated CEM.NKR$_{CCR5}$ cells as target cells. This dissertation further describes detailed titrations, validations and refinements of both the GranToxilux and PanToxilux assays to measure both direct NK cell killing and HIV-specific ADCC activity, and finally presents the optimised protocols for both assays. The PanToxilux assay (which measured both granzyme B and caspase activity) measured higher levels of direct NK cell killing of K562 tumour cells than the GranToxilux assay ($p<0.05$). In the ADCC assays in which NK cell killing was directed against gp120-coated CEM.NKR$_{CCR5}$ cells in an antibody-dependent manner, plasma from HIV-positive individuals yielded significantly higher levels of ADCC activity than the HIV-negative controls. In contrast to the direct killing measurement, the GranToxilux assay measured similar levels of ADCC killing as the PanToxilux assay while having significantly lower background cytotoxicity against target cells coated with HIV negative serum ($p=0.0028$). In conclusion, the study has optimised and compared both the GranToxilux and PanToxilux assays to measure HIV-specific ADCC within the laboratory, that will be useful for future studies. The PanToxilux assay was more sensitive for detecting direct NK cell killing of K562 cells than the GranToxilux assay, although both assays performed similarly at detecting HIV-specific ADCC activity against gp120-coated CEM.NKR$_{CCR5}$ cells.

LIST OF ABBREVIATIONS

ADCC	Antibody Dependent Cellular Cytotoxicity
ADCDC	Antibody Dependent Complement Dependent Cytotoxicity
ADCP	Antibody Dependent Cellullar Phagocytosis
ADVI	Antibody Dependent cell-mediated Viral Inhibition
AIDS	Acquired Immune Deficiency Syndrome
APC	Allophycocyanin
ART	Antiretroviral Therapy
ARV	Antiretroviral
BFA	Brefeldin
CCR5	Chemokine (C-C Motif) Receptor 5
CTL	Cytotoxic T Lymphocyte
CXCR4	Chemokine (C-X-C Motif) Receptor 4
CD4	Cluster of Differentiation 4
CD8	Cluster of Differentiation 8
DMSO	Dimethlysulphoxide
DNA	Deoxyribonucleic Acid
ELISA	Enzyme-Linked Immunosorbent Assay
Env	Envelope
FADD	Fas Associated Death Domain
FASL	Fas Ligand
FBS	Fetal Bovine Serum
FITC	Fluorescein Isothiocyanate
FMO	Fluorescence Minus One
Gp	Glycosylated Protein

HAART	Highly Active Antiretroviral Therapy
HIV	Human Immunodeficiency Virus
HLA	Human Leukocyte Antigen
HRP	Horseradish Peroxidase
IL	Interleukin
Ig	Immunoglobulin
KIR	Killer-cell Immunoglobulin-like Receptor
LAMP	Lysosomal Associated Membrane Protein
LILRB1	Leukocyte Immunoglobulin Like Receptor, subfamily B member 1
Ly9	Lymphocyte Antigen 9
min	Minutes
ml	Millilitres
MPER	Membrane Proximal External Region
NCR	Natural Cytotoxicity Receptor
NK	Natural Killer
NKG2D	Natural Killer Group 2, member D
NTBA	NK-T-B Antigen
PBMC	Peripheral Blood Mononuclear Cell
PE	Phycoerythrin
PerCP Cy5.5	Peridininchlorophyll protein Cy5.5
PHA	Phytohaemaglutinin
PMA	Phorbol myristate acetate
Qdot	Quantum Dot
RCF	Revolutions Per Minute
RNA	Ribonucleic Acid
RPMI	Roswell Park Memorial Institute Medium

RT	Room Temperature
SIV	Simian Immunodeficiency Disease
SSC	Side Scatter
TMB	Tetramethylbenzidine
UNAIDS	United Nations Program on HIV/AIDS
V	Variable
VIF	Viral Infectivity Factor
VIVID	Violet Fluorescent Reactive Dye
Vpr	Viral Protein R
Vpu	Viral Protein U
WHO	World Health Organisation
µl	Microlitres

CHAPTER 1

Literature Review

1.1. Introduction

Acquired Immune Deficiency Syndrome (AIDS), caused by Human Immunodeficiency Virus (HIV) (Sharp et al., 2011), was first described in 1981 in New York (reviewed by Greene, 2007) and first isolated by Montagnier in France and by Gallo in the USA (Gallo and Montagnier, 2003). Since then, HIV has become a pandemic with HIV type 1 (HIV-1) being the predominant type circulating worldwide and infecting ~60 million people and causing >25 million deaths (UNAIDS, 2013). HIV type 2 (HIV-2) is largely restricted to West Africa, although some spread to other parts of Africa, Europe, India and the USA have been described (Campbell-yesufu and Gandhi, 2011). Internationally, Africa has experienced the greatest AIDS/HIV morbidity and mortality, with the highest prevalence for HIV-1 infection being in Sub-Saharan Africa (UNAIDS, 2013). Sub-Saharan Africa, which only has 12% of the world populations but ~30 million people are living with HIV, has 71% of the total number of HIV-infected people in the world (Figure 1.1, UNAIDS, 2013). In this region, it was estimated that 2.7 million people were infected in 2010 alone (UNAIDS, 2012).

In Sub-Saharan Africa, HIV disproportionately affects women than men, with women accounting for 58% of all those infected, 77% of those who are newly infected between the ages of 15-24 years, with a prevalence that is 3-7 fold higher among adolescent females than adolescent males (Abdool-Karim et al., 2010; UNAIDS, 2012). Factors such as poverty, gender inequality and gender-based violence are contributors to this high prevalence observed in women as compared to their male counterparts in Sub-Saharan Africa (Shannon et al., 2012).

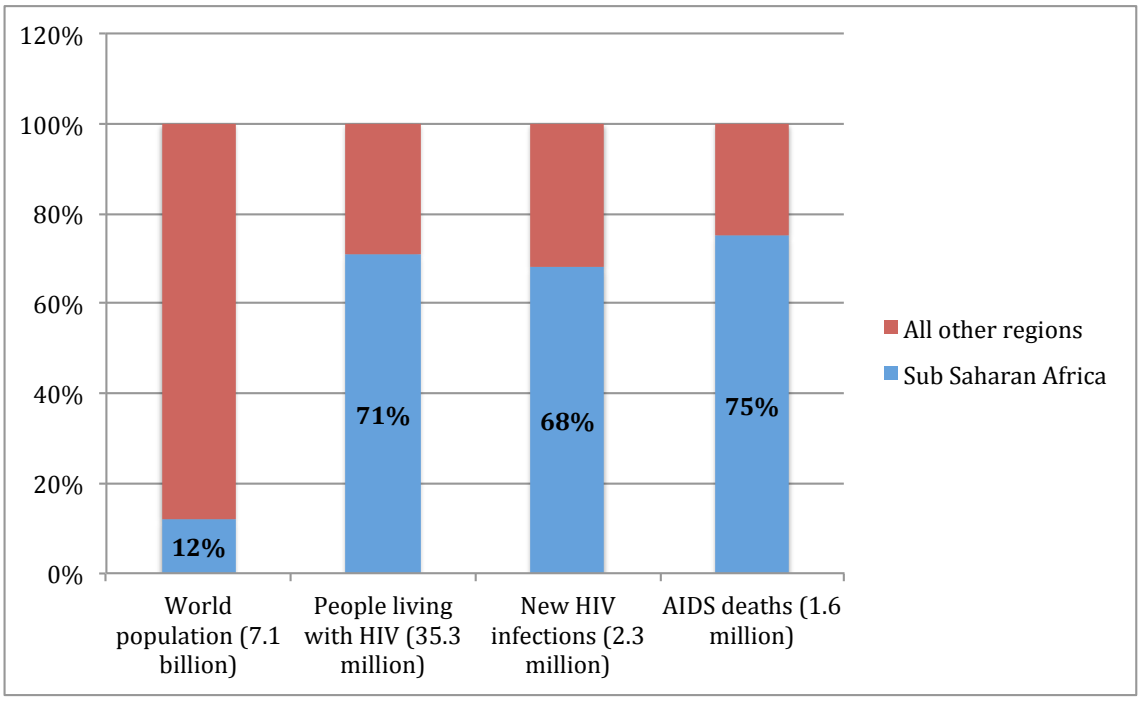

Figure 1.1. HIV-1 prevalence, incidence and AIDS deaths in Sub-Saharan Africa compared to the rest of the world. The blue bars represent all the countries in Sub-Saharan Africa, while the red bars represent all other regions in the world (taken from UNAIDS, 2012).

Since the introduction of potent antiretroviral drugs in the 1990's (which targeted various phases of the HIV life cycle within host cells) and their combination into highly active anti-retroviral therapy (HAART) in the early 2000's, the death rate associated with HIV/AIDS has declined (UNAIDS, 2013). Rollout of HAART to those who need it has become a major international focus. In Sub-Saharan Africa, it was estimated that ~47% of the people living with HIV who needed it were taking HAART at the end of 2010, increasing from 39% coverage in the previous year (UNAIDS, 2012).

Despite the positive effects of HAART on HIV-1 disease progression and life expectancy, HIV remains a huge public health problem and individual burden in the absence of a cure to rid the body of latent HIV reservoirs (UNAIDS, 2013). It is still a lifelong disease requiring daily medication until a way to completely deplete all latent reservoirs is found. Sub-Saharan Africa continues to bear the brunt of the pandemic, and further research is urgently needed to understand

how to eradicate HIV from those who are infected as well as protect those who are currently not HIV-infected.

1.2. HIV genes and organisation

HIV is a lentivirus belonging to the retroviridae family (reviewed by Sharp and Hahn, 2011). A mature virion has a diameter of ~100nm, making it medium size relative to other viruses. Figure 1.2 illustrates the organization of the enveloped HIV particle. The virion is enveloped by a lipid bi-layer derived from the host cell when the virion buds off from the infected host cell (Carlson et al., 2008; Garoff et al., 1998). The envelope contains glycosylated proteins (gp) 120 and 41, cleaved from the gp160 precursor by the host proteases (reviewed by Harris et al., 2011; Pollara et al., 2013). Within the envelope of HIV, the viral capsid composed of p24 protein contains three major enzymes (a protease, integrase and reverse transcriptase) and two identical single-stranded positive sense RNA strands bound to the nucleocapsid proteins (reviewed by Balasubramaniam and Freed, 2012).

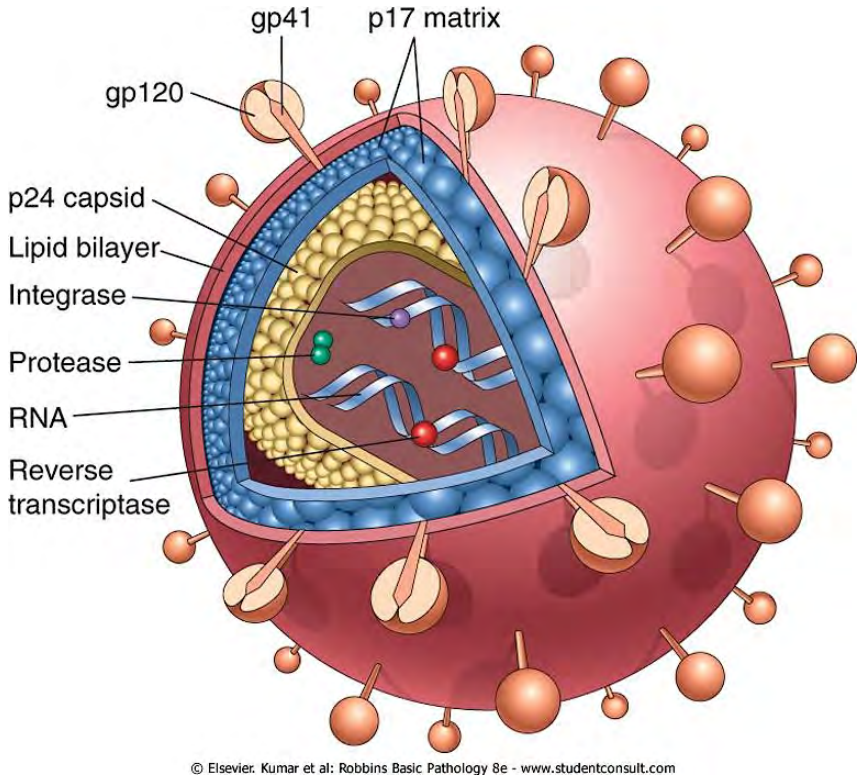

Figure 1.2. Structure of the HIV virion showing the two identical encapsulated single-stranded genomic RNA strands. The gp120, gp41 and p17 proteins are outside the envelope, while p24, integrase, protease and reverse transcriptase are encapsulated by the envelope (taken from php.med.unsw.edu.au/medwiki/index.php?title=Immunopathogenesis_of_HIV/AIDS).

HIV has a 9.2 kb genome, which contains 9 genes including structural genes (Env, Gag and Pol), regulatory genes (Rev and Tat) and accessory genes (Vif, Vpu, Nef and Vpr) (Table 1.1; Briggs et al., 2003; Frankel and Young, 1998; Harrich and Hooker, 2002; Kirchhoff, 2010; Kogan and Rappaport, 2011; Malim and Emerman, 2008; Marin et al., 2003; Melar et al., 2007; Pollard and Malim, 1998; Sierra et al., 2005; Suhasini and Reddy, 2009).

Table 1.1. Summary of HIV genes, proteins and their main functions

Genes	Proteins	Function
Proteins encoded by the structural genes (Frankel and Young, 1998; Sierra et al., 2005)		
Env	gp41	Mediates virus fusion to the target cell by achoring envelope glycoprotein complex to host surface membrane.
	gp120	Forms complexes with gp41 and binds to CD4 and chemokine receptors on target cells.
Gag	p24	Encapsidates genomic RNA and viral enzymes.
	p17	Important for virion maturation and stability.
	P9 nucleocapsid	Ensures packaging of the single stranded genomic RNA into virions.
Pol	p31 integrase	Mediates integration of reverse transcribed DNA into the host cell DNA.
	p6 proline-rich protein	Important in virion assembly and release.
	P66/p51 reverse transcriptase	Generates complementary DNA from the virus RNA genome.
Proteins encoded by the regulatory and accessory genes (Harrich and Hooker, 2002; Kirchhoff, 2010; Malim and Emerman, 2008; Marin et al., 2003)		
Rev	p19	Responsible for transcription regulation and mRNA nuclear transport.
Tat	p14 transcriptional activator	Regulates reverse transcription of the virus genome and the release of virions from infected cells.
Nef	p27	Down regulates cell surface expression of the CD4 molecule. Play a role in the virus infectivity by enhancing viral replication and therefore maintaining high viral load.
Vif	p23	Protects the virus from APOBEC inhibition.
Vpr	p14 viral protein R	Plays a role in the virus replication, specifically nuclear import of the pre-integration complex.
Vpu	P16 viral protein U	Involved in CD4 degradation and efficient release of viral particles from the infected cells.

1.3. HIV life cycle

HIV is transmitted through bodily fluids including semen, blood, breast milk and vaginal secretions (Keele and Estes, 2011; Sarnquist et al., 2013; Sharp and Hahn, 2011). The predominant routes of transmission include unprotected sexual intercourse, breastfeeding, needle sharing and transmission through direct contact with blood (Sarnquist et al., 2013).

1.3.1. Infection of host cells, HIV binding and entry

HIV infects new hosts by binding to specific host cell surface receptors. The primary HIV entry receptor is the CD4 trans-membrane protein found on T cells and cells of the macrophage lineage (König and Zhou, 2004; Schubert et al., 1998). HIV's envelope protein gp120 contains five relatively conserved domains (C1-C5) and five variable loops (V1-V5) which interacts with CD4 (reviewed by Wilen et al., 2012). Binding of the gp120 to the host CD4 receptor causes rearrangements of the variable loops V1, V2 and V3 regions, leading to formation of a bridging sheet (Kwong et al., 1998; Wilen et al., 2012). The bridging sheet is important in engaging the virus with the co-receptors (Kwong et al., 1998).

Host chemokine receptors CCR5 (C-C chemokine receptor type 5) and CXCR4 (C-X-C chemokine receptor type 4) are the necessary secondary co-receptors for HIV entry (Kwong et al., 1998; Llano and Est, 2005; Sterjovski et al., 2011). CCR5 is found on T cells and macrophages, while CXCR4 is only found on $CD4^+$ T cells (Baba et al., 2000; Trkola et al., 1999). HIV-1 strains that utilise the CCR5 co-receptor are known as macrophage tropic (M-tropic) viruses, and strains that utilise the CXCR4 are known as T cell-tropic (T-tropic) viruses (Sharp and Hahn, 2011). Some HIV strains can utilise both co-receptors and are known as dual tropic viruses (Li et al., 2012; Xiang et al., 2014). It has been shown that the binding avidity and tropism of HIV to new target cells depends on the protein structure of the gp120 (Harris et al., 2011; Kwong et al., 1998; Sterjovski et al., 2011). Once HIV gp120 has interacted with CCR5 or CXCR4 co-receptors, a gp41 fusion complex, consisting of six-helix bundle formation, is formed which result in viral fusion with the host cellular membrane leading to entry of the virus into the host cell (Figure 1.3; reviewed by Wilen et al., 2012).

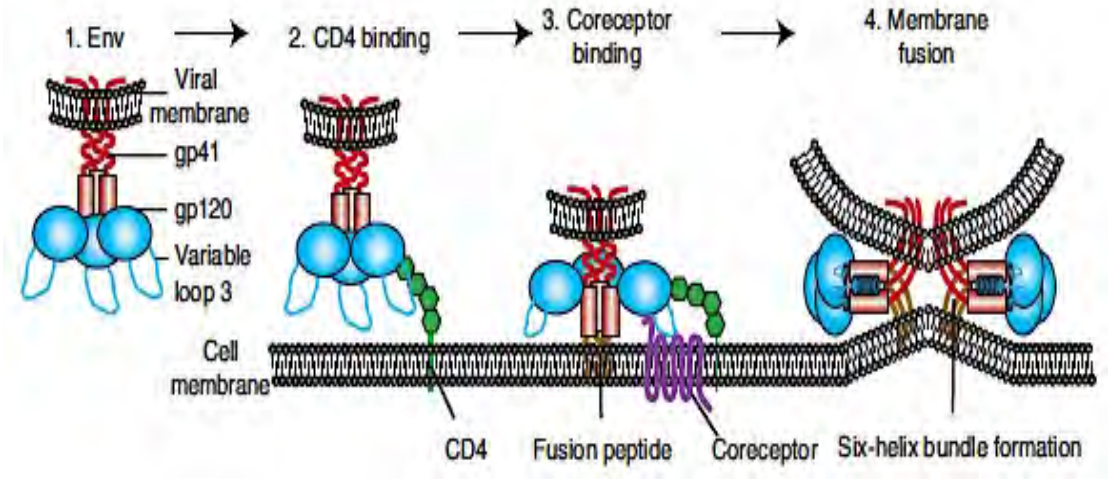

Figure 1.3. Entry of HIV into the host cell using viral envelope proteins. HIV gp120 and gp41 (1) bind to CD4 (2) causing conformational changes in the envelope. This brings the virus in close proximity with the co-receptors (CCR5 or CXCR4), allowing co-receptor binding and initiating formation of six-helix bundle (4), which leads to membrane fusion (taken from Wilen et al., 2012).

1.3.2. HIV replication and integration within host cells

Following HIV virus fusion with the new host cell, the viral core is released into the cytoplasm of the cell. HIV uncoating involves viral proteins Nef, Vif and other host cellular factors, leading to the release of virus RNA genome into the cytoplasm (Briggs et al., 2003; Balasubramaniam and Freed, 2012; Sierra et al., 2005). HIV reverse transcriptase enzyme use viral positive strand RNA as a template for synthesis of the negative strand DNA (Frankel and Young, 1998). Following formation of linear double stranded DNA, a pre-integration complex is formed, consisting of host proteins, viral proteins and DNA, that is translocated to the nucleus (Friedrich et al., 2011). Viral DNA is transported into the nucleus and integrated into the host DNA by the integrase enzyme forming a provirus (Friedrich et al., 2011). The provirus is replicated along with the host chromosome when it divides (Mogensen et al., 2010). This produces viral proteins, which then move to the cell surface and form new virions which bud off from the host cell, ready to infect a new target cell (Briggs and Kräusslich, 2011).

1.3.3. Clinical course of HIV infection in humans

During viral replication, HIV causes damage to the host immune system by lysing infected CD4+ T cells, leading to destruction of lymphoid tissues and immune deficiency (Lane, 2010; Weber, 2001). The clinical course of HIV infection has broadly been divided into three phases: the acute phase, chronic phase (asymptomatic) and the symptomatic phase of infection (Lane, 2010; Pantaleo et al., 1993). A more detailed Fiebig staging algorithm has been implemented for further definition within the acute (early) phases of infection, useful for initial diagnosis of HIV (Fiebig et al., 2003). Fiebig staging proposes that the acute phase of HIV infection is further divided into 6 phases based on the emergence of host immune markers (Figure 1.4; reviewed by Cohen et al., 2010). These phases are defined as follows:

- The *acute phase* of HIV infection is characterised by rapid growth and spread of the virus within the host cell lymphoid tissues in the absence of host adaptive immunity, which leads to high titres of plasma viremia and substantial loss of CD4+ T cells in the blood. At this stage, viral RNA can be detected in blood (corresponding to Fiebig stage I) (Figure 1.4B). During this early stage of infection, HIV has infected lymphoid tissues and established viral reservoirs throughout the body. HIV p24 (making up the viral capsid) can be detected in plasma at ~day 7 of infection although host immunity cannot yet be measured (corresponding to Fiebig stage II). After this, an expanded population of HIV-1 specific cytotoxic CD8+ T cells (CTLs) and HIV-specific binding antibodies develop and are measurable. Emergence of these HIV-specific adaptive immune responses have been implicated in bringing viral replication under control, and lowering the viral load to a steady set point (Koup et al., 1994). At this stage, HIV gp120 and gp41 antibodies can be detected by ELISA (corresponding to Fiebig stage III). Fiebig stages IV (antibody positive by ELISA but negative by western blot), stages V (antibody positive by ELISA and positive by western blot) and stages VI (ELISA positive; western blot positive, p31 antigen positive using ELISA or western blot) follows (Figure 1.4B).

- The *asymptomatic or chronic phase* of HIV infection is characterised by the establishment of viral "set point", as a result of emerging host adaptive immune responses. Viral set point represents the sum of ongoing viral replication in the presence of this immunity and the ability of the host's immunity to retard viral replication. The duration of this asymptomatic or chronic phase of infection varies from person to person and from country to country, with typical duration ranging from 5-15 years (Mlisana et al., 2014). Although binding antibodies emerge earlier, neutralizing antibodies against HIV appear at ~3-12 weeks and broadly cross-neutralizing antibodies typically emerge at ~3 years post-infection (Moore et al., 2008, 2012). Despite host adaptive immune responses against HIV, a steady yet slow decrease in CD4+ T cell numbers continues during chronic infection, ultimately resulting in exhaustion of both CD4+ and CD8+ T cells (Catalfamo et al., 2011; Leng et al., 2001; Ray et al., 2006). Although the typical duration of this asymptomatic phase of infection is <10 years, some HIV-infected individuals may have no AIDS-defining symptoms for longer than 10 years in the absence of treatment (Deeks and Phillips, 2009; Egger et al., 2002).
- The *symptomatic phase* (AIDS) is characterised by a rapid decrease of CD4+ T cells, corresponding to a decline in HIV-specific T cell responses and rapidly increasing viremia. In the absence of HAART, opportunistic infections usually appear leading to AIDS and death due to the collapse of host immunity (reviewed by An and Winkler, 2010). In the absence of treatment, AIDS typically occur at CD4+ T cell counts <200 cells/ml blood. Since the introduction of anti-retroviral therapy and then HAART, few HIV-infected individuals still progress to this stage of infection. Although 61% of individuals who need HAART are currently receiving it (UNAIDS, 2013), and HAART rollout is increasing annually, most recent statistics report that 1.6 million people died of AIDS in 2012 (UNAIDS, 2013). In South Africa, 200 000 HIV-infected individuals died of AIDS in 2010 (UNAIDS, 2011). South African National Guidelines are currently to start treatment at 350 cells/ml but are scheduled to increase to 500

cells/ml in 2015 (The South African Antiretroviral Treatment Guidelines, 2013).

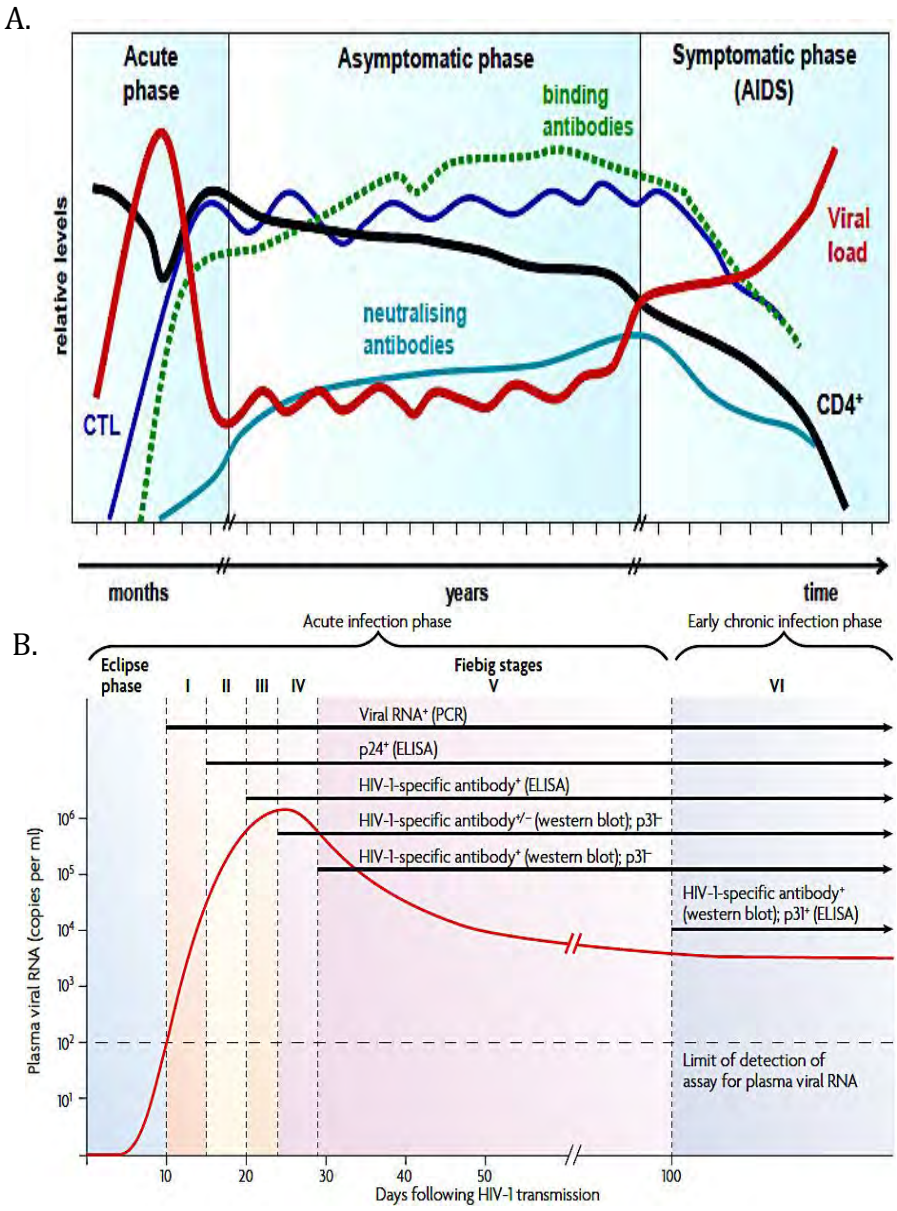

Figure 1.4. Typical clinical courses of HIV infection in humans and emergence of host adaptive immune responses. (A) Clinical course has broadly been divided into 3 phases: acute, asymptomatic and symptomatic phases. CD4+ T cell number (black line) drastically decreases during acute phase, rebound during the asymptomatic phase when host immunity emerges, achieving a relatively steady state. Viral loads (red line) increases during acute phase in the absence of host immunity, and decreases sharply when HIV-specific CTLs (blue line) and antibody responses emerge (green and turquoise lines respectively). (B) Acute phase has further been divided into six Fiebig stages (I-VI) based on the detection of HIV-1 RNA, viral antigens and emergence of host immunity (adapted from McMichael et al., 2010).

1.4. Immune responses to HIV

Both innate and adaptive host immune responses have been implicated in protection following HIV infection (Ackerman et al., 2012; Bergmeier and Lehner, 2006; Kasturi et al., 2011). Innate immunity (including, neutrophils, natural killer (NK) cells, dendritic cells, macrophages and monocytes) provides the earliest and first line of defense against HIV infection (Altfeld et al., 2011; Kasturi et al., 2011; Sharp and Hahn, 2011; Vivier et al., 2011). By definition, these innate responses were not thought to be HIV-specific although some recent studies have described HIV-specific responses directed by NK cells (Chung et al., 2012; Jost and Altfeld, 2012; Parsons et al., 2012; Tiemessen et al., 2009).

HIV-specific adaptive immune responses are characterised by the emergence of specific cellular immunity (involving both CD8+ CTLs and CD4+ helper T cells) and humoral immunity (B cells producing antibodies) (Alter and Moody, 2010; McMichael et al., 2010; Overbaugh and Morris, 2012; Vivier et al., 2011). HIV-specific antibodies neutralise or they mediate other effector functions including those that mediate antibody dependent cellular cytotoxicity (ADCC), those that mediate antibody dependent complement dependent cytotoxicity (ADCDC), and those that mediate antibody dependent cellular phagocytosis (ADCP) (reviewed by Ackerman et al., 2012). This dissertation will be focusing on the role of NK cells and HIV-specific antibodies in mediating ADCC in the control of HIV infection.

1.5. HIV-specific antibodies

B cell responses to HIV-infection can be detected as early as 1 week after HIV RNA is detectable in plasma (Tomaras et al., 2008). Detection of these HIV-specific B cells is followed by emergence of circulating anti-gp41 antibodies a few days later (corresponding to Fiebig stage I; Figure 1.4B), and anti-gp120 antibodies delayed a further few weeks (corresponding to Fiebig stage II; Figure

1.4B). Although HIV-specific antibodies that can neutralise HIV are an important and major focus of research, other classes and functions of antibodies exist that may play an important role in determining susceptibility and clinical course of HIV infection (reviewed by Overbaugh and Morris, 2012).

1.5.1. Evolution of HIV-specific antibody responses

An antibody is made up of a single constant domain (Fc), which interacts with cells of the innate immune system, and two identical variable domains from both light and heavy chains (Fab) that recognise antigens bound on the target cells (reviewed by Woof and Burton, 2004; Figure 1.5). Antibodies or immunoglobulins (Ig) can be divided into five major classes (isotypes) distinguished by their Fc regions: IgM, IgD, IgG, IgA and IgE. In humans, IgG has been further divided into four subclasses: IgG1, IgG2, IgG3 and IgG4 (reviewed by Pan and Hammarström, 2000).

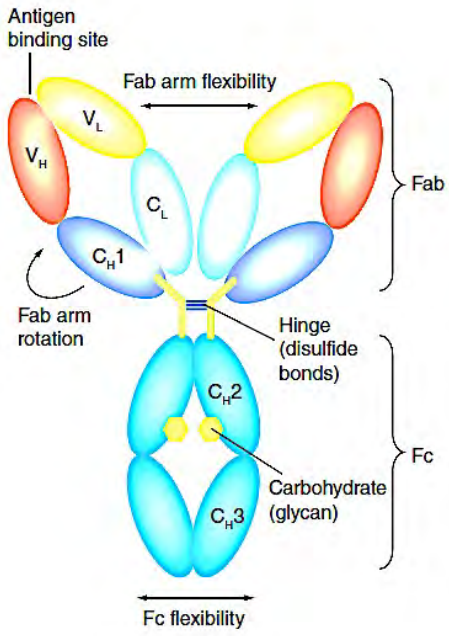

Figure 1.5. Basic structure of antibody domains with two identical heavy chains and two identical light chains. The antibody forms a Y shape linked together by disulfide bonds. The Fc region consists of carbohydrate glycans and two heavy chain constant (C) domains, and it mediates effector functions. The Fab region recognises antigens through its light and heavy chain variable domains (V_H and V_L) (taken from Chung and Alter, 2014).

During HIV infection, the first type of HIV-specific antibodies produced are gp41-specific IgM antibodies (Tomaras et al., 2008). At about two weeks, class switching occurs and HIV-specific IgM antibodies are replaced by IgA, IgG or IgE antibodies (Calame, 2001; Liao et al., 2011). Antibody class switching enables diversification of antibody effector functions by substituting the C region of IgM with that of IgG, IgA or IgE. Class switching happens in the germinal center of the lymph nodes, a specialised follicular compartment (He et al., 2006). After the initial IgM response following HIV infection, the predominant HIV-specific antibody subtype circulating are IgG1 (Doria-rose and Connors, 2010).

1.5.2. HIV-specific antibodies that neutralise

Neutralising antibodies (nAbs) against HIV play an important role in preventing infection (Alter and Moody, 2010; Li et al., 2012; Srisurapanon et al., 2005). HIV envelope proteins mediate entry into the cells and are the main target for nAbs (Li et al., 2012; Moog et al., 1997; Pilgrim et al., 1996). HIV-specific nAbs against the HIV variant to which they were raised (autologous nAbs) develop within weeks to months after infection (Mascola and Haynes, 2013). These autologous nAbs are usually restricted to the V1V2 region of the gp120 protein of the autologous virus, are usually potent, HIV type-specific to the infecting strain but not able to neutralise other viruses isolated from other individuals (Figure 1.6; Mascola and Haynes, 2013; Mikell et al., 2011). Autologous nAbs have been reported to drive HIV to escape neutralization leading to escaped viruses being less sensitive to early autologous nAbs overtime (Chung et al., 2011; Deeks et al., 2006). Mutations in N-linked glycosylation sites on gp120 (leading to changes in the glycan shield protecting HIV gp120), single amino acid substitutions within gp120, and insertions or deletions in gp120 V1-V4 regions were found to be the predominant mechanisms by which HIV escapes from these autologous nAbs (Gray et al., 2009; Overbaugh and Morris, 2012; Srisurapanon et al., 2005; Wei et al., 2003).

While autologous nAbs develop early during HIV infection, nAbs that have the ability to broadly recognise and neutralise heterologous HIV-1 variants take 2-3 years to develop (Overbaugh and Morris, 2012). Only about 30% of HIV-infected individuals develop these broadly nAbs and these individuals have been important for identifying new nAbs and HIV epitopes they target (Archary et al., 2013; Moore et al., 2012). Identification of HIV-specific nAbs capable of broadly neutralising HIV, are relevant in the development of HIV vaccines that can neutralise (Montefiori et al., 2011). NAbs are classified according to the epitopes that they recognise: those that recognise the CD4 binding site, the V1/V2 regions of gp120, the membrane-proximal external region (MPER) of gp41, and the glycan V3 region (reviewed by Kwong et al., 2013). NAbs that recognise the CD4 binding site target the site were the host CD4 receptor binds to the gp120 envelope (Muster et al., 1993; Sterjovski et al., 2011; Zhang et al., 2012). NAbs that recognise the V1/V2 target glycopeptides epitopes on the V1 and V2 regions (Sanders et al., 2002; Sterjovski et al., 2011; Wyatt et al., 1995). Nabs that recognise MPER target a site in gp41, proximal to the transmembrane-spanning region (Stiegler et al., 2001). NAbs recognizing V3 glycans are directed against epitopes that generally include residue Asn332 on gp120 (Su and Moog, 2014; Figure 1.6).

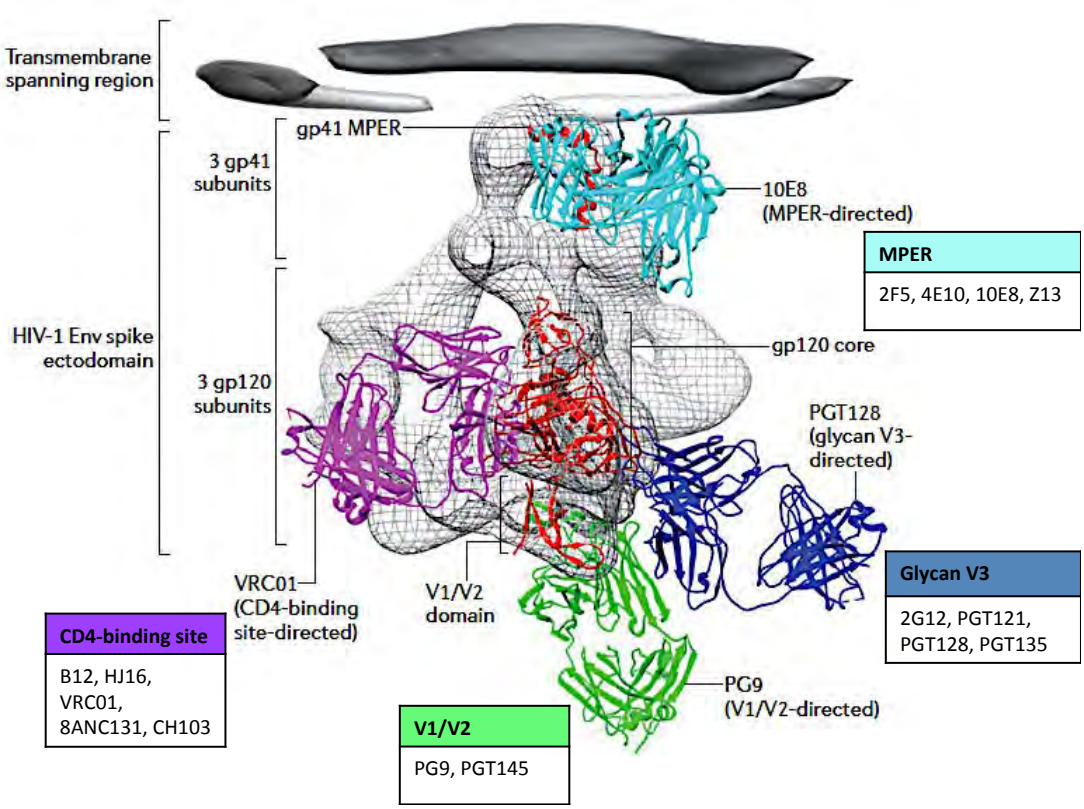

Figure 1.6. Epitopes on HIV-1 gp120 recognised by nAbs. NAbs that neutralise CD4 binding site are shown in purple, those that recognise V1/V2 binding site are shown in green, those that recognise Glycan V3 binding site are shown in blue, and those that recognise MPER binding site are shown in cyan (taken from Pollara et al., 2013).

1.5.3. Binding or non-neutralising HIV-specific antibodies

HIV elicits a number of antibodies that bind, but do not neutralise HIV infection of new host cells directly (Brocca-Cofano et al., 2011). These non-neutralising HIV-specific antibodies appear ~2 weeks after HIV infection, around the time that HIV-specific CTL's develop (Figure 1.4A). These antibodies form the basis for HIV diagnosis, which is based on seropositivity and can be measured using ELISA (HIV rapid test). Binding antibodies are thought to protect against HIV infection by several non-neutralising mechanisms, including ADCP, ADCDC and ADCC. Each of these will be discussed in detail in the following sections.

1.5.3.1. HIV-specific antibodies that mediate ADCP

Binding antibodies have also been shown to enhance phagocytosis of antibody-coated HIV particles by ADCP (Figure 1.7). Professional phagocytes, including monocytes, macrophages and neutrophils, bear the Fc receptor. These phagocytes can directly phagocytose antibody-coated HIV particles by binding to the antibody-coated viral particle through the antibody Fc portion (Fc-receptor mediated phagocytosis); or by engulfing whole HIV-infected target cells which have antibodies coating their cell surface at the point where new virions are budding off (reviewed by Ackerman et al., 2012). This antibody-mediated effector function is thought to play an important role in the rapid and early clearance of antibody-opsonised viral particles during HIV infection (Ackerman et al., 2013).

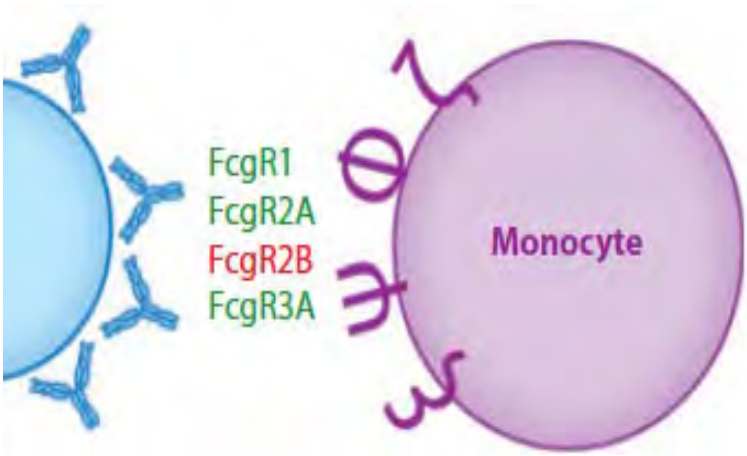

Binding antibodies mediate ADCP through monocytes, macrophages, neutrophils and mast cells, which act as professional phagocytes releasing cytokines or oxidants or by engulfing them and trafficking to phagolysosomes.

Figure 1.7. Fc receptor-mediated mechanism by which HIV-specific antibodies result in infected host cells being phagocytosed by professional antigen presenting cells. A monocyte effector cell (purple) would interact with the Fc portion on antibodies (coating an HIV-infected target cell in blue) via the FcgR2B receptors (in red). Other receptors (in green) may also be involved in ADCP (taken from Ackerman et al., 2012).

1.5.3.2. HIV-specific antibodies that mediate ADCDC

ADCDC is another effector function whereby antibodies recruit complement proteins through the classical or non-classical complement cascade (Figure 1.8; Stoermer and Morrison, 2011). The complement cascade initiates the formation of the membrane attack complex consisting of complement proteins C1q, C3b, C4b, mannose binding lectin (MBL) and IgG Fc binding proteins (FcγBP) (Ackerman et al., 2012; Stoermer and Morrison, 2011). This membrane attack complex forms pores in the target cell membrane allowing entrance of ions and other small molecules leading to osmotic cell lysis of the host cell and ultimately causing death (Ackerman et al., 2013). ADCDC is thought to be involved in the control of HIV replication during early infection (Ackerman et al., 2012; Stoermer and Morrison, 2011). Furthermore, IgG antibodies have been reported to eliminate heterologous virus in primary HIV infection through ADCDC (Aasa-chapman et al., 2005).

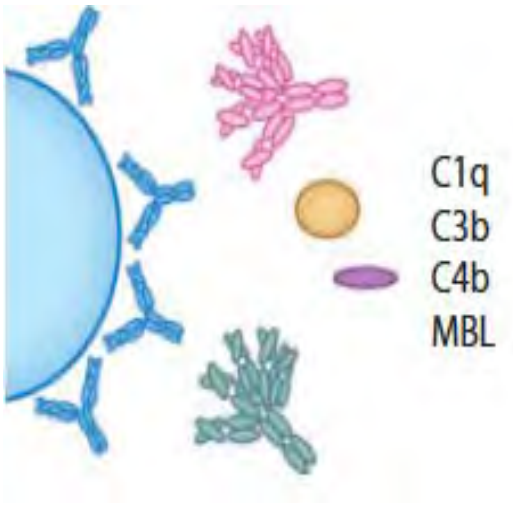

Binding antibodies can initiate the complement cascade either classical or non-classical routes, resulting in the formation of pores by the membrane attack complex, as well as contributing to increased uptake and toxicities mediated by other innate cells.

Figure 1.8. Possible mechanism by which binding antibodies recruit complement proteins C1q, C3b, C4b and MBL during ADCDC. These complement proteins mediate cytotoxicity by forming a complement cascade. HIV-infected host cells (in blue) which are coated with HIV-specific antibodies, become targets for these cytotoxic complexes (taken from Ackerman et al., 2012).

1.5.3.3. HIV-specific antibodies that mediate ADCC

ADCC involves components of both the innate immune system (including NK cells, macrophages, monocytes and eosonophils) and the acquired immune system (antibodies) (Lanier et al. 1986; Jewett et al., 1990; Lopez et al., 1985). During ADCC, IgG antibodies recognise and bind to the HIV antigen on the surface of target cells (Chung et al., 2008). Bound antibody is then recognised by effector cells through the Fc region on IgGs. Effector cells bind to this Fc region using FcγRIIIa (CD16) receptors on their cell surface. The FcγR-mediated binding between antibody coated HIV-infected target cells to effector cells during ADCC triggers the release of cytokines, granzymes and perforin by effectors cells that enter the target cell and causes apoptosis (Figure 1.9; Chung and Alter, 2014; Cox et al., 1999).

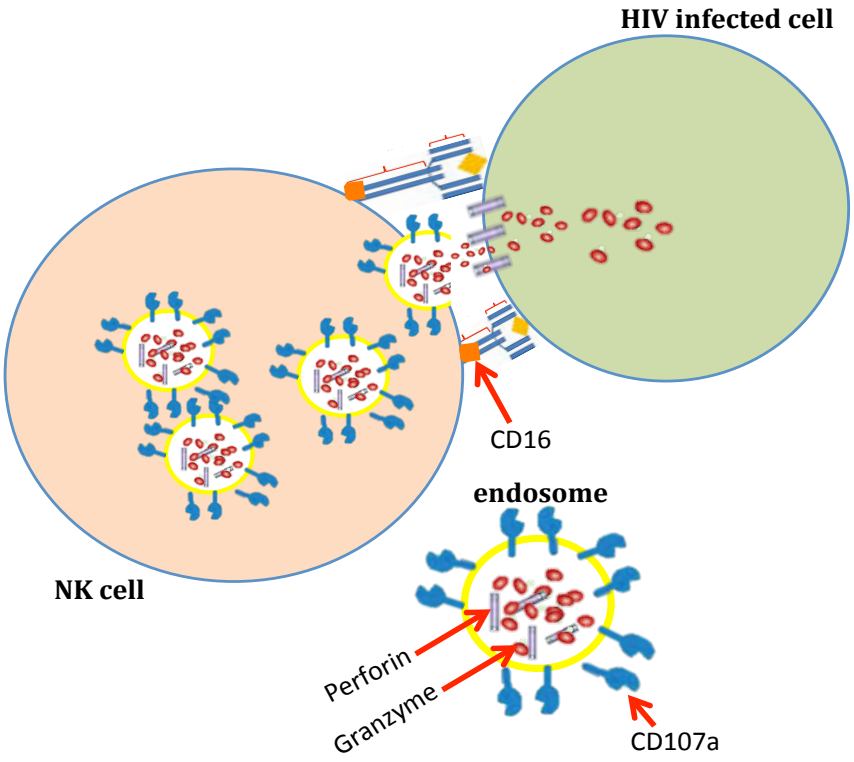

Figure 1.9. Mechanism by which HIV-specific antibodies bind to HIV-infected target cell, thereby recruiting NK cells, interacting with their FcγRIIIa (CD16) and mediating ADCC. NK cell endosomes (membrane lined with CD107a) contain cytolytic granules (granzymes and perforin), which are released into the target cell.

1.6. Natural killer cells

NK cells are important components of the innate immune response to tumors and virally-infected cells (Caligiuri, 2008). NK cells can be identified by their expression of FcγRIIIa (CD16), CD56+ and lack of expression of CD3 (Lanier et al., 1986; Vivier et al., 2011). NK cells are the major effector cells for ADCC during HIV infection, mediated primarily through their FcγRIIIa (CD16) receptors that bind to the Fc component of IgG (Cooper et al., 2001; Tyler et al., 1989). Using these markers, distinct subpopulations of NK cells have been described: $CD56^{Bright}$ CD16- NK cells that predominantly secrete cytokines (Poli et al., 2009), $CD56^{Dim}$ CD16+ NK cells that are predominantly cytotoxic (Funke et al., 2011), and CD16+ CD56- NK cells that predominantly release chemokines, and are much more rare than the other two subsets (Björkström et al., 2010; Bluman et al., 1996; Walzer et al., 2005). $CD56^{Dim}$ CD16- NK cells do express the CD56 receptor but to a lesser extent than $CD56^{Bright}$ CD16+ NK cells, while

CD16+ CD56- NK cells do not express CD56.

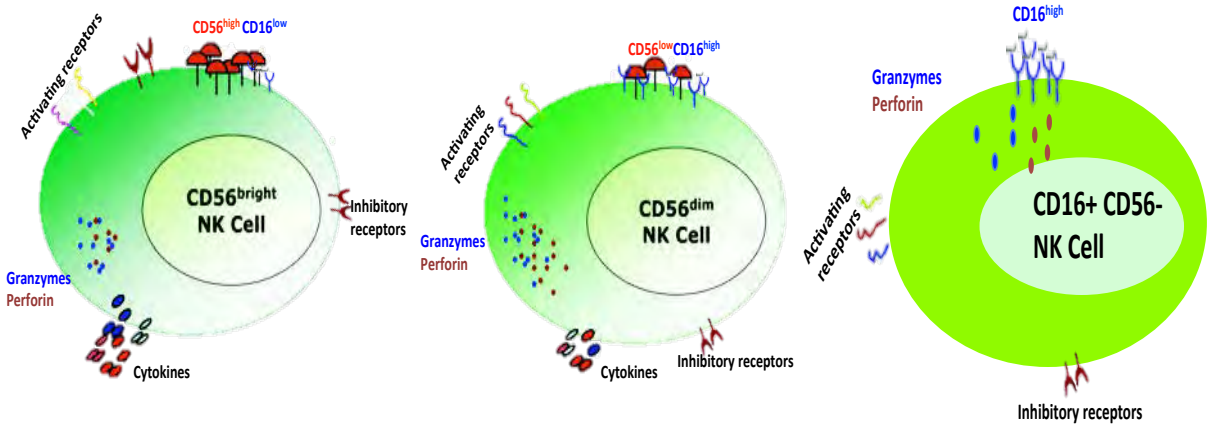

Figure 1.10. Distinct NK cell subsets (CD56^{Bright}, CD56^{Dim} and CD16+ CD56-) exhibit distinct immune functions. CD56^{Bright} NK cells produce more cytokines than the other subsets, CD56^{Dim} NK cells are more cytolytic (releasing more granzymes and perforin) than the other subsets, and CD16+ CD56- NK cells produce low levels of granzymes and perforin (adapted from Hong et al., 2013).

In addition to phenotypic markers CD56 and CD16, NK cells also express activating, inhibitory, cytokine, chemotactic and adhesion receptors (Figure 1.11; reviewed by Vivier et al., 2011). Activating receptors on NK cells include natural cytotoxicity receptors (NCRs) (NKp30, NKp44 and NKp46), killer cell immunoglobulin-like receptors (KIRs) (KIR-2DS and KIR-3DS) and C-type lectin receptors (CD94/NKG2C), while inhibitory receptors include KIRs (KIR-3DL and KIR-2DL) and C-type lectin receptors (CD94/NKG2A/B). Activating receptors interact with soluble ligands and trigger cytolytic activity mainly against virus-infected cells and malignantly transformed cells (Caligiuri, 2008; Cooper et al., 2001). Of these, NCRs are the major activating receptors and they recognise a broad spectrum of ligands, ranging from viral, parasite, bacteria derived and cellular ligands (reviewed by Hudspeth et al., 2013). Inhibitory receptors on NK cells recognise HLA class I molecules on the surface of target cells (Caligiuri, 2008; Cooper et al., 2001). Regulation of NK cells occurs through integration of these activating and inhibitory signals, triggered by ligands binding to these different activating and inhibitory surface receptors (reviewed by Koch et al., 2013). Cytokine, chemotactic and adhesion receptors are involved in NK cell

development, retention, relocation, localization and effector functions (Caligiuri, 2008; Cooper et al., 2001).

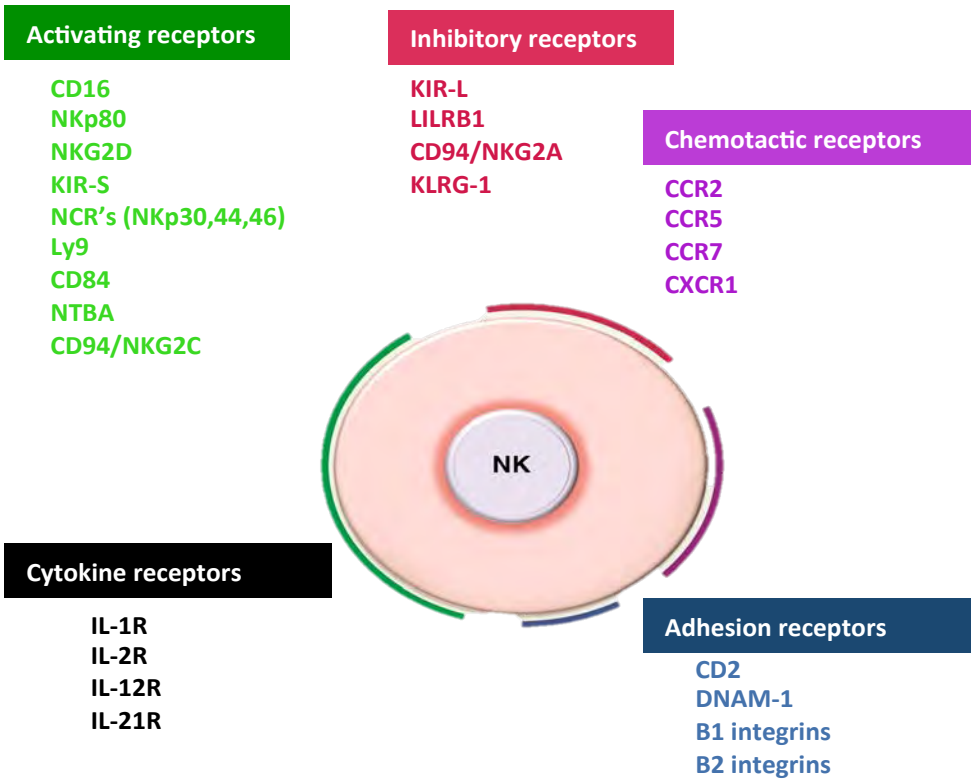

Figure 1.11. Overview of NK cell surface receptors. NK cell receptors can be broadly grouped into inhibitory receptors (red), activating receptors (green), those that mediate adhesion with other host cells (blue), bind to cytokines (black), or mediate chemotaxis (purple) (adapted from Vivier et al., 2004).

1.6.1. NK cell cytotoxicity pathways

NK cells are able to kill target cells using two major mechanisms that require direct contact between NK cells and target cells (Rauf et al., 2012; Caligiuri, 2008). The first NK killing mechanism involves engagement of death receptors on the host target cells, and is called the FAS-ligand (FAS-L) pathway (Rauf et al., 2012). The second NK killing pathway involves the release of cytotoxic molecules (perforin/granzyme) into the cytolytic synapse between NK cells and their targets and causes apoptosis of the target cells (Caligiuri, 2008; Lanier, 2003; Vivier et al., 2004).

1.6.1.1. FAS-L/FAS pathway of NK killing

FAS transmembrane protein is a member of the tumor necrosis factor (TNF) receptor superfamily and is broadly distributed in tissue. Tumor cells do not normally express FAS, but can be induced to do so via IFN-γ secretion by NK cells (Screpanti et al., 2001). Expression of FAS-L is restricted to a highly selective cellular pool including activated T cells, NK T cells and NK cells (Kaufmann et al., 2012). Crosslinking of FcγRIIIa on NK cells can induce transcriptional upregulation of FAS ligands, enabling NK cells to bind to target cells expressing FAS receptors (Figure 1.12; Rauf et al., 2012). The binding of FAS-L to the FAS receptor recruits the FAS-associated death domain (FADD), which then activates caspase-8. Caspase-8 activates downstream effector caspases (caspase-3, -6, -7) leading to target cell apoptosis (Figure 1.12; Elmore, 2007; Rauf et al., 2012).

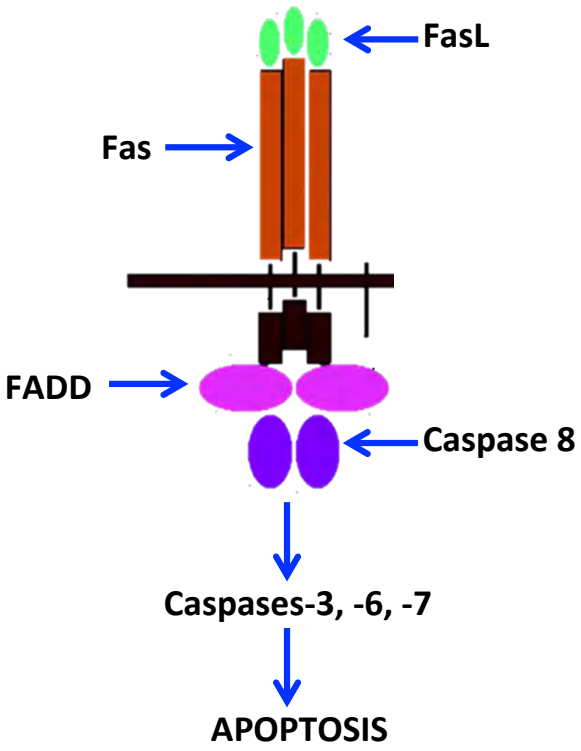

Figure 1.12. FAS-L/FAS pathway of killing by NK cells. The binding of FAS-L (green) to the FAS receptor (red) on the target cells recruits FADD (purple), which then activates caspase activity (including caspases 8, 3, 6 and 7) leading to target cell apoptosis (adapted from Cheema et al., 2004).

1.6.1.2. Perforin and granzyme pathway of NK killing

The perforin and granzyme pathway is the most commonly used NK cell cytolytic pathway during direct killing of tumor cells and ADCC clearance of virus infected cells (Vivier et al., 2004). Upon NK cell CD16 cross-linking with IgG Fc region on antibodies (Figure 1.13), a macromolecular complex containing granzymes, perforin and other molecules is formed within NK cell granules (Bryceson et al., 2011; Trapani and Sutton, 2003). Perforin is a membrane disruptive protein, which forms pores in the target cell (Anthony et al., 2010). Granzymes are a family of structurally related protease enzymes (Bots and Medema, 2006; Hoves et al., 2010). In humans, five granzymes (A, B, H, K and M) have been described, each with their own substrate specificity and cytotoxic potential (van Domselaar and Bovenschen, 2011). Granzyme B is a major

constituent of NK cell granules (Hoves et al., 2010; Trapani and Sutton, 2003), and it promotes apoptosis through proteolysis at aspartate residues that activate caspase activity (Figure 1.13 point 1), including downstream caspases (caspase-3, -6 and -7), and upstream caspases (caspase-2, -8, -9 and -10) (Figure 1.13; Anthony et al., 2010). Processing of caspase-3 and caspase-7 by granzyme B promotes caspase-mediated degradation of hundreds of protein substrates and ultimately leads to cell death (Afonina et al., 2010; Trapani and Sutton, 2003). Granzyme B can also activate apoptosis by cleaving Bid (Figure 1.13 point 2), a pro-apoptotic protein into its truncated form (tBid) (Figure 1.13 point 3), which activates two pro-apoptotic proteins (Bak and Bax) (Figure 1.13 point 4) in the outer mitochondrial membrane (Afonina et al., 2010; Trapani and Sutton, 2003). These proteins induce the release of cytochrome c (Figure 1.13 point 5), which binds to cytoplasmic protein APAF-1 (Figure 1.13 point 6), recruiting caspase-9 (Figure 1.13 point 7; Sharif-Askari et al., 2001; Smyth et al., 2005). Activated caspase-9 can activate other effector caspases (Figure 1.13 point 1) (such as caspase 3 and 7) that promote rapid cell death through proteolysis of their diverse repertoire of substrates. Within NK cells, the endosomal membrane of these cytolytic granules contains lysosome-associated membrane protein (LAMP or CD107a), which is exposed onto the surface of NK cells when granzyme B and other granules are released. NK cell surface expression of CD107a has been used as a marker for NK cell degranulation (Alter et al., 2004; Krzewski et al., 2013). Silencing LAMP has been shown to inhibit granzyme B delivery but not perforin delivery to target cells (Krzewski et al., 2013).

In addition to activation of caspase activity, granzyme B had been reported to initiate target cell death via other mechanisms (Afonina et al., 2010; Rauf et al., 2012; Trapani and Sutton, 2003). Granzyme B can promote DNA fragmentation in cells lacking functional caspases, which activates nucleases, which then mediates the internucleosomal degradation of DNA, one of the hallmarks of apoptosis induced by NK cells (Liu et al., 1998; Sharif-Askari et al., 2001; Thomas et al., 2000). Furthermore, granzyme B may directly target mediators of viral replication and inhibit viral spread without causing apoptosis of infected cells (Kinchington and Hendricks, 2008).

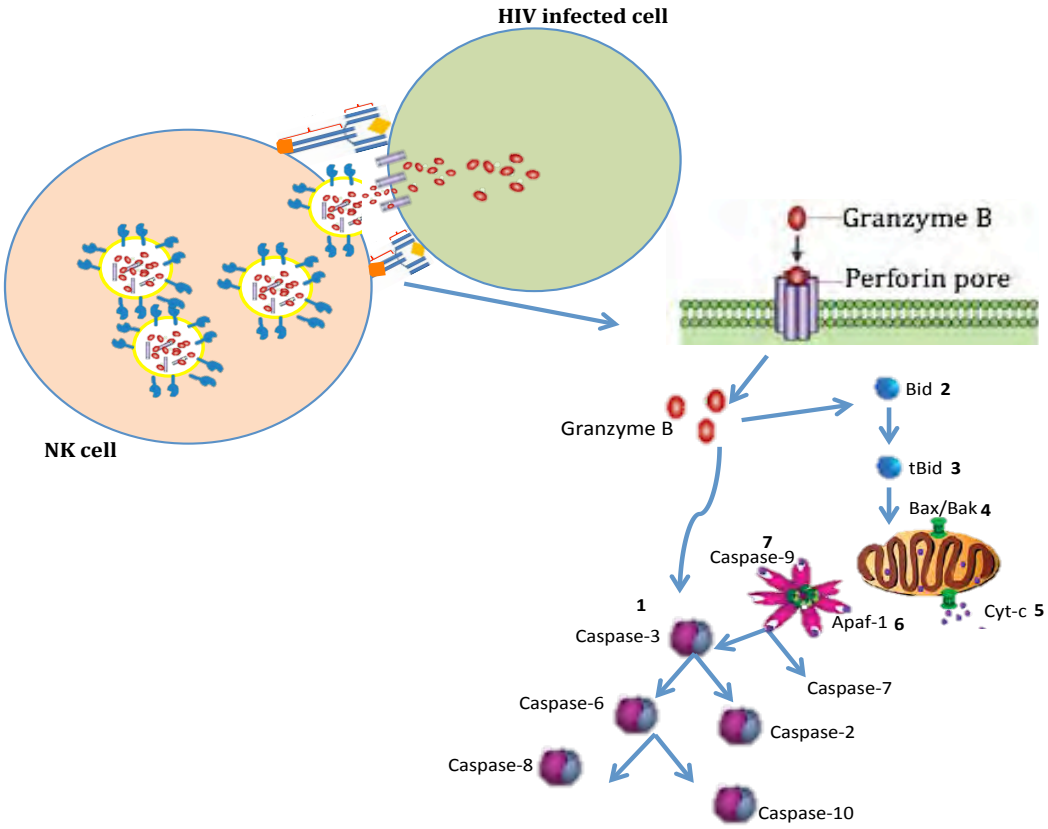

Figure 1.13. NK cells mediating ADCC by binding to HIV-infected cells and releasing preformed granules containing granzyme B and perforin, leading to the activation of caspase activity. Secretory lysosomes are formed within the NK cell and travel to the cell membrane when cells are activated. The proteins are released at the synapse formed between the NK cell and target cell. Granzyme B enters the target cells by a perforin-dependent manner and activates caspase activity (1). Granzyme B can also activate bid (2), which is truncated to tbid (3) to induce oligomerization of bax/bak. This facilitates cytochrome c release (5), which mediates the formation of a caspase-activating complex between Apaf-1 and caspase-9. Activated caspase-9 activates downstream effector caspase activity, which promote apoptosis (adapted from Afonina et al., 2010).

1.6.2. Characteristics of NK cells that influence ADCC activity

Characteristics of NK cells, such as polymorphisms in their FcγRIIIa receptor, expression of inhibitory versus activating KIRs or cytokine secretion, may also determine the efficiency or magnitude of ADCC activity (Wren et al., 2013).

1.6.2.1. NK cell education and cumulative signals

Effector functions of NK cells develop in two stages (Figure 1.14). The first stage during which an NK cell is educated, is initiated during early NK cell ontogeny in the bone marrow (Figure 1.14 left panel; Caligiuri, 2008; Cooper et al., 2001; Valiante et al., 1997), and determines whether the NK cell will be directly cytolytic or indirect antibody-dependent killers (Wren et al. 2013). During this early process within the bone marrow, the activating and inhibitory receptors interact with normal healthy self-environment. NK cells with inhibitory receptors for self-ligands are stimulated to mediate enhanced effector functions including ADCC, while those that carry activating receptors for self-ligands are less likely to mediate ADCC (Parsons et al., 2012; Wren et al., 2013). With regards to anti-HIV ADCC, education of NK cells through the inhibitory receptor KIR-3DL1 (section 1.6) has been demonstrated to be important (Parsons et al., 2012). There is evidence that KIR-3DL1-educated NK cells mediate higher anti-HIV ADCC against autologous targets than non-educated NK cells (Parsons et al., 2012; Ward et al., 2004).

The second stage involves the regulation of NK cells through the cumulative effects of NK cell inhibitory and activating receptor interaction with cognate ligands on the surface of potential target cells (Figure 1.14; Wren et al., 2013). Activation of NK cells to mediate effector functions requires cumulative positive (activating) signals to be delivered from these surface interactions (Lanier, 2003). Moreover, the strength of the signal determines the exact effector functions. For example, lower cumulative activating signals induce NK cells to degranulate and secrete chemokines, while stronger cumulative activating signals allow NK cells to secrete cytokines such as IFN-γ (Fauriat et al., 2010). In addition to CD16, a role for activating and inhibitory receptors during HIV-specific ADCC activity has been observed during the stimulation of NK cells. For example, KIRs that interacts with HLA-C and HLA-E binding inhibitory NKG2A receptor has been reported to dramatically decrease ADCC (Ward et al., 2004).

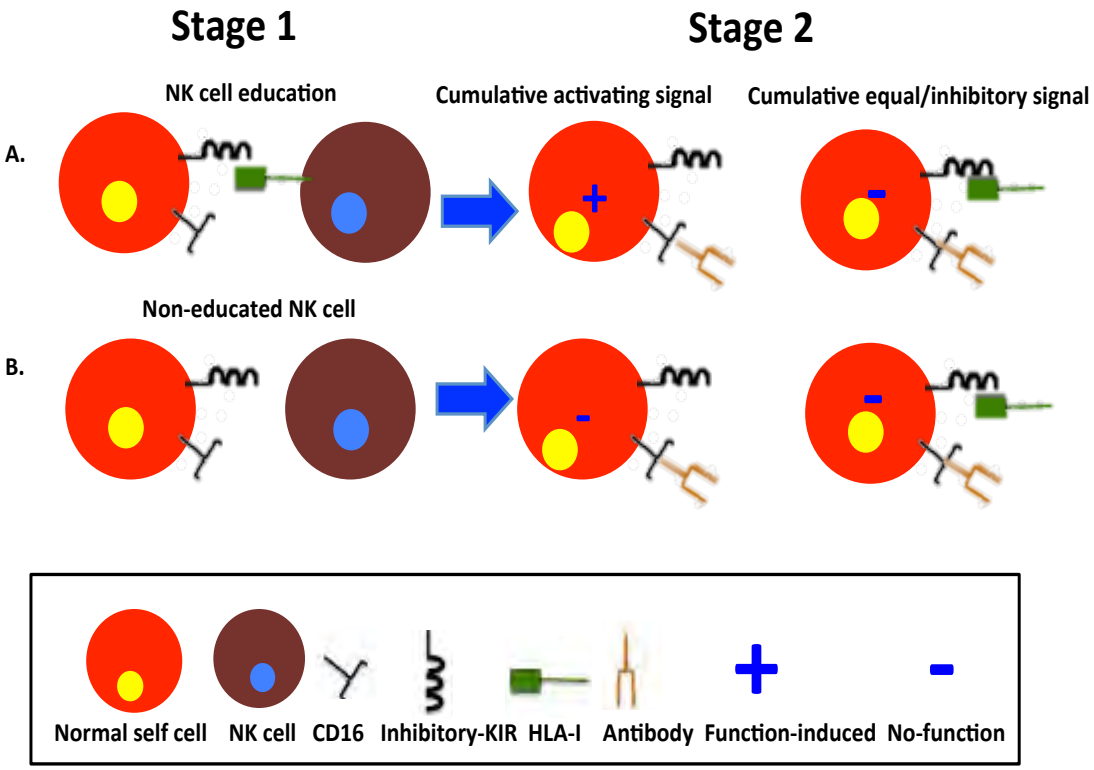

Figure 1.14. Education (stage 1) and regulation (stage 2) of NK cell activity. (A) NK cells (red) screen cellular surface of normal healthy cells (brown) and if NK cell inhibitory receptors find self-ligand (HLA-I), the NK cell is educated (stage 1) with a potential to mediate effector functions that results in cumulative activating signals (stage 2). (B) If NK cell inhibitory receptors fail to recognise self-ligand (stage 1), NK cell remains uneducated and unable to stimulate effector functions that results in cumulative activating signals (stage 2) (adapted from Wren et al., 2013).

1.6.2.2. NK cell exhaustion

Exhaustion of NK cells as a result of HIV infection has also been shown to reduce their potency to mediate ADCC (Mavilio et al., 2005; Wren et al., 2013). Like other chronic viral infections, HIV infection induces changes in the phenotype, functionality and subset distribution of NK cells during the course of infection (Björkström et al., 2010; Mavilio et al., 2003). Highly cytolytic $CD56^{Dim}$ CD16+ NK cells becoming depleted during long-term HIV infection, resulting in reduced ADCC activity (Bayigga et al., 2014; Sips et al., 2012). The cell surface density of NCRs (NKp30, NKp44 and NKp46) was shown to be reduced during HIV infection, decreasing the activation of NK cells and their ability to mediate ADCC activity (De Maria et al., 2003; Garcia-Iglesias et al., 2009; Mavilio et al., 2003).

1.6.2.3. FcRIIIγ polymorphisms and ADCC activity

The ability of NK cells to mediate ADCC have been shown to be influenced by polymorphism in the FcR receptors (Wren et al., 2013b). Polymorphism in CD16 (FcγRIIIa) at amino acid position 158 (resulting in a switch from valine to phenylalanine in this position), have been shown to influence both the density of CD16 expression on the surface of NK cells, the affinity for IgG Fc component, and therefore influences the magnitude of the ADCC responses in individuals with this polymorphism (Brown et al., 2012; Hatjiharissi et al., 2007; Naranbhai et al., 2013).

1.6.2.4. Role of cytokines in enhancing ADCC activity of NK cells

NK cells functionality can also be altered by exogenous factors such as cytokines (Wren et al., 2013b). During viral infections, cytokines (such as type I IFNs, IL-10, IL-12, IL-15 and IL-18) are responsible for early NK cell activation and expansion (Iannello et al., 2008). Exogenous addition of IL-10 and IL-15 has been shown to significantly increase NK cell-mediated ADCC effector functions during HIV infection (Brenner et al., 1989; Carson et al., 1994; Wren et al., 2013). Furthermore, the effect of exogenous addition of IL-15 was more potent on NK cells educated through co-expression of KIR3DL1 and HLA-Bw4, previously associated with protection against HIV infection (Boulet et al., 2010; Parsons et al., 2010). Although the exact mechanism whereby IL-10 and IL-15 enhances NK cell ADCC during HIV infection is not understood, they may increase NK cell sensitivity to ADCC antibodies (Wren et al., 2012). In contrast, IL-4 and TGF-β have been reported to suppress NK cell function (Iannello et al., 2008).

NK cell ability to mediate ADCC is therefore influenced by these characteristics of the Fc receptor used, the level of maturity, activation or inhibition, and exhaustion of these effector cells as well the cytokine environment in which NK cells are functioning.

1.7. HIV epitopes targeted by ADCC

During HIV infection, antibodies have been identified that target various HIV epitopes on free virus particles and on the host cell surface of the HIV-infected cells (Figure 1.15 and Table 1.2; reviewed by Pollara et al., 2011). HIV-specific ADCC responses have been reported to target both linear and conformational epitopes in HIV gp120 and gp41 (Ferrari et al., 2011; Kwong et al., 1998; Lyerly et al., 1987). An important characteristic of the ADCC HIV epitopes are that these epitopes are exposed to antibodies when HIV is entering the host cell or when the HIV envelope is maturing on the host cell membrane of HIV-infected cells, before budding (Briggs and Kräusslich, 2011). Within gp120, epitopes within variable regions V1-3 and the CD4 binding site have been identified as targets for ADCC (reviewed by Pollara et al., 2013). Within gp41, the MPER, cluster A, B and C regions were shown to be targets for ADCC (Figure 1.15; reviewed by Pollara et al., 2013).

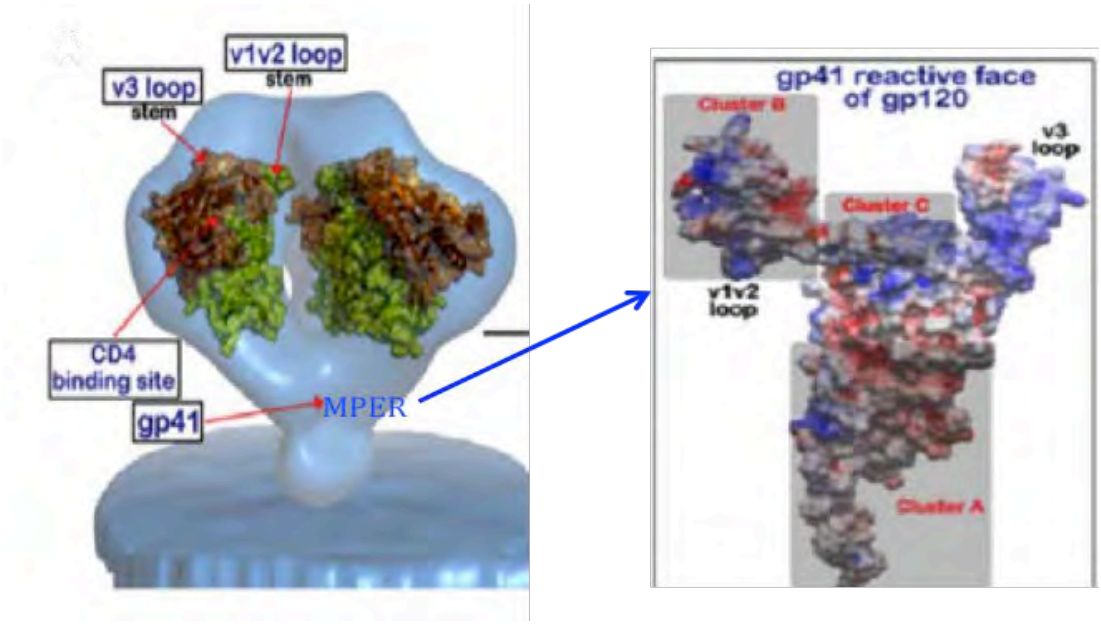

Figure 1.15. HIV gp120 and gp41 epitopes recognised by ADCC antibodies. The red arrows indicate the regions of the HIV-envelope glycoprotein targeted by ADCC activity. The V1, V2 are indicated in green and the V3 region is indicated in yellow. The CD4 binding site is indicated in brown. On the right panel is the gp41 reactive face of gp120, showing the clusters (A-C; red) identified in gp41 and the V1-3 regions (purple) (adapted from Pollara et al., 2013).

Table 1.2. Defined regions on the HIV-envelope targeted by human monoclonal antibodies with ADCC activity (reviewed by Pollara et al., 2013).

HIV-1 Envelope Glycoprotein	Envelope Region	mAb	Discontinuous Or Linear Epitope	Neutralizing or Non-neutralizing	References
gp41	Cluster I	245-D	Linear	Non-neutralizing	(Forthal et al., 1995; Moog et al., 2014)
		4B3	Linear	Non-neutralizing	(Moog et al., 2014)
		98-43	Linear	Non-neutralizing	(Tyler et al., 1990)
		50-69	Discontinuous	Non-neutralizing	(Tyler et al., 1990)
	Cluster II (HR2)	98-6	Discontinuous	Non-neutralizing	(Forthal et al., 1995; Tyler et al., 1990)
		126-50	Discontinuous	Non-neutralizing	Tyler et al., 1990)
	Not defined	31710B	Not defined		(Alsmadi et al., 1998)
	MPER	120-16	Linear	Non-neutralizing	(Forthal et al., 1995; Tyler et al., 1990)
		2F5	Linear	Non-neutralizing	(Moog et al., 2014, Tudor et al., 2011)
		4E10	Linear	Non-neutralizing	(Moog et al., 2014)
gp120	CD4i C1 region (Cluster A)	A32	Discontinuous	Non-neutralizing	(Ferrari et al., 2011)
	CD4i CoRBS (Cluster C)	17B	Discontinuous	Neutralizing	(Ferrari et al., 2011)
	CD4i	CH08	Discontinuous	Neutralizing	(Friedman et al., 2012)
	CD4i Cluster A	C11, L9-i1, N5-i5, L9-i2, N12-i3, N26-i1	Discontinuous	Non-neutralizing	(Guan et al., 2013)
	CD4i Cluster B	N12-i15	Discontinuous	Non-neutralizing	(Guan et al., 2013)
	CD4i Cluster C.1	L9-i3, N5-i1, N5-i3, N5-i4, N5-i8, N10-i1.1, N10 15.3, N12-i1, N12-i2, N12-i4, N12-i5, N12-i7, N12-i8	Discontinuous	9/10Neutralizing	(Guan et al., 2013)
	CD4i Cluster C.2	N12-i10, N12-i17, N12-i18, N12-i19	Discontinuous	2/6Neutralizing	(Guan et al., 2013)
	CD4 Cluster C.3	N5-i2, N5-i6, N5-i9, N5-i14, N5-i7, N5-i12, N10-i3.1, N12-i12, N12-i9, N12-i11	Discontinuous	Non-neutralizing	(Guan et al., 2013)
	CD4 Cluster C.4	L9-i4, N5-i10.1, N5-i13, N10-i2, N12-i14, N12-i16	Discontinuous	Non-neutralizing	(Guan et al., 2013)
	CD4i	N10-i4, N10-i6.1	Discontinuous	Neutralizing	(Guan et al., 2013)
	CD4i C1 region	CH20, CH29, CH38, CH40, CH49, CH51, CH52, CH53, CH54, CH55, CH57, CH77, CH78, CH80, CH81, CH90, CH91, CH92, CH94	Discontinuous	Neutralizing	(Bonsignori et al., 2012)
	C2, C3, C4, V4 glycansites	2G12	Discontinuous	Non-neutralizing	(Trkola et al., 1996)
	C5	670-D	Discontinuous	Non-neutralizing	(Forthal et al., 1995)
		750-D	Not defined	Neutralizing	(Forthal et al., 1995)
		42F, 43F	Linear	Non-Neutralizing	(Alsmadi et al., 1997)
	CD4 binding site	15e	Discontinuous	Neutralizing	(Koup et al., 1991)
		F105	Discontinuous	Neutralizing	(Posner et al., 1992)
		448-D	Discontinuous	Neutralizing	(Forthal et al., 1995)
		1125H, 5145A	Discontinuous	Neutralizing	(Alsmadi et al., 1998)
		b12	Discontinuous	Neutralizing	(Hezareh et al., 2001)
		VRC01	Discontinuous	Neutralizing	(Ferrari et al., 2011)
	V2	CH58, CH59, HG107, HG120	Linear	Neutralizing	(Liao et al., 2013)
		PG9	Discontinuous	Neutralizing	(Biedma ME, 2013)
	V3	694/98D	Linear	Neutralizing	(Forthal et al., 1995)
		4117C, 41148D	Linear	Neutralizing	(Alsmadi et al., 1998)
		CH22, CH23	Linear	Neutralizing	(Bonsignori et al., 2012)

Many ADCC epitopes coincide with epitopes previously shown to be recognised by nAbs (Bonsignori et al., 2012; Pollara et al., 2013; Veillette et al., 2014). Even though the HIV envelope protein has been shown to be the major target for HIV-specific ADCC, antibodies that recognise Nef, Vpu and Pol HIV proteins have also been described that mediate ADCC (Isitman et al., 2011; Veillette et al., 2014; Wren et al., 2013). The specific epitopes where the HIV-specific ADCC antibodies bind on these proteins are yet to be identified.

Although it is well established that HIV readily escapes from HIV-specific nAbs and that this is the major driver of genetic variation in gp120 and other HIV proteins (Deeks et al., 2006; Moore et al., 2012; Wei et al., 2003), similar escape from ADCC antibodies has only recently been demonstrated (Chung et al., 2011). It is thought that HIV-specific ADCC activity exerts significant pressure on HIV, resulting in HIV escape mutations (Chung et al., 2011b; Isitman et al., 2012). As has been shown for nAbs, HIV-specific ADCC antibodies have been shown to loose ability to recognise viral sequences from earlier autologous time points (Isitman et al., 2012). Isitman and colleagues (2012) suggested that conformational ADCC antibodies are also likely to elicit HIV escape mutants, but are likely to be more difficult to map than linear epitopes and therefore it would be difficult to detect immune escape (Isitman et al., 2012).

1.8. Protective role of ADCC in HIV infection

Longitudinal studies in SIV-infected non-human primates have shown that the presence of SIV-specific ADCC activity correlated with better disease outcome (Banks et al. 2002). In humans, the presence of HIV-specific ADCC antibodies during acute infection predicted better control of viremia by leading to lysis of HIV-infected cells and reduced viremia (Forthal et al., 2001; Go´mez-Roma´n et al., 2005; Baum et al., 1996). Elite controllers of HIV (individuals who are infected with HIV but maintain undetectable plasma viral loads without HAART) were found to have levels of ADCC activity (Okulicz et al., 2009; 2012).

Antibodies that mediate HIV-specific ADCC have also been detected in secretions from the female genital tract, and women with ADCC antibodies in their genital secretions had lower genital viral loads compared to women with no genital ADCC antibodies (Nag et al., 2004). In addition, HIV-specific ADCC antibodies have been found in breast milk of HIV-infected women, and low levels of ADCC envelope specific IgGs in breast milk has been identified as a correlate of transmission that may impact infant infection risk to infants (Mabuka et al., 2012).

1.9. Properties of antibodies that influence the magnitude of ADCC activity during HIV infection

Properties of antibodies may influence the magnitude of ADCC responses during HIV infection (reviewed by Wren et al., 2013). The isotype, subclass or glycosylation of the Fc component (including the precise composition of major sugar residues) of antibodies may influence ADCC responses (Bruhns et al., 2009). Previous studies have reported that IgG1 and IgG3 antibodies are the most potent inducers of anti-HIV ADCC (Ljunggren et al., 1988; Niwa et al., 2005). The removal of the major sugar residue fucose has been shown to increase ADCC ~100-fold, while the addition of the sugar siliac acid during glycosylation of the Fc component has been shown to decrease ADCC activity (Boyd et al., 1996; Shinkawa et al., 2003). Some studies reported that galactosylation of IgG Fc enhances ADCC, while others were unable to replicate this enhancement (Boyd et al., 1996; Shinkawa et al., 2003; Wren et al., 2013).

1.10. ADCC antibodies mediate protection against HIV

Recently, the "RV144" HIV vaccine trial was conducted in 16000 HIV-negative Thailand women and men at risk for HIV infection via heterosexual exposure in Thailand (Rerks-Ngarm et al., 2009). This vaccine trial included a total of four inoculations of a recombinant avian poxvirus live vector ALVAC-HIV (vCP1521), expressing Gag-Pro of HIV clade B and a membrane-anchored clade E gp120

and two simultaneous inoculations of the AIDSVAX B/E gp120 proteins (Karnasuta et al., 2004; Rerks-Ngarm et al., 2009). Thorough investigation of the immune correlates of protection in the RV144 trial demonstrated that protection was associated with HIV-specific CD4+ T cells, binding (non-neutralizing) IgG antibodies, and gp120 V1V2 antibodies associated with ADCC activity (Haynes et al., 2012). This RV144 vaccine trial highlighted importantly that protection could be achieved in absence of nAbs or HIV-specific CTLs. Also, this study suggested that IgA vaccine responses were not protective and that individuals with the highest titers of HIV-specific IgA were most at risk of becoming infected (Gottardo et al., 2013; Haynes et al., 2012; Karasavvas et al., 2012).

1.11. Methods to measure ADCC

Different approaches have been used to study NK cell-mediated ADCC activity (Chung et al., 2009; Gómez-Román et al., 2006; Karnasuta et al., 2005; Pollara et al., 2011). Measurement of ADCC activity of NK cells is a complex process because three distinct important components are involved in ADCC and therefore need to be considered (Chung et al., 2008). These 3 components to consider are: (1) properties of the target cells that express HIV antigens; (2) properties of the effectors cells (NK cells); and (3) properties of the HIV-specific antibodies. Therefore, ADCC assays that have been widely used in the past measured either properties of effector cells; or the amount of killing of the HIV-infected target cells.

1.11.1. ADCC assays measuring properties of the effector cells

1.11.1.1. CD107a flow cytometry assay

During ADCC, NK cell effectors degranulate, releasing cytolytic granules into the immunological synapse between the effector and target cell to induce target cell lysis (section 1.6.1). The membrane of the lysomal compartment that releases cytolytic granules (containing perforin and granzyme) contains CD107a, which

can be useful as a cell surface marker to measure the extent to which NK cells have degranulated (Alter et al., 2004). Other markers such as CD16 and cytokines (TNF-α and IFN-γ) can also be measured simultaneously by multi-parameter flow cytometry (Alter et al., 2004). NK cell surface expression of CD107a was shown to correlate significantly with target cells lysis measured by Cr^{51}-release and with secretion of cytokines by NK cells (Alter et al., 2004).

1.11.1.2. Esterase release assay

An alternative to the CD107a assay, Kato et al (1991) described measurement of esterase activity by the effector cells as a measure of effector cell degranulation. Effector cells release granules containing esterases (mainly granzyme A) that can cleave the substrate N-α-benzyloxycarbonyl-ι-lysine thiobenzyl ester (BLT), which can be used to measure the frequency of effector cell degranulation (Kato et al., 1991).

1.11.1.3. Perforin deposition assay

Since effector cell degranulation results in the release of granules containing perforin and granzymes, Zaritskaya et al (2010) proposed measuring perforin deposition as a measure of effector cell function. Using this approach to measure ADCC, effector cells were stained with a perforin-specific monoclonal antibody and perforin-deposition within the target-effector synapses can be visualised using monitored using microscopy (Zaritskaya et al., 2010).

1.11.2. ADCC assays measuring properties of the target cells

1.11.2.1. Chromium release assay

Historically, ADCC assays have relied on labeling target cells with radioactive sodium chromate (Chromium^{51} or Cr^{51}; Brunner et al., 1968) and this approach has also been used to measure HIV-specific ADCC (Chung et al., 2008). This traditional approach to evaluating target cell death during ADCC has several

disadvantages, such as low sensitivity, need for potent radioactive isotopes, and that certain target cells are difficult to label in this manner (Go´mez-Roma´n et al., 2006).

1.11.2.2. Rapid fluorometric ADCC assay

More recently, fluorescence based assays have been developed to measure ADCC (Chung et al., 2008). These involve labeling the target cells with a membrane and intracellular fluorescent dyes and using flow cytometry to measure loss of fluorescence as a measure of lysis. These rapid and fluorometric ADCC assays rely on double staining target cells with a membrane marker (PKH-26) and a viability dye (CSFE) prior to addition of effector cells (Go´mez-Roma´n et al., 2006).

1.11.2.3. Lactate dehydrogenase (LDH) release assay

The principle of this assay is the release of lactate dehydrogenase (LDH) from the dying target cells whereby LDH participates in a colourmetric reaction in which a yellow tetrazolium salt is converted to a red colour that is measured as a marker of target cell lysis during ADCC (Broussas et al., 2013).

1.11.2.4. ADCC-GranToxilux and PanToxilux assays

Recently, Pollara et al. (2011) described a sensitive high-throughput flow cytometry based assay to measure ADCC. The GranToxilux assay measures granzyme B activity in target cells and relies on hydrolysis of a cell-permeable fluorogenic peptide substrate containing a sequence recognised by the serine protease, granzyme B (Packard et al., 2007; Pollara et al., 2011). Granzyme B is delivered to target cells following degranulation of NK cells during ADCC, and this assay quantifies this delivered granzyme B by flow cytometry. The PanToxilux assay is a variation of the GranToxilux assay, with the main difference being the cell permeable fluorogenic substrate (Packard et al., 2007).

While GranToxilux detects granzyme B only, PanToxilux detects granzyme B as well as upstream caspase activity.

1.12. Aims and objectives

The aim of this study was to optimise and compare the GranToxilux and PanToxilux assays to measure (1) direct killing and (2) HIV-specific ADCC activity.

Objective 1:

To optimise the GranToxilux and PanToxilux assays to measure direct NK cell killing of the tumour cell line K562.

Hypothesis:

The PanToxilux assay will be more sensitive to detect direct killing of K562 tumour cells than the GranToxilux assay because it measures both granzyme B and caspase activity.

Objective 2:

To optimise and compare the GranToxilux and PanToxilux assays for measurement of HIV-specific ADCC activity.

Hypothesis:

The PanToxilux assay, which detects both granzyme B and caspase activity in target cells, will be more sensitive at measuring ADCC activity in HIV-infected individuals than the GranToxilux assay, which only detects granzyme B.

CHAPTER 2

Materials and Methods

2.1. NK target cell lines

The human erythroleukemic cell line K562 was used as the target cells for measuring direct killing of NK cells in this study (Chapter 3). K562 are highly undifferentiated human erythroleukemic cell line that do not express HLA class I molecules, making these cells sensitive to NK cell lysis (Naumann et al., 2001). K562 cells (1 x 10^6 cells/ml) were cultured in RPMI-1640 medium (Sigma-Aldrich®; St. Louise, MO) containing 10% FBS (fetal bovine serum) and 1% penicillin-streptomycin-glutamine (R10) at 37°C in a humidified 5% CO_2 incubator. The growth medium was checked and replaced ~2 days. This cell line was maintained in a 50ml tissue culture flask in R10 and split ~4 days.

CEM.NKR_{CCR5} cells, modified to express CD4 and CCR5 receptor on the cell surface, are not directly sensitive to NK cell killing but become sensitive to killing following coating them with HIV gp120 and adding HIV-specific antibodies, making them useful target cells for measuring ADCC (Trkola et al., 1999). In addition, CEM cells which do not express CCR5 were used as a negative control (Chapter 4). CEM.NKR_{CCR5} cells were cultured in a 50ml plastic cell culture flask (Sigma-Aldrich®) as described above. This cell line was maintained in R10 in 50ml tissue culture flask at 37°C in a humidified 5% CO_2 incubator. The growth medium was checked and replaced ~2 days and split ~3 days. The growth kinetics of CEM.NKR_{CCR5} cells differed slightly from K562 cells, growing faster. A sub-passage of cells was done before any experiment to ensure that the cells were in log-phase of growth.

2.2. Study participants and sample collection

Blood "buffy" packs were obtained from 8 HIV-negative individuals from Western Province Blood Transfusion Service (Pineland, Cape Town) and processed within four hours of collection for isolation of peripheral blood mononuclear cells (PBMCs), as a standardised source of NK cell effector cells for this study (used in Chapter 3 for direct killing and in Chapter 4 for ADCC-

mediated NK killing). In addition, whole blood (40ml) was collected by venipuncture from 9 chronically HIV-infected individuals who were naïve to HAART. Plasma from these HIV-infected donors was used as the source of HIV-specific antibodies for the ADCC assays (Chapter 4). Whole blood was collected into vacutainer tubes containing acid citrate dextrose as an anti-coagulant (ACD; BD Bioscience, San Diego, CA). The University of Cape Town's Faculty of Health Sciences Research Ethics committee (REC REF 258/2006) approved all aspects of this study, and written informed consent was obtained from all the participants.

2.3. Processing of PBMCs and blood plasma

PBMCs were isolated from HIV-negative buffy packs using Ficoll-Hypaque (Sigma-Aldrich®) density gradient centrifugation. This method takes advantage of the density differences between mononuclear cells (such as NK cells, B cells, T cells, monocytes, macrophages and dendritic cells) and other blood elements and cells (red blood cells, platelets and neutrophils). Ficoll-Hypaque is a hydrophilic polymer, which serves as a solute that produces a density gradient for the separation of cells. Briefly, 15ml of Ficoll-Hypaque was added to a 50ml Leucosep® tube (Greiner Bio-one; Frickenhausen, Germany) containing porous membrane. The porous membrane separates the Ficoll-Hypaue from the blood sample thus avoiding their accidental mixture before centrifugation. This was then centrifuged at 1258rcf for 1 min to allow the Ficoll-Hypaque solution to descend below the membrane. Buffy packs from HIV-negative blood donors were dispensed into the 50ml Leucosep® tubes and centrifuged at 1258rcf for 15 min. The PBMC layer was carefully removed using a Pasteur pipette and transferred to a 15ml tube. PBMCs were washed with 1% FBS in phosphate buffer saline (PBS) by centrifugation. The cell pellet was resuspended in 6ml of RPMI 1640 (Gibco™) supplemented with 10% FBS (R10) and counted using the automated Guava cell counter.

2.4. Counting cells and viability assessment

2.4.1. Trypan blue exclusion manual counting of cell lines

K562 and CEM.NKR$_{CCR5}$ cell lines were manually counted using the light microscopy and Trypan blue exclusion dye test to differentiate live from dead cells. Trypan blue exclusion dye does not stain live cells (that have intact cell membranes and cannot be penetrated by the Trypan blue dye) but does stain dead cells (that have damaged cell membrane that allows uptake of the dye). Briefly, cells were stained with 0.4% Trypan blue at a 1:2 dilution (10µl cells: 10µl Trypan blue) in a 96-well microtiter plate and thoroughly mixed with a pipette. Ten µl of the cell-trypan mixture was then loaded onto a plastic disposable Blaubrand Neubauer slide into the counting chamber/haemocytometer with a glass coverslip (Blaubrand®, Germany). A haemocytometer is a device used to determine the number of cells per defined unit volume of suspension. The haemocytometer was placed under a 40x objective of a light microscope (Figure 2.1). The live and dead cells in the two opposite chambers are counted and the absolute cell count and viability were calculated using the formulas shown in Figure 2.1. After counting the live cells, concentration was adjusted to $1x10^6$ cells/ml for continued culturing or 10x 10^6cells/ml for cryopreservation. Only cells with viability >95% were cryopreseved or used in the experiments.

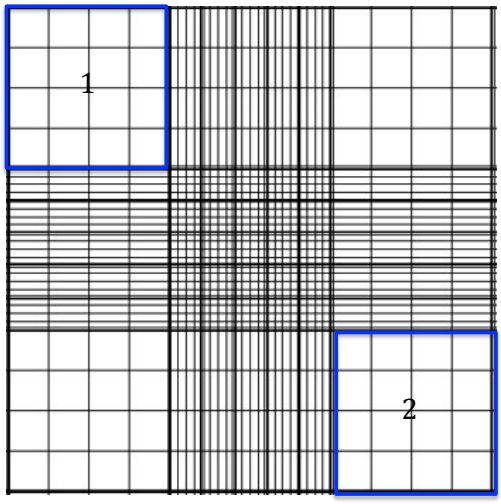

FORMULAS:

(a) Viable cells = [(1+2)/2] x (dilution factor) x 10^4 x total volume (ml)

(b) Percent viability = (live cell count/ total cell count) x 100

Figure 2.1. Schematic of a haemocytometer chamber and the formulas used to calculate viability of cells following Trypan blue staining. Cells in any of the two opposite squares are counted and the viability is calculated using the two formulas (taken from www.microbehunter.com).

2.4.2. Automated cell counting of PBMCs using the Guava cell counter

PBMCs from HIV-negative individuals were counted using an automated Guava cell counter (Guava Technologies Inc, San Fransisco, CA) before cryopreserving them, and after thawing or preparing them for experiments. The Guava automated cell counter counts the number of nucleated cells in a PBMC sample in addition to testing the viability of the sample using Guava ViaCount reagent consisting of a nuclear and viability dye. For Guava ViaCount cell counting, PBMCs were diluted at a 1:20 in Guava ViaCount reagent (10µl PBMCs added to 190µl of the ViaCount reagent). According to the manufacturer instructions, the mixture was vortexed and incubated for 8 min at RT before counting. Viable PBMCs were adjusted to 10x10^6cells/ml and cryopreserved immediately as described in section 2.5. Resting PBMCs were adjusted to 1x10^6cells/ml. As with the cell lines, viability of the PBMCs after thawing had to be >95% to be included in any experiment.

2.5. Cryopreservation of PBMCs

For long-term storage of PBMCs, cells were cryopreserved in a media containing 10% dimethyl sulfoxide (DMSO; Sigma-Aldrich®) as a cryoprotectant, diluted in FBS as freezing medium. DMSO is a polar solvent that can penetrate cell membranes during the freezing process, without damaging them, to protect freezing cells from damage caused by ice crystals formation (Frackman et al., 1998). Briefly, PBMCs for cryopreservation were first resuspended in 100% FBS (Invitrogen) at $20x10^6$cells/ml. Freezing media (20% DMSO FBS) was then added drop-wise, with continual mixing, to obtain a final concentration of PBMCs at $10x10^6$cells/ml. The mixture was then aliquoted into pre-cooled cryovials (Greiner Bio-one) at 1ml per cryovial ($10x10^6$ cells) and placed into pre-cooled controlled rate freezing unit, containing isopropyl alcohol to control the rate of freezing. 'Mr Frosty®' (Nalgene; Rochester, NY) unit ensured that PBMCs froze at a rate of 1˚C/min. 'Mr Frosty®' units containing PBMCs were placed at -80˚C overnight and cryovials containing PBMCs were then transferred to liquid nitrogen for long-term storage within 48 hours.

2.6. Thawing cryopreserved PBMCs

Because thawing of cryopreserved cells can be stressful to cells, working quickly and maintaining sterile techniques throughout ensured that a high proportion of the cells survived thawing. In this study, cryopreserved cells were thawed rapidly in a 37˚C water-bath until a pea-size of ice crystal remained. At this point, the cryovial containing the thawed cells was transferred into the biosafety cabinet and 1ml of R1 media [RPMI 1640 (Gibco™), 1% FBS (Invitrogen)] at RT containing [50U penicillin, 50mg/ml glutamine (Gibco™) and 0.8mg/mL Fungin (InvivoGen)] was added drop-wise while shaking the cryovial gently. The contents of the cryovial was then transferred to a 50ml Falcon Tube using a sterile pipette and 15ml R1 was added and the sample was centrifuged at 290rcf for 10 min. The supernatant was discarded and the pellet resuspended in 500µl of 0.02mg/ml DNAse I (Roche Diagnostics). Addition of DNAse to thawing cells prevents them from clumping by digesting the DNA

released by some cells that lysed during cryopreservation or thawing. Samples with DNAse added were incubated at RT for 2 min to facilitate DNA digestion, following which they were then washed with 30ml R1 at 290rcf for 10ml. The pellet was resuspended in 5ml R20 for cell counting, adjusted to the required concentration with R20 and incubated at 37°C, 5% CO_2 overnight.

2.7. Characterisation of NK cells by flow cytometry

2.7.1. Staining of NK cells

The phenotype and function of NK cells from HIV-negative PBMC donors (section 2.3) used in the direct killing and ADCC assays were characterised by flow cytometry. Table 2.1 describes the antibodies used in this study, their fluorochrome, clone and manufacturer. NK cell phenotype was evaluated using antibodies against CD3 (to exclude T cells), CD56 and CD16 (to differentiate distinct NK cell subsets). Furthermore, the functional ability of distinct NK cell subsets was evaluated using antibodies against CD107a (to measure NK cell degranulation, Alter et al., 2004) and intracellular IFN-γ (to measure cytokine production). In addition, a dump channel containing antibodies directed against cells to be excluded from analysis (cells that were not of interest to this study including $CD19^+$ B cells and $CD14^+$ monocytes) and dead cells (ViVid stain to exclude dead cells) was also included in the panel to increase the specificity of staining.

To phenotype and functionally characterise the universal HIV-negative NK cell donor, PBMCs were stimulated with Phorbol 12-myristate 13-acetate (PMA)/ionomycin, Phytohaemaglutinin (PHA) (both positive controls) or left unstimulated (negative control). For stimulation with PHA and PMA/ionomycin, $1x10^6$ cell/ml PBMCs from the HIV-negative donor was added to the individual FACS tubes. To each of these tubes, 10µl of Brefeldin A [(BFA; 5mg/ml) to prevent the exocytosis of cytokine production containing vesicles allowing for the visualization of cytokine production following stimulation], 10µl of

ionomycin and 12,5µl of PMA (2.5µg/ml) or PHA (2.5µg/ml) was added, together with 5µl of CD107a. These tubes were mixed well and then placed in the incubator for 2 hours at 37°C and 5% CO_2. For all experiments, an unstimulated control tube was also included. To these tubes, 10µl BFA, 10µl Monensin (10µg/ml) and 5µl CD107a was added. The tubes were mixed well and placed in the incubator at 37°C and 5% CO_2 for the same length of time.

After stimulating, the PBMCs were washed twice in PBS by centrifuging at 290rcf for 4 min. The supernatant was discarded and the pellet was resuspended in 50µl of ViVid dye (to stain dead cells) and transferred to a 96-well V-bottomed microtiter plate (Corning; Tewksbury MA) for staining. The plate was incubated in the dark at RT for 20 min. The cells were then washed twice with 150µl PBS by centrifugation at 887rcf for 5 min. After the second wash, the PBMCs were resuspended in a volume of 50µl containing the master-mix of antibodies to stain for extracellular markers (Table 2.1). The plate was covered with aluminium foil and incubated on ice for 20 min. The cells were then washed twice as previously described. To enable fixation and permeabilization, 100µl of Cytofix/Cytoperm (BD Biosciences) was added to the cells and incubated at RT for 20 min. Cells were washed twice using permwash. The antibody cocktail against (intracellular) markers (Table 2.1) was added and the plate incubated for 20 min at RT. The CD3 T cell marker was included to distinguish NK cells (which lack expression of CD3) from T cells (which express high levels of CD3). Staining for CD3 was done following permeabilisation (intracellularly) as stimulation of cells can sometimes cause the internalization of the CD3 receptor, which is usually expressed on the surface of T-cells. Cells were washed twice as previously described. Cells were resuspended in 150µl of cellfix and contents were transferred to the FACS tubes (BD Biosciences). The wells were rinsed with 150µl of cellfix and added to the tubes. All the samples were acquired within 6 hours of staining using the BD LSRFortessa™ and approximately 500 000 events were acquired for each tube.

Table 2.1. Antibodies included in the optimised flow cytometry panel

Fluorochrome	Antibody	Clone	Function	Manufacturer
		Extracellular		
PerCP-Cy5.5	CD4	L200	CD4 T cell marker	BD Bioscience
Qdot 605	CD8	3B5	CD8 T cell marker	BD Bioscience
PE	CD16	3G8	Fc Receptor and NK cell marker	BD Bioscience
PE-Cy7	CD56	NCAM16.2	NK cell marker	BD Bioscience
FITC	CD107a	H4A3	LAMP-1 and marker of degranulation	BD Bioscience
PacBlue	CD19	MHCD1928	Dump channel: B cell marker	Invitrogen
PacBlue	CD14	M5E2	Dump channel: Monocyte marker	BD Bioscience
PacBlue	Vivid		Dump channel: Viability marker	BD Bioscience
		Intracellular		
APC-Cy7	CD3	SK7	T cell marker	BD Bioscience
Alexa Fluor 700	IFN-γ	B27	Functional marker	BD Bioscience

All antibodies were first titrated to determine the optimal amount to use in the experiment (see Appendix II).

2.7.2. Colour compensation tubes to correct for spectral overlap

During multicolor flow cytometry (including multiple fluorochromes against distinct antigens) that may have overlapping spectral ranges, it is always necessary to include compensation tubes to correct for spectral overlap (Seddon et al., 2003). This ensures that the fluorescence detected by a particular detector derives solely from the fluorochrome conjugated on the specific antibody and not from fluorochromes on other emission spectra. For each of the fluorochromes used in the panel (Table 2.1), a single-stained positive control tube is prepared containing just the fluorochrome of interest. A negative control (unstained) is also prepared to set voltages for the fluorescence channels.

For the panel in Table 2.1, eight compensation tubes each having one of the different fluorochromes were prepared using BD CompBeads™. BD positive CompBeads™ are beads that have been coupled to an antibody specific Kappa light chain of Ig from mouse or rats (Bishop et al., 2004). The beads are easily stained and have a robust fluorescence signal. In contrast, BD negative CompBeads™ have no binding capacity. The positive and negative CompBeads™ were vortexed thoroughly for 1 min to avoid aggregation. Using 5ml FACs tubes, 100µl of PBS was added to each tube followed by a drop of negative and positive CompBeads™. Tubes were singly stained with the corresponding volume of each antibody that had been used during the staining of samples, followed by incubation on ice for 20 min. The beads were washed by adding 1ml PBS and centrifuging at 290rcf. The supernatant was discarded and the pellet was re-suspended in 100µl of 1X cellfix (BD Biosciences) and stored at 4˚C until acquisition with the BD LSRFortessa™. The CompBeads were acquired along with the PBMCs stained with all the panel antibodies using the optimised voltages and settings. During analysis using Flowjo (Treestar Inc, Ashland, OR), the compensation matrix was calculated using the positive CompBeads while the unstained gated on the negative population.

2.7.3. Fluorescence Minus One (FMO) controls

In addition to compensation tubes, fluorescence minus one (FMO) controls were also used to evaluate spill over of fluorescence from other channels into each specific channel being evaluated. This control contains all fluorochrome in the panel except the one being measured. This ensures that any spread of the fluorochrome in the channel of interest is properly identified. One would expect no staining in the channel for which the antibody had been left out. The presence of staining in the channel for which the antibody had been left out would indicate that fluorescence from another channel was spilling over into the negative channel which would have been contributing to a false positive signal had the FMO approach not been implemented.

Preparation of the FMO controls included staining $1x10^6$ cells per well in a 96-well V-bottomed plate with 50µl of vivid. The plate was incubated at RT in the dark for 20 min. Cells were washed twice with PBS. Intracellular (CD107a, CD3, IFN-γ) and extracellular (CD4, CD8, CD56, CD16 and CD107a) antibodies were added as previously described; making sure the antibody of interest is not added. The cells were resuspended in 100µl cellfix and transferred to 5ml FACS tube. The tubes were then stored at 4˚C until acquisition using the BD LSRFortessa™.

2.8. Collection of HIV-positive plasma as source of antibodies for ADCC

PBMCs and plasma were isolated from ACD anti-coagulated whole blood from HIV-infected individuals using Ficoll-Hypaque (Sigma Aldrich®) density gradient centrifugation, as described above. Plasma (5ml) from the top of the gradient was collected using a plastic disposable Pasteur pipette, aliquoted into 1ml cryovials and transferred immediately into a -80˚C freezer. This HIV-positive plasma was used as the source of HIV-specific antibodies for the ADCC

assays (Chapter 4). PBMCs from HIV-positive individuals were collected and stored as described above.

2.9. Measurement of HIV-1 specific antibodies in plasma

2.9.1. Measurement of GP120 ELISA IgG concentration by sandwich ELISA

To quantify gp120 IgG titres in the plasma from HIV-positive individuals, a Corning® high binding ELISA plate (Sigma-Aldrich®) was coated with purified envelope gp120 consensus C (kindly donated by Prof Lynn Morris, NICD, Johannesburg) at a concentration of 4µg/ml diluted in bicarbonate buffer (Sigma-Aldrich®) at 100µl per well. The plate was covered with film and incubated in the fridge at 4˚C overnight. Next, the wells were washed four times with 0.05%Tween-20 in PBS (Sigma-Aldrich®). Wells were then blocked with 100µl of 5% non-fat dry milk in PBS/0.05% Tween20 (dilution buffer) and incubated at 37°C for 1 hour. The contents from the blocking step were discarded. Next, a 3-fold serial dilution of HIV-positive plasma starting with a 1:10 dilution was carried out using the dilution buffer. Diluted plasma (50µl) was then added to the wells and plate was incubated for 1 hour at 37˚C. The wells were washed as previously with 0.05% Tween 20/PBS and 50µl of anti-human IgG-HRP (1:1000 dilution in dilution buffer; Sigma-Aldrich®) was added to each well and incubated for 1 hour at 37˚C. The wells were washed as previously and 100µl of 1-Step Ultra TMB-ELISA substrate (Thermo Fisher Scientific, Waltham, USA) was added to each well for 3-5 minutes. Development of colour was stopped by addition of 25µl of $1H_2SO_4$. The plate was read on the VersaMax® microplate (Molecular Devices) reader using the SOFTmax PRO 4.3.1 set at a wavelength of 450nm.

2.9.2. Profiling of HIV-1 specific antibodies by Western Blot

Western blot analysis was carried out on the HIV-positive samples using the genetic systems (GS) HIV-1 Western Blot kit (Bio-Rad, California, USA). The kit provided nitrocellulose strips onto which HIV-1 proteins fractionated by SDS gel electrophoresis and trans-blotted, and the proteins were resolved into bands according to their molecular weight. In this study, the nitrocellulose strips with immobilised HIV proteins were reacted with plasma from HIV-infected individuals. If HIV-specific antibodies are present in the plasma samples, they bound to their corresponding viral protein bands which were visualised using phosphatase-labeled goat anti-human immunoglobulin conjugate, followed by a substrate for the enzyme. Recognised HIV-1 viral proteins produce bands at the proteins indicated in Figure 2.2.

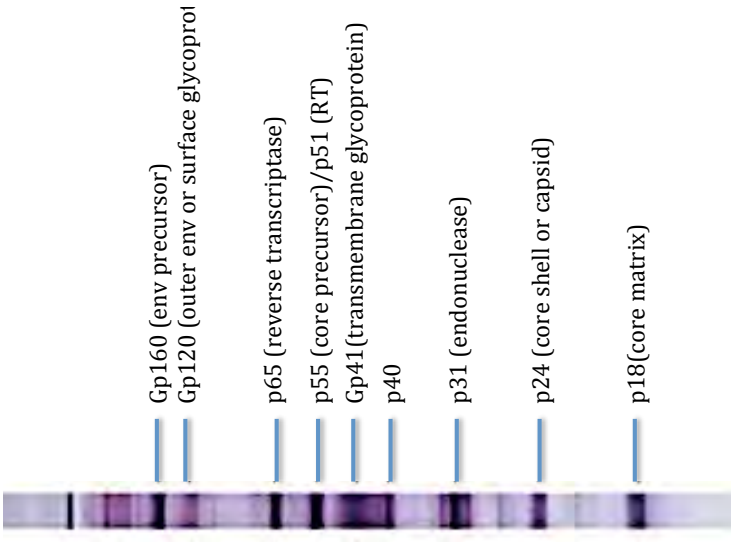

Figure 2.2. Western blot strip showing the position of each HIV protein band reacting to plasma from an HIV-seropositive individual. Three envelope proteins (gp120, gp160 and gp41), three reverse transcriptase proteins (p65, p51 and p31) and four poly-proteins (p55, p51, p40 and p18) can be resolved using this kit (taken from www.bio-rad.com).

According to the manufacturer, the specimen diluent/wash buffer provided in the kit was diluted 1:5 with deionised water. Specimen/diluent wash (1ml) was added to each tray (provided with the kit) with one tray per sample being tested. Plasma samples (10µl) from each HIV-infected individual were then loaded into the tray. Using a clean forceps, one western blot strip was put into each trough, immersed in the specimen/diluent wash, and incubated for 65 min at RT on a 96-well plate shaker (Labnet). Samples were carefully aspirated using a Pasteur pipette and washed four times with the specimen diluent/wash buffer. Anti-human IgG, IgA and IgM (goat) alkaline phosphatase conjugate solution was added to the strips immediately after the fourth wash and incubated for 50 min at RT on a plate shaker. Next, samples were aspirated; the strips washed and soaked using deionised water for 6 min on a plate shaker.

The deionised water was aspirated completely from each trough. Color development reagent (5-bromo-4-chloro-3-indolyl phosphate) was added for 4 min at RT and the tray was gently rocked back and forth twice. Aspirating the color development reagent and adding deionised water for 10 min stopped the reaction. The strips were allowed to air dry away from direct light to avoid fading before reading the bands. To compare the band intensity of the proteins, the strips were scanned into the computer and analyzed using UVIband (UVITEC, Cambridge, UK).

2.10. Measurement of NK cell direct killing of K562 cells

The ability of NK cells to kill target cells directly was investigated using two high-throughput approaches that measured properties of the target cells. GranToxilux assay is a flow cytometry based approach that measures granzyme B activity (Pollara et al., 2011). The PanToxilux assay, a more recent variation of the GranToxilux assay, measures both granzyme B and caspase activity (Packard et al., 2007).

2.10.1. Preparation of NK effector cells

Prior to the GranToxilux or PanToxilux assays, PBMCs from the HIV-negative donors (section 2.3) were thawed (section 2.6), counted (section 2.4), adjusted to $1x10^6$ cells/ml, and rested overnight in R10 at 37°C and 5% CO_2. Immediately before the assay, PBMCs were assessed for viability and only those with >95% where used in the assay.

2.10.2. Preparation of K562 target cells

Prior to the assay, a sub-passage of K562 cells was made to ensure that the cells were >95% viable and in logarithmic phase of growth. The GranToxilux assay kit provides a TFL4 red fluorescent probe used to label target cells, and NFL1 as a viability marker (Table 2.2; OncoImmunin Inc, Gaithersburg, MD). The manufacturer recommends that TFL4 should be optimised for the specific target cell used. To determine the optimal amount of TFL4 to use and the time required for staining, K562 cells were adjusted to $1x10^5$ cells/ml in R10 and labeled with 0.5µl or 1µl TFL4 and 1µl of the viability stain NFL1. The cells were incubated in the dark for 15 min or 30 min at RT, then washed twice with wash buffer. The cells were resuspended in wash buffer and approximately 100 000 events were acquired using the BD LSRFortessa™.

Once the optimal concentration of TFL4 and the optimal staining time had been determined, control tubes for the experiment were setup. Since the GranToxilux and PanToxilux assays do not require compensation because of the non-overlapping spectral properties of the fluorochromes used (APC, PacBlue and FITC), these control tubes were used to set the flow cytometry channels and to determine the background activity. Briefly, $1x10^5$ K562 cells were labeled with TFL4, 1µl NFL1 and 75µl of either the GranToxilux substrate (a substrate for granzyme B) or PanToxilux substrate (a substrate for granzyme B and caspase), which are both detected in the FITC channel (Table 2.2). The following set up tubes were used in each experiment: (1) K562 target cells alone; (2) K562 cells with GranToxilux substrate; (3) K562 with PanToxilux substrate; (4) PBMC

effectors alone; (5) PBMC effectors with GranToxilux substrate; and (6) PBMC effectors with PanToxilux substrate. The cells were incubated at RT for 15 min and then washed as previously described. Cells were resuspended in wash buffer and approximately 100 000 events acquired using the BD LSRFortessa.

Table 2.2. Markers and fluorochromes included in the GranToxilux and PanToxilux kits

Marker	Fluorochrome	Laser	Detector
TFL4	APC	Red	640 nm/40 mW
NFL1	PacBlue	Violet	405 nm/50 mW
FITC	GzB substrate	Blue	488nm/ 20 mW
FITC	PS substrate	Blue	488 nm/20 mW

2.10.3. Measurement of NK cell direct killing with the GranToxilux and PanToxilux assays

Following channel setting of APC, PacBlue and FITC on the flow cytometry using the control tubes, an experiment was carried out to measure direct K562 target cell killing by NK cells from HIV-negative donors. K562 cells pre-labeled with TFL4 and NFL1 were combined with PBMCs adjusted to an effector to target ratio of 5:1. GranToxilux substrate (75 µl) or PanToxilux substrate (75 µl) were added to each tube. In addition three control tubes were included: (1) K562 target cells alone; (2) K562 cells with GranToxilux substrate; and (3) K562 cells with PanToxilux substrate. The cells were incubated at 37°C 5% CO_2 for 60 min. The cells were washed twice using wash buffer and resuspended in 200µl of wash buffer for acquisition. Approximately 100 000 events were acquired for K562 cells only, and the whole sample was acquired of the K562 and PBMC mixture (~500 000 events) using the BD LSRFortessa. The data obtained was then analyzed using FlowJo software (version 9.7.5; Treestar; Ashland, OR).

2.11. Measurement of NK cell ADCC killing of CEM.NKR$_{CCR5}$ cells

Next, the GranToxilux and PanToxilux assays were optimised to investigate HIV-specific ADCC activity using CEM.NKR$_{CCR5}$ target cells.

2.11.1. Preparation of NK effector cells

Cryopreserved PBMCs from (section 2.5) were used as the source of the NK cells. The day before the ADCC assay was to be performed, frozen PBMCs were thawed (section 2.6), counted (section 2.4.2), adjusted to 1x10^6/ml, and rested overnight in R10 at 37°C and 5% CO^2. The following day, the cells were re-counted for viability and adjusted to the right concentration to obtain an effector to target ratio of 30:1 (E:T = 30:1).

2.11.2. Preparation of CEM target cells

Prior to the assay, a sub-passage of the CEM.NKR$_{CCR5}$ target cells and CEM control cells was made to ensure that these cell lines were >95% viable and in logarithmic phase of growth. To confirm CCR5 expression by CEM.NKR$_{CCR5}$ cells, they were initially stained with PE anti-human CCR5 antibody (Biolegend, San Diego, CA) and expression evaluated by flow cytometry. Three 5ml FACS tubes were prepared for this confirmatory experiment: (1) unstained CEM.NKR$_{CCR5}$, (2) CEM.NKR$_{CCR5}$ stained with PE-conjugated CCR5, and (3) CEM cells (which do not express CCR5) stained with CCR5 (as a negative control). To each tube, 1x10^5 cells CEM.NKR$_{CCR5}$ or CEM cells were added suspended in 100µl of PBS. Pre-titrated volume of CCR5-PE antibody (5µl) was added and the tubes were incubated at 4°C for 20 min. Cells were washed twice and resuspended in 200µl cellfix. The samples were acquired immediately with the BD LSRFortessa™ and analyzed using Flowjo (version 9.7.5; Treestar; Ashland, OR).

2.11.3. Coating of CEM.NKR$_{CCR5}$ target cells with HIV-1 gp120

The recombinant gp120 HIV-1 proteins representing the subtype C (a kind gift from Prof Lynn Morris from the NICD, Johannesburg) were used to coat CEM.NKR$_{CCR5}$ target cells in preparation for the ADCC assay. The amount of recombinant gp120 used to coat the target cells was determined by competitive binding of the CD4-FITC conjugated antibody (BioScience, San Jose, USA), to the CD4 receptor expressed on the surface of the CEM.NKR$_{CCR5}$ cells. Briefly, 1x10^6 CEM.NKR$_{CCR5}$ cells were incubated with serial two-fold dilutions of recombinant gp120 starting at 20µg/ml. CEM.NKR$_{CCR5}$ cells were coated in this way with recombinant gp120 for 90 min at 4°C in R10 medium. The cells were washed twice and stained with a saturating concentration of the CD4-FITC antibody for 15 min. After two washes, cells were resuspended in 200µl of cellfix. The samples were acquired using the BD LSRFortessa and analyzed using Flowjo (version 9.7.5; Treestar; Ashland, OR). The first concentration of gp120 to reduce the mean fluorescence intensity (MFI) by >50% of the uncoated CEM.NKR$_{CCR5}$ cells was chosen to coat the cells in the final assay (described in more detail in Chapter 4; section 4.2.3).

2.11.4. Measurement of NK cell ADCC activity using the GranToxilux and PanToxilux assays

To determine the optimal amount of TFL4 to use and the time required for staining, gp120 coated CEM.NKR$_{CCR5}$ cells were adjusted to 1 x 10^5 cells/ml in R10 and labeled with 0.5µl or 1µl TFL4 and 1µl of the viability stain NFL1. The cells were incubated in the dark for 15 min or 30 min at RT, and then washed twice with PBS.

After optimising the concentration of TFL4 and the time required for staining, control tubes to set the APC, PacBlue and FITC channels on the flow cytometer for both the GranToxilux and PanToxilux assays were setup. Briefly, 1x10^5 gp120 coated CEM.NKR$_{CCR5}$ cells were labeled with TFL4, 1µl NFL1 and 75µl of either the GranToxilux substrate or PanToxilux substrate, both detected in the

FITC channel (Table 2.2). Approximately $1x10^5$ CEM.NKR_{CCR5} target cells and $4x10^5$ PBMC effector cells were used giving an effector to target ratio of 5:1. The following tubes were used in each experiment: (1) CEM.NKR_{CCR5} cells alone; (2) and CEM.NKR_{CCR5} cells with GranToxilux substrate; (3) CEM.NKR_{CCR5} cells with PanToxilux substrate; (4) PBMC effectors with GranToxilux substrate; (5) PBMC effectors with PanToxilux substrate; and finally (6) PBMC effectors, CEM.NKR_{CCR5} cells and GranToxilux substrate together; and (7) PBMC effectors, CEM.NKR_{CCR5} cells with PanToxilux substrate together. The CEM.NKR_{CCR5} cells were pre-labeled with the optimal TFL4 concentration before mixing them with target cells. The plate was incubated for 15 min in CO_2 at 37°C. Cells were then washed twice in PBS by centrifugation at 2100rp for 5 min and acquired using the BD LSRFortessa. The data obtained was analyzed using FlowJo software (version 9.7.5; Treestar; Ashland, OR).

After setting up the APC, PacBlue and FITC channels, the ADCC assay was carried out. Briefly, CEM.NKR_{CCR5} cells were coated with 5µg/ml recombinant gp120 for 90 min at 4°C in RPMI, and thereafter washed using R10 by centrifugation at 887rcf for 5 min. CEM.NKR_{CCR5} cells were labeled with 1µl TFL4 and 1µl NFL1 for 15 min at 37°C in water bath and then washed twice using 10ml R10. For each assay, PBMCs and CEM.NKR_{CCR5} cells were counted using a Guava PCA counter (Guava Technologies Inc, California, USA) and adjusted to a final viable effector to target ratio of 30:1. Next, 25µl of each target ($\sim 2x10^5$) and effector ($\sim 6x10^6$) cell suspension and 75µl of the GranToxilux or PanToxilux substrate (OncoImmunin Inc, Gaithersburg, MD) were dispensed into each well of a 96-well V-bottom plate according to the manufacturer instructions. Wells containing controls as previously described were also included for this experiment. The plate was incubated at RT for 5 min. Twenty five µl of 1:1000 dilution of each plasma sample was added to the cell suspension and incubated for 15 min at RT. The plates were centrifuged for 1 min 290rcf, and incubated for 1 hour at 37°C and 5% CO_2. After washing with wash buffer (WB), cells were re-suspended in 150µl of WB and transferred to 5ml FACS tubes. The cells were acquired using the BD LSRFortessa™ and at least

500 000 events were acquired. Analysis was performed using Flowjo 9.7.5 software.

2.12. Statistical analysis

Statistical analysis was performed using GraphPad Prism (version 6.0; San Diego). The non-parametric Wilcoxon paired test was used to compare matched samples while the non-parametric Mann-Whitney U test was used to compare unmatched samples. The Bland-Altman test was used to analyze agreement between GranToxilux and PanToxilux assays. A p-value of ≤0.05 was considered significant.

CHAPTER 3

Optimising the GranToxilux and PanToxilux flow cytometry assays to measure NK cell cytotoxicity against the tumour cell line K562

3.1. Introduction

NK cells are an important component of the host innate response during both viral infections including HIV and against tumor cells (Jost and Altfeld, 2013; Valiante et al., 1997). NK cells can be subdivided into distinct populations, based on their expression of CD56, into two main subsets - $CD56^{Dim}$ and $CD56^{Bright}$. $CD56^{Dim}$ NK cells represent the majority of NK cells in blood (~90%), are potent cytotoxic cells, express high levels of perforin and granzymes and can mediate antibody dependent cytotoxicity, while $CD56^{Bright}$ NK cells represent the minor population of NK cells in blood (5-10%) and they produce cytokines such as IFN-γ upon stimulation (Cooper et al., 2001; Smyth et al., 2005). In addition to these two major subsets, other NK cell subsets have been describe which do not express CD56 (CD56-) but do express CD16 (CD16+). These NK cells only have relatively weak expression of perforin and have defect in ADCC activity (Björkström et al., 2010). They are relatively rare in healthy individuals but elevated in individuals chronically infected with HIV-1 (Lopez-verge et al., 2010; Mavilio et al., 2005; Williams, 2007).

NK cell secretory lysosomes, containing perforin and granzymes, are imperative for cytotoxicity because their release results in the induction of target cell apoptosis (Jiang et al., 2013; Krzewski et al., 2013; Smy, 2002). When NK cells degranulate and release these secretory lysosomes containing perforin and granzymes during killing, the lysosomal membranes surrounding these cytolytic proteins contains CD107a, which is expressed on the cell surface and can be used as a marker of degranulation (Krzewski et al., 2013; Penack et al., 2005). CD107a is upregulated on the surface of activated NK cells and assays to measure degranulation, based on CD107a expression, have been shown to correlate with both NK cell-mediated lysis of target cells (measured by Cr^{51}-release) and cytokine secretion (Mata et al., 2014; Wren et al., 2012).

Different approaches have been used to evaluate NK cell cytotoxicity, either directly or indirectly, allowing a comprehensive evaluation of the NK cell

function (He et al., 2013; Mata et al., 2014; Morice, 2007). The Cr^{51}-release assay is the gold standard in evaluating cytolytic effector function for NK cells (Chung et al., 2008; Mata et al., 2014; Richard et al., 2014). Recently, the GranToxilux and PanToxilux flow cytometry based high-throughput assays have been developed that measures cytotoxicity against fluorescent labeled targets, granzyme B and caspase loss or degranulation (Alter et al., 2004; Pollara et al., 2011). When evaluating direct NK cell-mediated cytotoxicity, the NK-sensitive HLA class I deficient K562 cells are traditionally used as target cells (Geiger et al., 2012; Koeffler and Golde, 1980).

The aim of this Chapter was to optimise and compare the GranToxilux and PanToxilux assays for measuring NK cell direct killing of K562 cells. In addition to optimising these assays for measurement of direct tumour cell killing, an aim of this Chapter was the selection of a suitable NK cell donor for the HIV-specific ADCC assays described in Chapter 4.

3.2. Results

3.2.1. Optimising growth of K562 target cells and staining with the nuclear marker TFL4

To ensure that the K562 target cells that will be used to measure NK cell direct killing in this study were viable and in logorithmic phase of growth during the assay, the growth kinetics of K562 cells were initially monitored for a few growth cycles prior (Figure 3.1). For this study, K562 cells were considered to be in log phase between day 11 and 15, with a viability of >95% determined by Trypan blue.

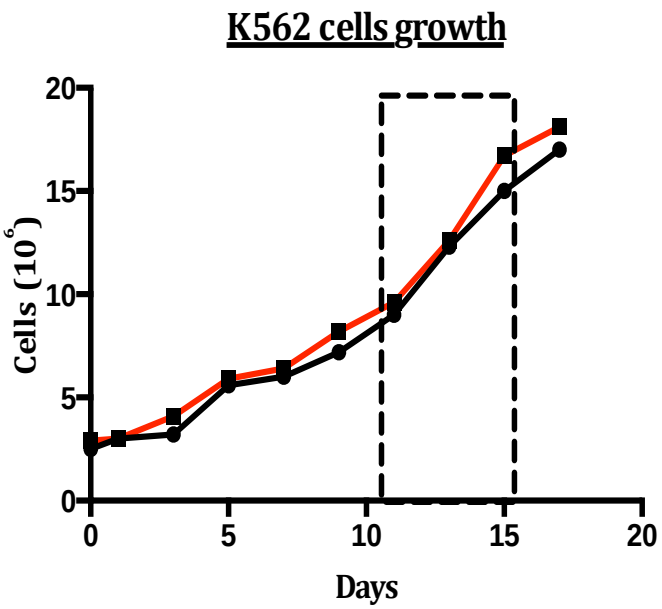

Figure 3.1. K562 cells growth kinetics. Cell numbers and viability in this experiment were counted by Trypan blue staining and manual counting. Counting was performed every day from days 1-17. The experiment was repeated twice, and the dotted lines indicate the days during which K562 cells were in log phase of growth, with viability >95%.

The TFL4 cellular fluorophore is used to label all target cells in both the GranToxilux and PanToxilux assays (Packard et al., 2007; Pollara et al., 2011). To optimise the concentration of TFL4 dye needed to label K562 target cells, cells were labeled with either 0.5µl or 1 µl TFL4 for 15 or 30 min (Figure 3.2).

Labeling K562 cells with 0.5µl TFL4 for 15 min was chosen as the optimal target cell staining conditions for further assays. The volume of the viability marker NFL1, GranToxilux fluorogenic substrate (GzB) and PanToxilux fluorogenic substrate (PS) are standard for any target cells used in the high-throughput assays.

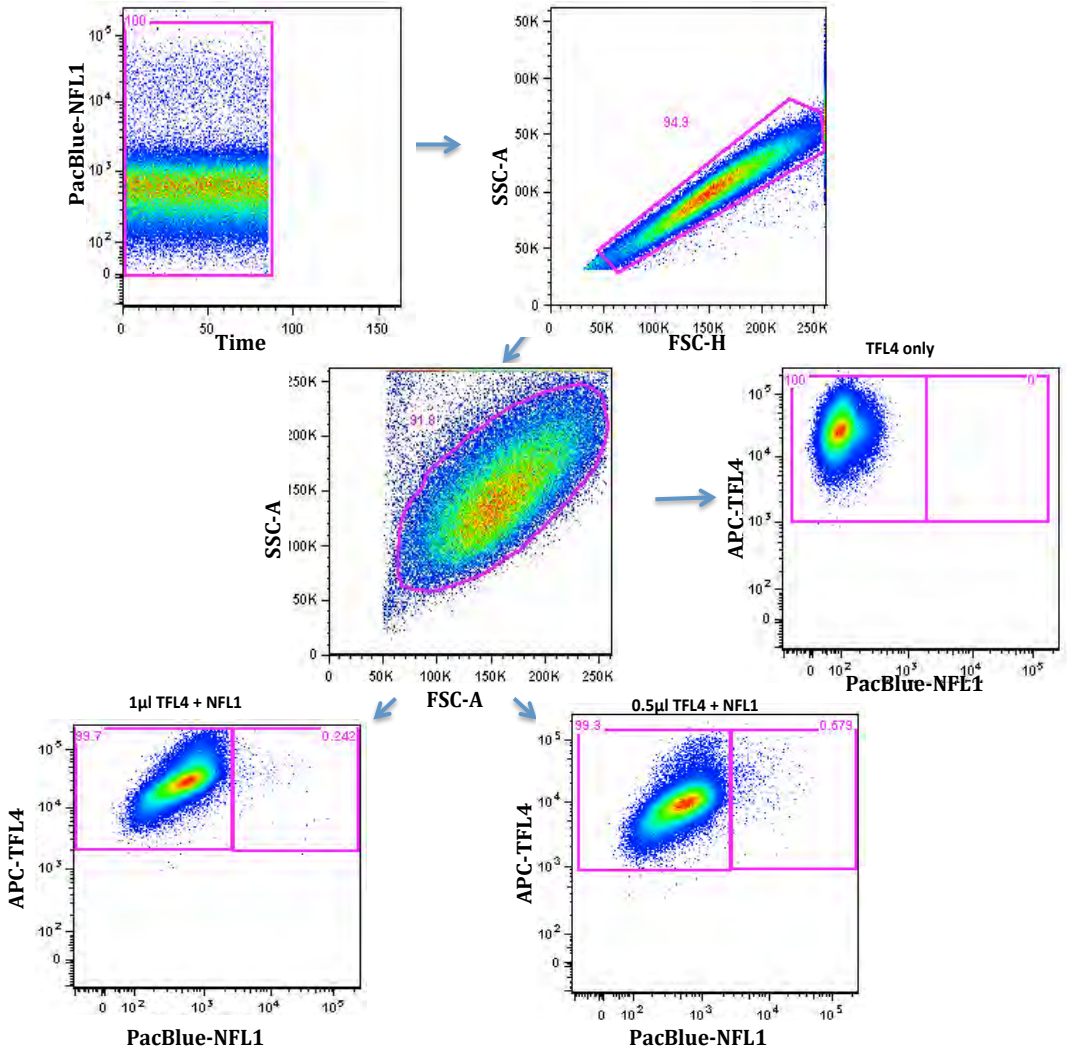

Figure 3.2. Representative flow cytometry plots showing optimisation of K562 target cell staining using TFL4 dye. Two different TFL4 concentrations (1µl and 0.5µl) and two different incubation times (15 and 30 mins) were compared for staining of K562 cells. The time gate was set to exclude any irregularities in the flow cytometer's pressure and laser output. Next, a singlets gate was set to exclude doublets. The K562 cell population was gated using the FSC-A vs SSC-A plot. Identifying the viable target population was based on TFL4 and NFL1 (viability) signals.

To set the gates for the GranToxilux and PanToxilux assays, a panel of controls were used: TFL4-K562 cells alone; TFL4-K562 with GzB substrate alone; and TFL4-K562 with PS substrate alone; PBMCs (source of NK effector cells) alone; PBMCs with GzB substrate alone; and PBMCs with PS substrate alone. The gating strategy used for the GranToxilux and PanToxilux assay is shown in Figure 3.3.

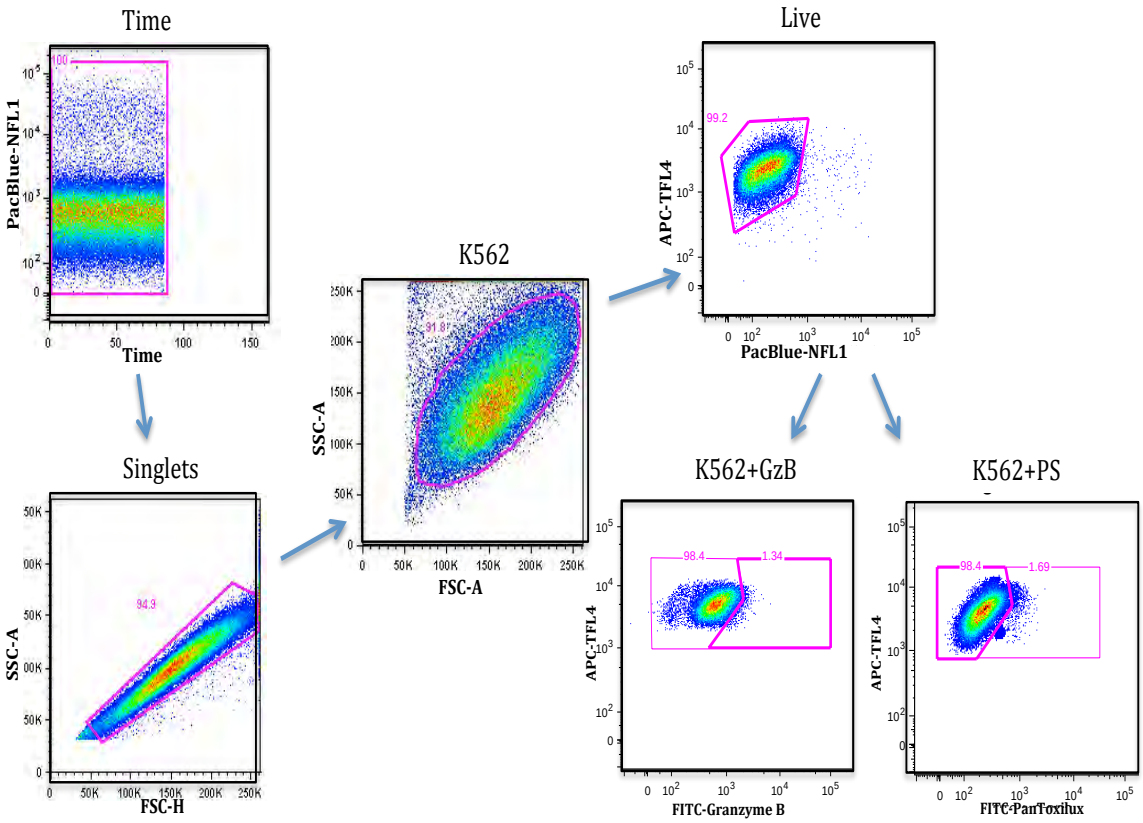

Figure 3.3. Overview of the gating strategy used for the GranToxilux and PanToxilux assays. The time and singlet gates were used to gate out irregularities in the flow and exclude doublet cells. The side scatter and forward scatter plot were used to gate out K562 cells. Viable K562 cells were identified as being TFL4+ but NFL1-. Granzyme B+ (GzB substrate for the GranToxilux assay) and dual granzyme B and caspase+ (PS substrate for the PanToxilux assay) were then measured.

3.2.2. Screening of NK cell donors for direct killing using the GranToxilux and PanToxilux assays

To select a universal ADCC effector NK cell donor for this study, eight HIV-negative samples were evaluated for NK cell activity against K562 targets. HIV-negative donors were screened as universal donors for NK cells since they do not have antibodies against HIV that could confound measurement of ADCC activity in the subsequent Chapter. Briefly, PBMCs (as a source of NK cells) were incubated with K562 target cells in presence of the granzyme B substrate (for the GranToxilux assay) or granzyme B and caspase substrate (for the PanToxilux assay) for 60 min at an effector to target ratio of 5:1. Figure 3.4 summarises the gating strategy used to measure direct killing of K562 target cells by NK cells in the GranToxilux and PanToxilux assays. The results are expressed as percentage of viable target cells staining positive for the proteolytically active form of granzyme B (for the GranToxilux)**,** or for granzyme B and upstream caspase activity (for the PanToxilux assay; Figure 3.4C). In the GranToxilux assay, granzyme B activity in the 8 donors ranged from 2.0-8.4%. The highest frequency of direct NK cell activity was detected in PBMC donor F (8.4%). In the PanToxilux assay, the frequency of granzyme B and caspase activity detected in K562 target cells ranged between 6.9-35.2%, with the highest frequencies of killing also being detected in PBMC donor F (Figure 3.4C).

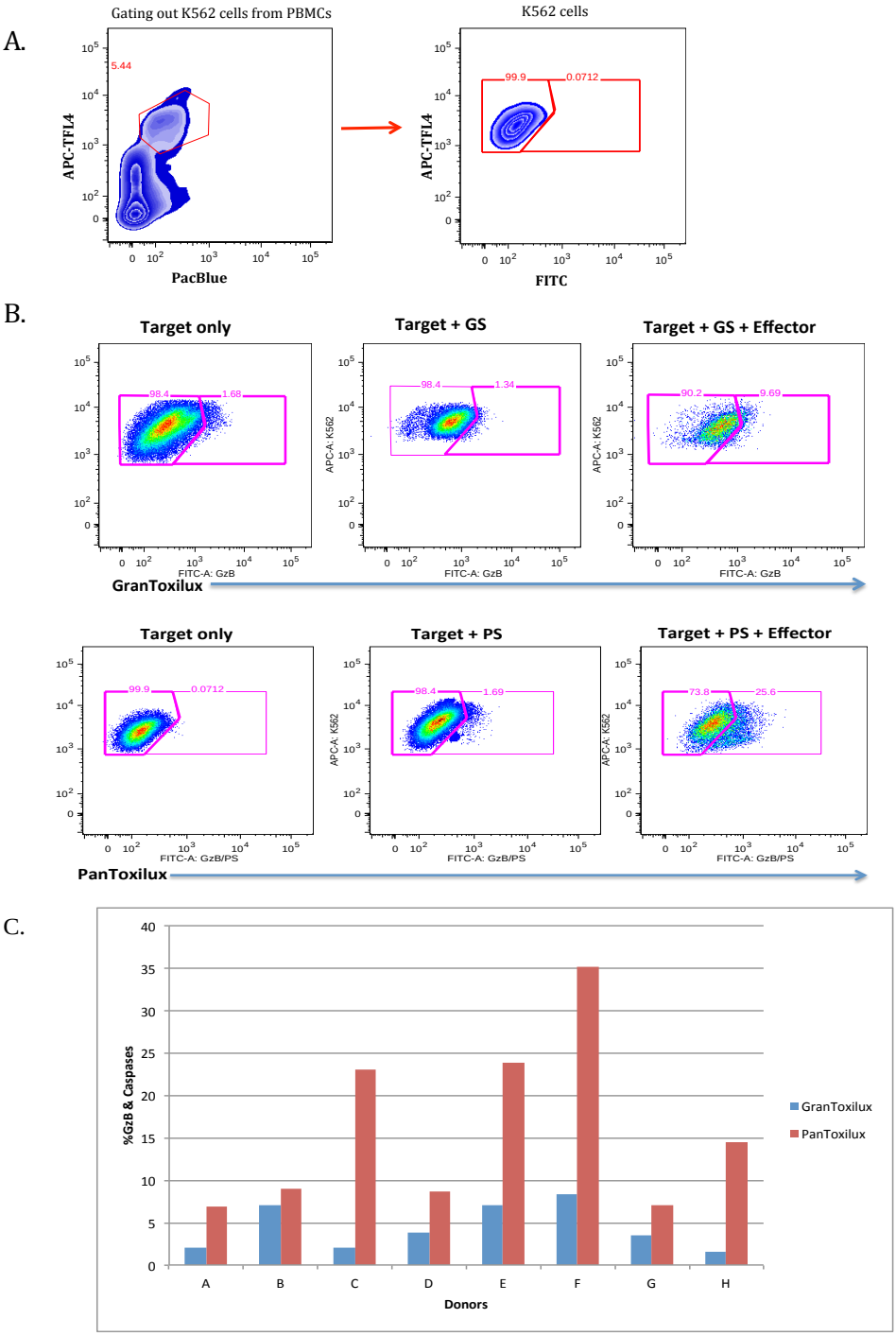

Figure 3.4. Screening for NK cell activity for direct killing of K562 target cells in the GranToxilux and PanToxilux assays from 8 HIV seronegative PBMC donors. (A) Representative flow cytometry plots showing gating strategy to identify viable K562 cells using TFL4, NFL1 and FITC markers. (B) Representative flow cytometry plots showing the gating strategy used for the GranToxilux (top row plots) and PanToxilux assays (bottom row plots). (C) NK cell frequencies of granzyme B (blue bar) and frequencies of dual granzyme B and caspase activity (red bar) across the eight donors screened. This experiment was performed only once so no error bars are shown.

Since the PanToxilux assay (measuring granzyme B and caspase activity) has been developed by the same manufacturer and marketed as a modification of the GranToxilux assay (which measure granzyme B activity alone), the two assays were compared in their ability to measure direct killing of K562 cells (Figure 3.5). All of the 8 PBMC donors showed higher direct cytolytic activity in the PanToxilux assay than the GranToxilux assay against K562 cells (p=0.007; Figure 3.5A).

A Bland-Altman statistical test was performed to evaluate whether the two assays were in agreement (Figure 3.5B). This test calculates the mean difference between two assays of measurement (the "bias'') and 95% limits of agreement as the mean difference, which is for visual judgement (Bland and Altman, 1999). If the bias is close to zero, then the assays are in agreement. This analysis showed that the two assays were not in agreement, with a bias of –11 and 95% limits of agreement from -29.82 to 6.69.

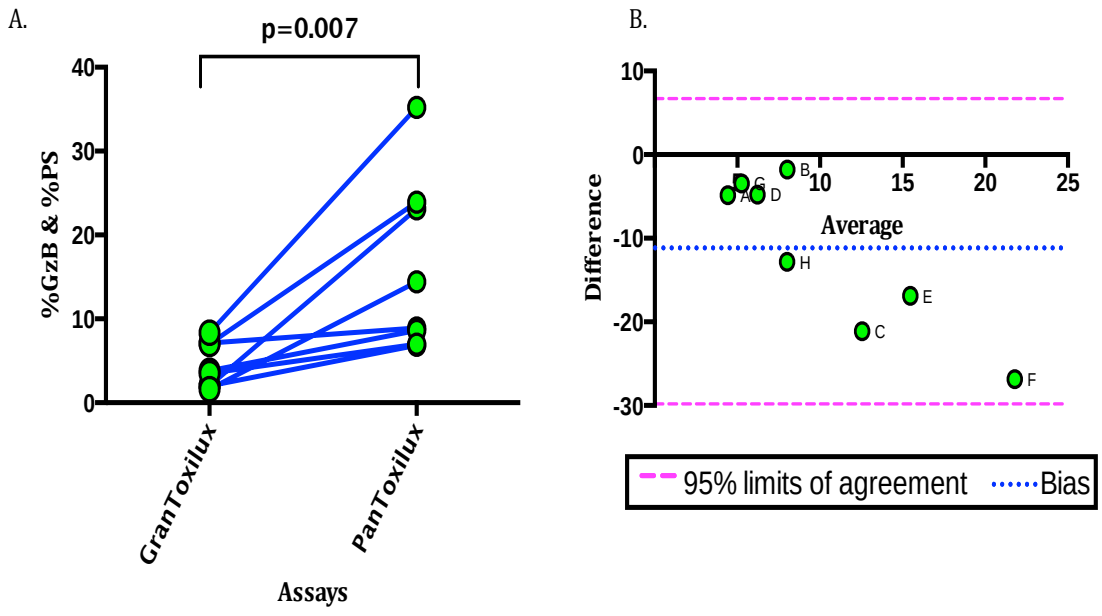

Figure 3.5. Comparison between the GranToxilux and PanToxilux assays for measuring direct NK cell killing of K562 tumour cells. (A) Paired comparison between GranToxilux and PanToxilux assays. A Wilcoxon paired test was used to compare responses in the matched analysis. P-values <0.05 were considered significant. (B) Bland-Altman plot of assessing agreement between the GranToxilux and PanToxilux assays. Each dot represents an individual NK cell donor (A-H).

3.2.3. Phenotypic and functional characteristics of NK cells from donor F

To phenotype NK cells from 3 of the 8 donors with the highest levels of direct killing against K562 cells, PBMCs from donor F, E and H were stained for the NK cell markers CD56 and CD16 and NK cell subsets evaluated by flow cytometry (Figure 3.6). $CD56^{Bright}$ CD16- NK cells have previously been reported to be the minor subset, and less cytotoxic NK cell subsets than $CD56^{Dim}$ CD16+ NK cells (Cooper et al., 2001). $CD56^{Dim}$ CD16+ NK cells are predominantly cytotoxic and comprise ~90% of human NK cells (Cooper et al., 2001). In all 3 healthy HIV-negative NK cell donors, $CD56^{Dim}$ CD16+ NK cells were the major NK cell subset, whereas $CD56^{Bright}$ CD16- NK cells and CD56- CD16+ NK cells were the minor subsets (Figure 3.6B). This is similar to previous studies showing that ~90% of NK cells in blood were $CD56^{Dim}$ CD16+ NK cells whereas only ~10% were $CD56^{Bright}$ CD16- (Bayigga et al., 2014; Björkström et al., 2010; Cooper et al., 2001). NK cells expressing the CD16 receptor (FcγRIIIa) are the major effector cells for ADCC activity (Chapter 4, Cooper et al., 2001), thus the $CD56^{Dim}$ CD16+ NK cells are the predominant NK cell subset mediating ADCC activity. Since the CD16 (FcIIIRγ) is the receptor that binds to antibody-coated target cells during ADCC, its high level of expression is positively associated with ADCC activity (Hatjiharissi et al., 2007; Jia et al., 2013), and its low level of expression has functional consequences for ADCC (Bayigga et al., 2014; Lichtfuss et al., 2011; Mandelboim et al., 1999).

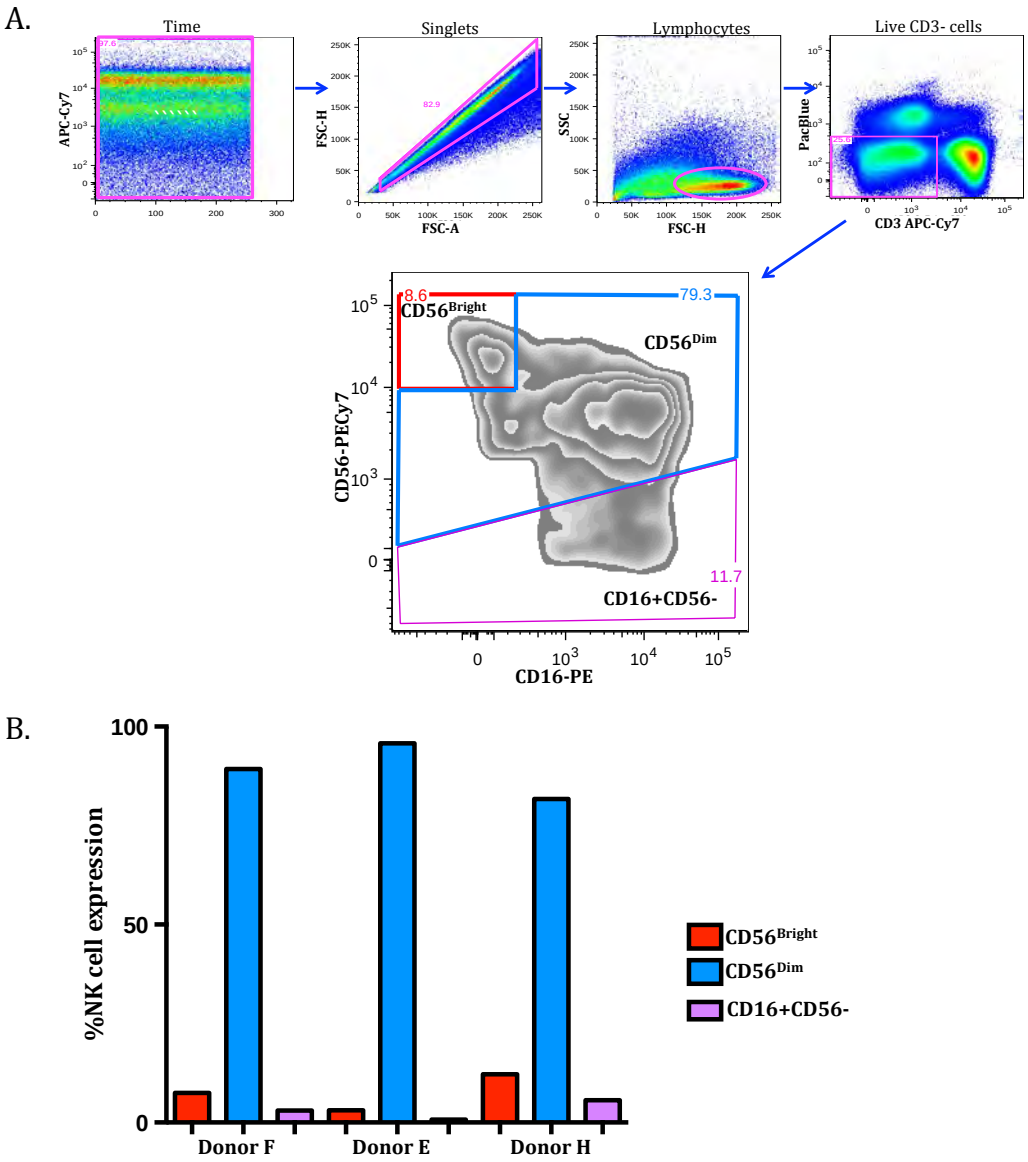

Figure 3.6. Flow cytometry analysis of CD56^{Bright}, CD56^{Dim} and CD16+ CD56- NK subsets in PBMCs from HIV-negative individuals. (A) Representative flow cytometry plot showing the gating strategy used to evaluate NK cell phenotypes. A time gate was set to exclude acquisition artefacts, followed by a singlets gate and then lymphocytes. Viable CD3- NK cells were gated on and these CD3- viable lymphocytes were then assessed for expression of CD56 or CD16. (B) Frequency distribution of NK cell subsets. This experiment was only conducted once so no error bars are shown.

To further characterise the functional ability of NK cell subsets, PBMCs from donor F were stimulated with the mitogen PHA and PMA/Ionomycin and assessed for their ability to degranulate (measured by expression of CD107a) and produce cytokines (measured by intracellular IFN-γ; Figure 3.7). The frequency of NK cells from donor F that have degranulated (expressed CD107a) following PHA-stimulation ranged from 6.0-14.0% compared to 2.0-14.0% following PMA/ionomycin stimulation. $CD56^{Dim}$ CD16+ NK cells expressed the highest frequencies of CD107a+ cells compared to $CD56^{Bright}$ and CD16+ CD56- NK cells (Figure 3.7B). The frequency of NK cells expressing IFN-γ following PHA stimulation ranged from 7.1-31.0%, compared to 1.0-4.0% following stimulation with PMA/ionomycin. $CD56^{Dim}$ NK cells were the subset most frequently producing IFN-γ following stimulation with PHA (31.0%), while $CD56^{Bright}$ NK cells were the subset most frequently producing IFN-γ (4.0%) when stimulated with PMA/ionomycin. It was interesting that more NK cells produced IFN-γ following PHA stimulation than PMA/ionomycin stimulation.

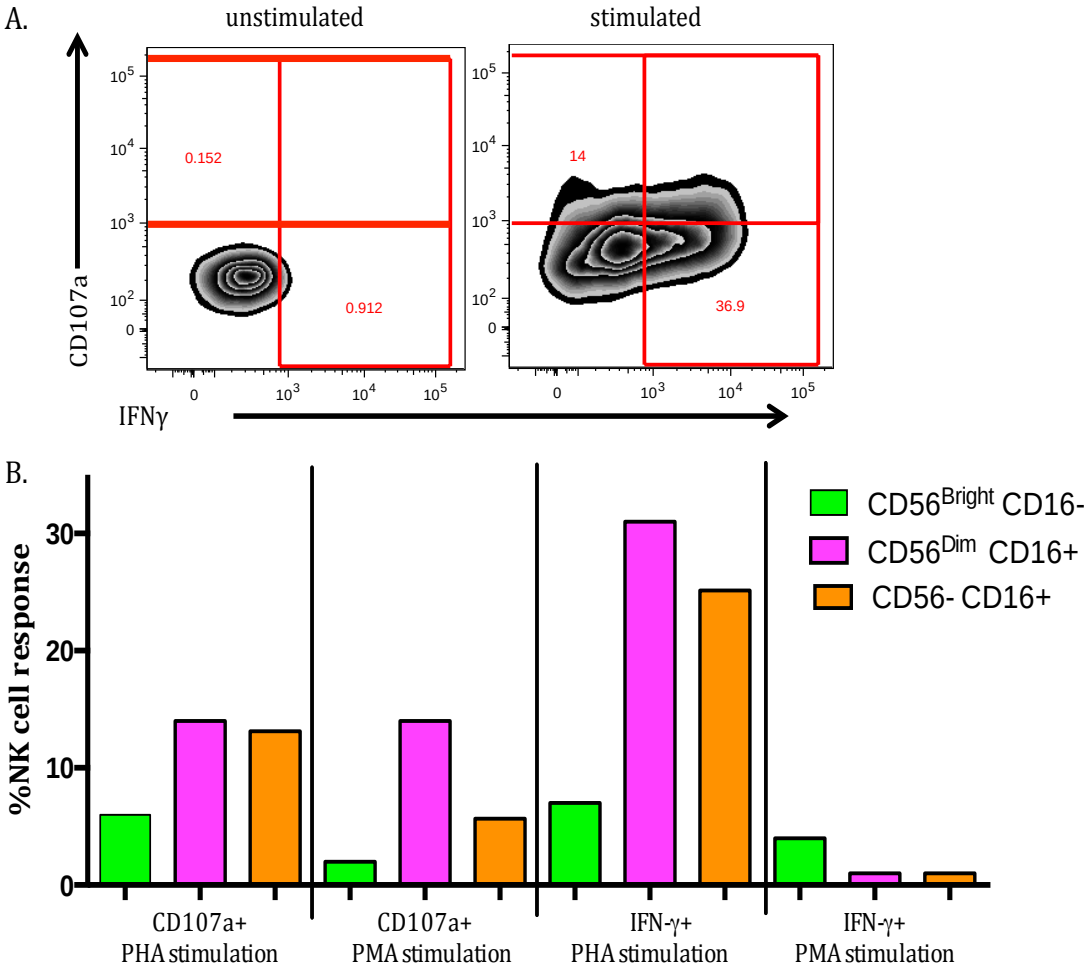

Figure 3.7. Functional analysis of NK cell subsets. (A) Degranulation was measured by the expression of CD107a on the surface of NK cell subsets, while cytokine production was measured by the intracellular expression of IFN-γ. This repesentative plot shows $CD56^{Dim}$ CD16+ NK cell subset expression of CD107a and IFN-γ before and after stimulation with PHA. Approximately 500 000 events were captured and analyzed using Flowjo. (B) NK cell subsets expression of CD107a or production of IFN-γ following stimulation with PHA or PMA/ionomycin. Results have been corrected for background measured in the unstimulated controls. $CD56^{Bright}$ CD16- NK cells are shown as green bars, $CD56^{Dim}$ CD16+ NK cells are shown as pink bars and CD16+ CD56- NK cells are shown as orange bars. This experiment was performed only once, so no error bars are shown.

3.3. Discussion

Flow cytometry based assessment of immune cell cytotoxicity allow sensitive and reliable measurement of *in vitro* cytotoxicity. Several high-throughput flow cytometry-based methods have been used for detection of NK cell activity (Alter et al., 2004; Chung et al., 2009; Gómez-Román et al., 2006; Hwang et al., 2012; Parsons et al., 2012; Thobakgale et al., 2012; Wren et al., 2012). These include the GranToxilux and PanToxilux assays that measure delivery of the cytotoxic granules and enzymes to NK target cells (Packard et al., 2007; Pollara et al., 2011). The aim of this Chapter was to optimise and compare the GranToxilux and PanToxilux assays to measure direct NK cell killing of K562 tumour target cells.

The K562 cell line has been widely used as targets in assays to measure direct NK cell killing (Alter et al., 2004; Fauriat et al., 2010; Garcia-Iglesias et al., 2009; Lichtfuss et al., 2011; Romee et al., 2013), because of their sensitivity to NK cell killing. NK cells kill by releasing cytolytic granules containing perforin and granzymes, which activates caspase activity during interaction with target cells, resulting in granzymes and caspases being detectable in the cytoplasms of the target cells (Caligiuri, 2008; Jost and Altfeld, 2013). While the GranToxilux substrate detects granzyme B activity in target cells, the PanToxilux substrate detects granzyme B and caspase activity.

HIV-negative PBMC donors were screened for selection of a suitable universal NK cell donor for optimisation of the GranToxilux and PanToxilux assays in this Chapter and for use in ADCC assays in Chapter 4. All of the 8 HIV-negative NK cell donors screened had detectable granzyme B activity in the GranToxilux assay and granzyme B and caspase activity in the PanToxilux assay against K562 cells. However, the PanToxilux assay was more sensitive than the GranToxilux assay at detecting direct killing of K562 cells in all donors, with significantly higher levels of cytotoxicity detected than against the GranToxilux assay. This is likely because the PanToxilux detects both granzyme B and

upstream caspase activity, while the GranToxilux assay detects only granzyme B activity (Packard and Komoriya, 2008). Of the 8 donors screened, PBMCs from donor F exhibited the highest frequency of killing against K562 target cells using both assays and was therefore chosen as a universal NK cell donor for the rest of this study.

Expression of NK cells phenotypic markers CD56 and CD16 and functional markers of degranulation (CD107a) and cytokine production (IFN-γ) by NK cells from donor F were investigated using flow cytometry following stimulation with mitogenic PHA and PMA/ionomycin. Like previous studies (Hubert and Amigorena, 2012; Sansoni et al., 1993; Timmons and Cieslak, 2008), $CD56^{Dim}$ were found to be the major NK cell subsets in PBMCs identified in this study, and this NK cell subset exhibited high levels of CD107a expression following stimulation. This NK cell subset has been shown to be responsible for natural cytotoxicity against tumor target cells (Penack et al., 2005). Interestingly, $CD56^{Dim}$ NK cells also expressed high levels of IFN-γ following PHA but not PMA/ionomycin stimulation, compared to $CD56^{Bright}$ NK cells, which are known to be the most potent producers of IFN-γ (Caligiuri, 2008; Cooper et al., 2001). In T cells, previous studies have reported that PHA stimulates a wider range of intracellular cytokine production than PMA/ionomycin (Baran et al., 2001). The differences observed in the expression of CD107a and IFN-γ by CD16+ NK cells following stimulation with either PHA or PMA-/ionomycin might also be attributed to the fact that PMA causes shedding or cleavage of CD16 from the cell surface, which would result in failure to detect NK cells using CD16 as a marker (Huth et al., 2014; Romee et al., 2013). While these $CD56^{Dim}$ CD16+ NK cells are the subset of most interest to this study due to their ability to mediate ADCC activity via their FcγIIIa receptor (CD16), it is notable that other subsets ($CD56^{Bright}$ and CD56- CD16+) evaluated expressed CD107a and IFN-γ.

Direct NK cell cytotoxicty against tumour or virally-infected cells is dependent on both phenotypic and functional characteristics of the cell (Biron, 2012; Cooper et al., 2001; Mandelboim et al., 1999; Morice, 2007). NK cells employ a

variety of activating receptors to kill virally infected and tumour cells. Prominent among these receptors are the natural cytotoxicity receptors (NKp30, NKp44, NKp46;De Maria et al., 2003; Garcia-Iglesias et al., 2009; Mavilio et al., 2003). NK cells expressing NKp46 were shown to be important in mediating direct killing of tumour cells (Glasner et al., 2012; Hwang et al., 2012).

A limitation of this study was that the PBMCs screened for NK cell activity using the GranToxilux and PanToxilux assays were all cryopreserved prior to testing. Previous studies have shown that cryopreserved PBMCs which are not rested overnight after thawing have decreased cytotoxic function compared to fresh PBMCs or those that have been rested appropriately after thawing (Callery et al., 1980, Strong et al., 1982, Hirsen et al., 1983). However, PBMCs for this study were thawed the day before the GranToxilux and PanToxilux assays were performed and allowed to rest overnight to allow cells to recover cytolytic functions and for cells destined for apoptosis to die. More recent studies have demonstrated that cryopreservation of PBMCs do not affect cytotoxicity if they are allowed to rest in media for more than 5 hours to recover cytotoxic function (Gómez-Román et al., 2006; Mata et al., 2014; Pollara et al., 2011). In these more recent studies, NK cells obtained from cryopreserved PBMCs were found to mediate significantly higher cytolytic activity compared to those obtained from fresh PBMCs (Mata et al., 2014). Although the focus of this Chapter was selection of a universal NK cell donor to use in subsequent HIV-specific ADCC assays (Chapter 4), another possible limitation was that universal NK cell donor selection was based on measuring direct NK cell killing which may not completely reflect their cytolytic function in ADCC assay.

In summary, two high-throughput assays for measuring NK cell-mediated direct cytotoxicity against a tumour cell line K562 were optimised and compared in this study. The GranToxilux and PanToxilux assays differed in their ability to detect NK cell direct killing of K562 target cells, with the PanToxilux assay (measuring granzyme B and caspase activity) proving to be more sensitive than

the GranToxilux assay (which measures granzyme B alone). In addition, a universal NK cell donor (donor F) was selected for subsequent experiments in Chapter 4 on the basis that this donor exhibited the highest granzyme B and caspase activity against K562 target cells of the 8 donors screened. $CD56^{Dim}$ NK cells from this donor were shown to produce IFN-γ and degranulate, measured by expression of CD107a, a good marker for cytolytic activity mediated directly or via ADCC.

CHAPTER 4

Optimisation and comparison of the GranToxilux and PanToxilux assays to measure HIV-specific ADCC

4.1. Introduction

Although several different assays have been used over the years to measure ADCC activity, these have traditionally made use of radioactivity (Chung et al., 2008; Gómez-Román et al., 2006; Karnasuta et al., 2005) and the majority are labour intensive and not suited to high-throughput screening of ADCC applicable such as in large HIV trials (Alpert et al., 2012; Chung et al., 2008; Larson et al., 2011). High-throughput non-radioactive assays have been developed recently that are less labour intensive, and these include the GranToxilux and PanToxilux assays . The GranToxilux assay measures the number of target cells into which granzyme B has been delivered (Pollara et al., 2011), while the PanToxilux assay measures both granzyme B and caspase activity within target cells (Kute et al., 2012). The GranToxilux assay was intended as an assay which detects cytotoxicity (Packard et al., 2007). Pollara et al. (2011) subsequently modified and optimised it to detect cytotoxicity mediated by HIV-specific antibodies. To my knowledge, there are currently no published studies using the PanToxilux assay to measure HIV-specific ADCC responses. Therefore, the same modifications applied to the GranToxilux assay by Pollara et al. (2011) were used to optimise the PanToxilux assay in this study.

One of the challenges of studying ADCC during HIV infection has always been choosing the most appropriate way to express HIV antigens on the surface of target cells and the best target cells to use (Stratov et al., 2008; Wren et al., 2013). Several studies have used HIV-infected CD4 T cells as targets in the ADCC assay (Davis et al., 2011; Isitman et al., 2011; Pegu et al., 2013; Smalls-Mantey et al., 2012; Tomaras et al., 2013), while others have used immortalised cell lines coated with recombinant HIV proteins (Ahmad et al., 2001; Chung et al., 2008; Pollara et al., 2011; Trkola et al., 1999). Choice of ADCC target cells and HIV antigens are likely to influence what is being measured, as target cells need to be coated with the right HIV epitopes to be recognised by ADCC antibodies. Most HIV-specific antibodies that mediate ADCC that have been identified thus

far have been directed against specific epitopes within HIV-1 envelope proteins gp120 and gp41 (Table 1.2; Pollara et al., 2013; Srisurapanon et al., 2005).

In this Chapter, the immortalised cell line CEM, stably transfected with CCR5 (CEM.NKR$_{CCR5}$ cells), were used as target cells as they can be either infected directly with HIV or coated with recombinant gp120 to measure ADCC. The aim of this Chapter was to optimise and compare the GranToxilux and PanToxilux assays for measuring ADCC activity to HIV.

4.2. Results

4.2.1. Clinical characteristics of HIV-infected individuals used for antibodies

Nine HIV-positive women were included in this study as the source of HIV-specific antibodies. These chronically infected women were healthy despite having been infected with HIV for >5 years, maintaining CD4+ T cell counts >300cells/µl in absence of HAART. Two of the women maintained viral loads <50 RNA copies per ml and were likely to be considered to be HIV controllers. In addition, plasma from 6 HIV-negative women were included as a negative controls. Table 4.1 summarises the clinical characteristics of the HIV-positive women in this study.

Table 4.1. Clinical descriptions of the HIV-positive women

	Age	Duration of HIV-1 infection at enrollment	HIV-1 load	CD4 count
PID	**(Years)**	**(Months)**	**(RNA copies/ml)**	**(cells/µl)**
NY010	41	60	<50	334
NY040	41	78	7200	322
NY064	27	84	930	383
NY094	38	72	1700	465
NY099	26	66	10000	525
NY100	33	78	53000	778
NY219	33	78	16000	551
NY234	35	72	2600	680
NY292	42	108	<50	529
Median [CI]	35 [33:41]	78 [72:78]	2600 [930:10,000]	525 [383:551]

[a] **PID (Participant Identification); CI (Confidence Intervals)**

4.2.2. Measurement of HIV-1 specific antibody titres

The titre of HIV-specific antibodies against gp120 were measured in plasma from 9 HIV-infected and 6 HIV-negative women by ELISA (Figure 4.1). Plasma from HIV-negative women were included as negative controls. The HIV-positive individuals had significantly higher HIV gp120-specific antibodies than HIV-negative individuals (at 1:100 plasma dilution, p=0.0004; at 1:1000 plasma dilution, p=0.0007). All HIV-infected individuals had detectable IgG responses to HIV gp120 and were therefore suitable for testing the ability of this sera to mediate ADCC activity against CEM.NKR$_{CCR5}$ target cells.

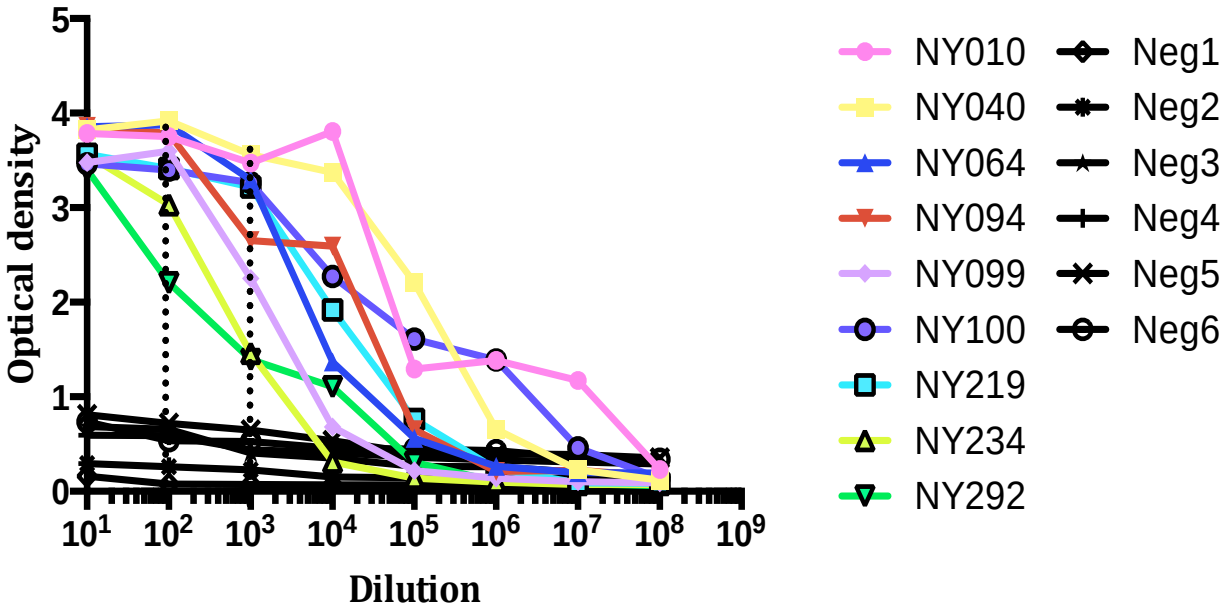

Figure 4.1. Measurement of gp120 specific IgG titres by ELISA in plasma from HIV-positive and HIV-negative individuals. The different colour curves represent plasma IgG titres for the HIV-positive individuals while the black curves represent plasma titres for the HIV-negative samples. Plasma was diluted using a 10-fold serial dilutions. The OD wavelength used was 450nm. Titers in HIV-positive plasma differed significantly from HIV-negative plasma at 1:100 and 1:1000 dilutions, indicated in the figure by the dotted lines.

To further characterise the breadth of HIV-specific antibodies in the HIV-positive women plasma samples, HIV-specific western blot analysis was carried out (Figure 4.2). In addition to gp120-specific antibodies, the western blots show that all 9 HIV-positive plasma samples had antibodies binding to gp160,

p65, p55/51, p41, p40, p31, p24 and p18 (Figure 4.2), while plasma from the HIV negative individual tested did not bind. By western blot, the most strongly recognised protein in all HIV-positive plasma samples was gp160 and gp41 followed by p24 and p55/51. Densitometry values of the protein band intensities was measured using Uviband software (UVItec, UK), and relative density of recognition of each HIV protein was expressed as a ratio to the most abundent protein recognised, gp160 (Figure 4.2B). The ratio of gp120:gp160 was a median of 0,90 (1,05-0,80) in the HIV-positive samples screened. This analysis confirmed that the HIV-positive plasma samples chosen to optimise the GranToxilux and PanToxilux assays had binding antibodies to gp120 as well as other HIV antigens.

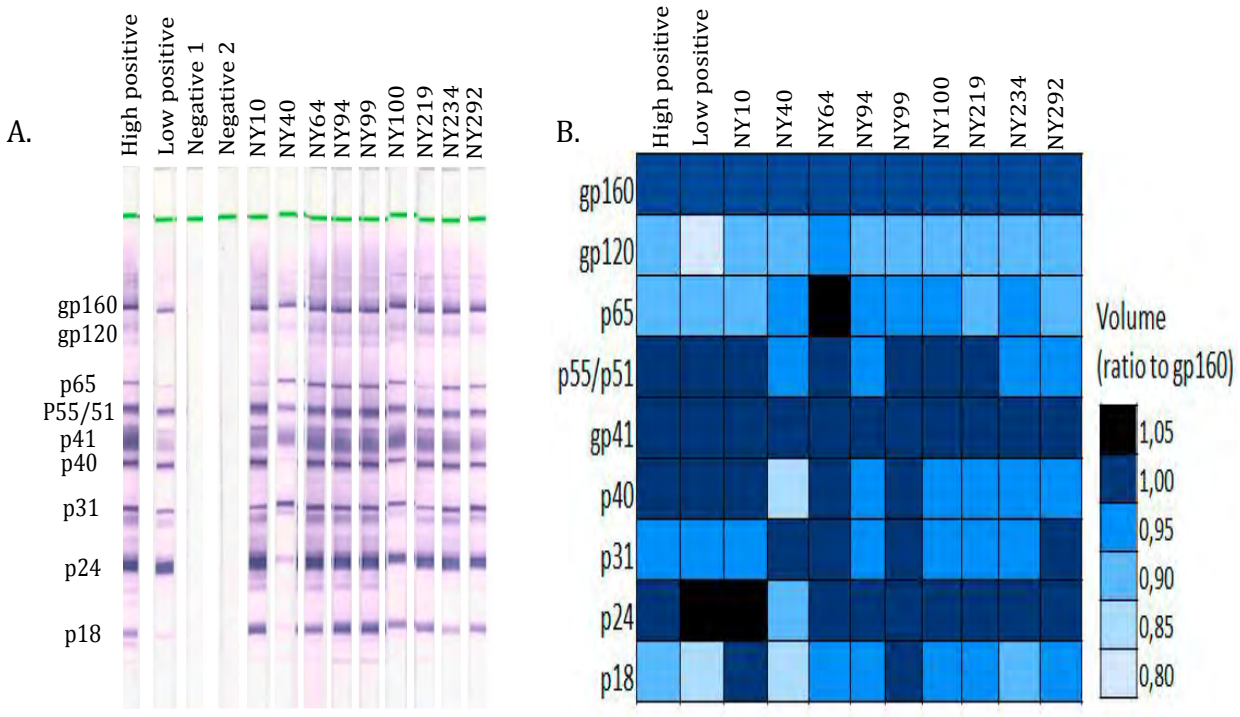

Figure 4.2. Western blot profiling of HIV proteins recognised by plasma from HIV-infected and HIV-negative individuals. From left to right (A) Blot 1 is a high positive control (provided with the kit), blot 2 is a low positive control (provided with the kit), blot 3 is a negative control (provided with the kit) and blot 4 is one of the six HIV-negative plasma sample. Blots 5-13: Plasma samples from HIV-infected women. (B) Heatmap showing the relative abundence of HIV-specific antibodies recognising different HIV proteins, compared to gp160, in the HIV-positive plasma.

4.2.3. Preparation of target and effector cells for ADCC assays

4.2.3.1. Optimisation of gp120- coating of CEM.NKR$_{CCR5}$ cells

To ensure that the CEM.NKR$_{CCR5}$ cells used in the GranToxilux and PanToxilux ADCC assays were viable and in the logarithmic phase of growth, growth kinetics of the cells were monitored for a few growth cycles prior to setting up the experiments (Figure 4.3). CEM.NKR$_{CCR5}$ cells grew more rapidly than K562 cells (Chapter 3), used to measure direct killing by NK cells. CEM.NKR$_{CCR5}$ cells were considered to be in the log phase at around day 6 of culture and showed good viability (>95%) and were used in all subsequent experiments in this phase.

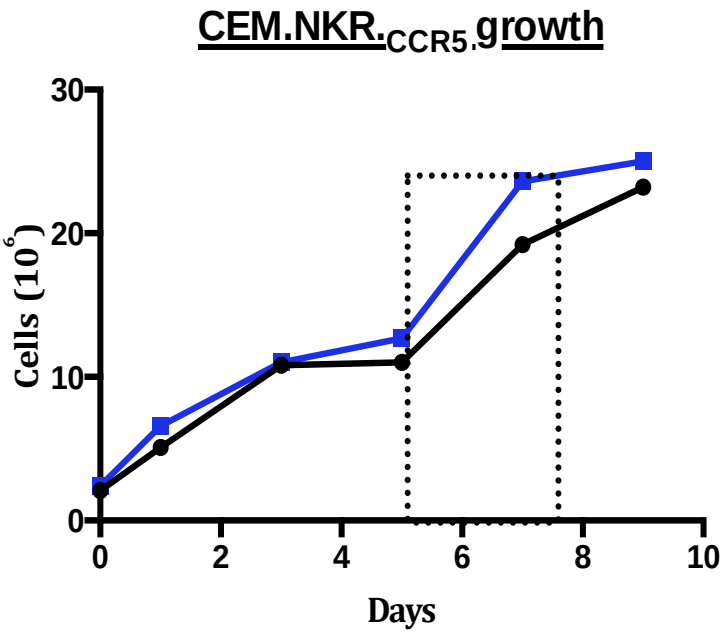

Figure 4.3. Measurement of CEM.NKR$_{CCR5}$ cells growth kinetics. Cell numbers and viability in this experiment were counted by Trypan blue staining and manual counting. Counting was performed at days 1 until 9. Two independent experiments were carried out, indicated by the different colour lines. The dotted box indicates the days of culture considered to represent CEM.NKR$_{CCR5}$ cells in log phase when viability was >95%. The black line is the first experiment of labeling CEM.NKR$_{CCR5}$ cells, while the blue line is the growth of cells used for the ADCC experiments.

CEM.NKR$_{CCR5}$ cells have been transfected to stably express the HIV-1 co-receptor CCR5 on their cell surface (Trkola et al., 1999). To confirm that the CCR5 receptor was expressed by the CEM.NKR$_{CCR5}$ cells used in these experiments, cells were initially stained with PE anti-human CCR5 antibody (Figure 4.4). The majority of CEM.NKR$_{CCR5}$ cells (99.3%) expressed CCR5 on their cell surface. In addition to CEM.NKR$_{CCR5}$ cells, CEM cells were also included as a negative control target cell line. CEM cells do not express CCR5 (Gervaix et al., 1997) and this was confirmed by flow cytometry (Figure 4.4).

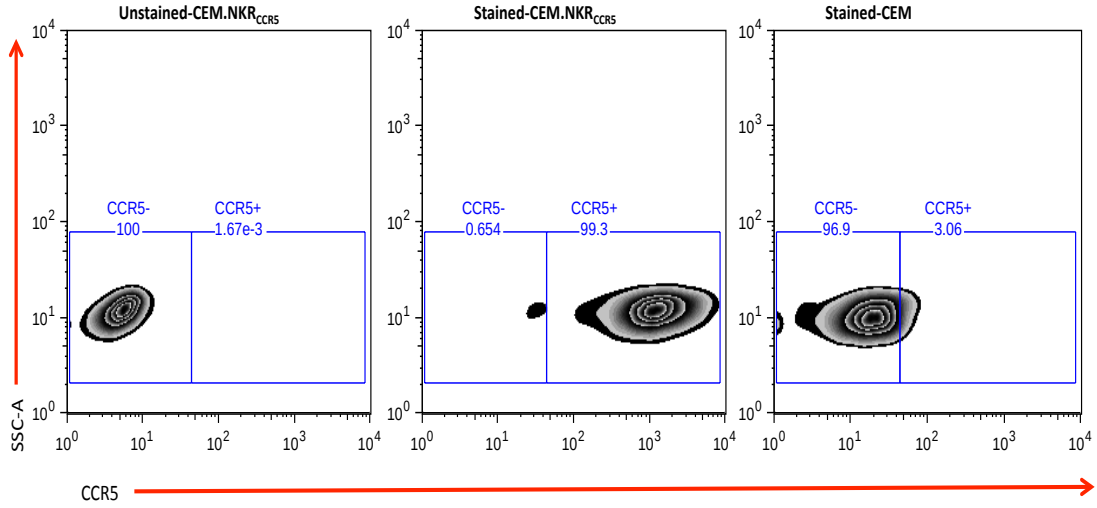

Figure 4.4. Measurement of cell surface expression of CCR5 by CEM.NKR$_{CCR5}$ and CEM cells. The cell lines were examined for stable surface expression of CCR5 by flow cytometry. Approximately 100 000 events were captured and CCR5 expression by these cells was assessed using Flowjo. The negative and positive gates were set using the unstained control.

After determining the expression of CCR5 on CEM.NKR$_{CCR5}$ cells, the optimal amount of recombinant gp120 to coat the CEM.NKR$_{CCR5}$ cells was determined by competitive staining of CD4 on the cell surface of CEM.NKR$_{CCR5}$ cells (according to the method described by Pollara et al., 2011). CEM.NKR$_{CCR5}$.cells were coated with varying amounts of gp120 to block the CD4 receptor, and then subsequently labeled with a standard saturating concentration of CD4-FITC (Figure 4.5). The concentration of gp120 that reduced the CD4 median fluorescence intensity (MFI) of unstained CEM.NKR$_{CCR5}$ cells by ~50% was chosen as the optimal concentration to coat CEM.NKR$_{CCR5}$ cells. This was determined to be 5µg HIV subtype C gp120. From this point forward, all the

CEM.NKR$_{CCR5}$ cells used in all experiments were coated with 5µg gp120 for use in the ADCC assays.

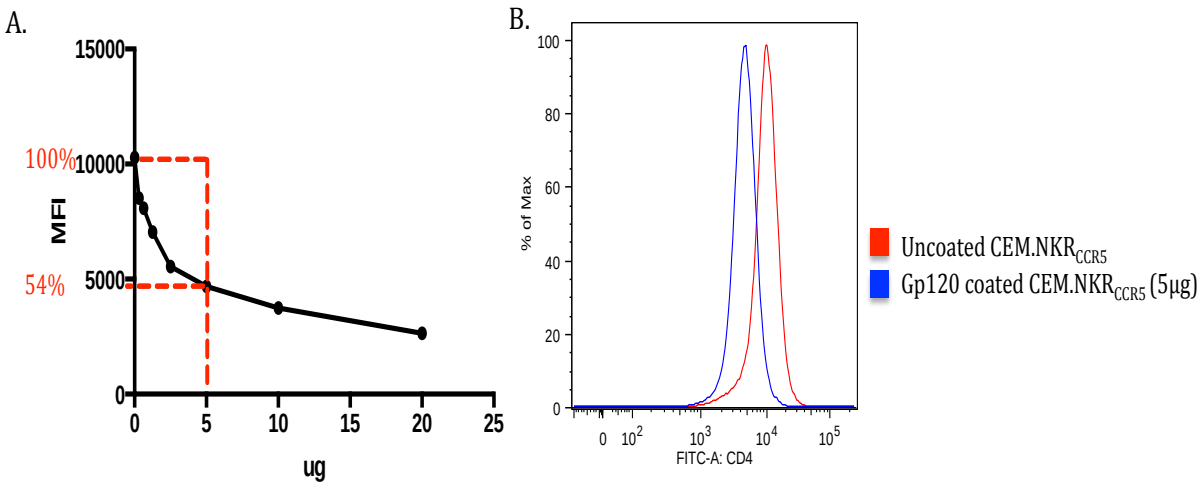

Figure 4.5. Titration of recombinant gp120 for coating CEM.NKR$_{CCR5}$ cells in order to block CD4 antibody binding in the ADCC assay. (A) Impact of recombinant gp120 coating at varying concentrations (20, 10, 5, 2.5, 1.25, 0.625 and 0.3125 µg) on changes in CD4-FITC staining, measured by changes in MFI relative to uncoated CEM.NKR$_{CCR5}$ cells. Five µg (at the dotted red line) reduced the CD4-FITC (100%) MFI by 54%. (B) Histogram overlay of uncoated and gp120 coated (5µg/ml) CEM.NKR$_{CCR5}$ cells.

4.2.3.2. Optimisation of TFL4 target cell fluorescent marker

For CEM.NKR$_{CCR5}$ cells, the amount of TFL4 needed to stain target cells with was initially optimised. TFL4 is a red fluorescent marker which labels the target cells before co-incubating them with the NK effector cells. Although TFL4 concentrations were optimised for K562 cells (Chapter 3), the amount of TFL4 needed to be optimised for CEM.NKR$_{CCR5}$ cells because each cell line has slightly differing growth kinetics, metabolism and morphology, and hence dye permeability might differ. Optimisation of the TFL4 marker was carried out similarly to the K562 cells. Briefly, 1x10^6 gp120 coated CEM.NKR$_{CCR5}$ cells were put into wells with either 0.5µl or 1µl TFL4 for 15 min or 30 min (Figure 4.6). The optimal condition of TFL4 chosen was labelling CEM.NKR$_{CCR5}$ cells with 1µl TFL4 for 15 min. At this concentration, CEM.NKR$_{CCR5}$ cells appeared as a single population and there was no cell spread compared to the other incubation conditions.

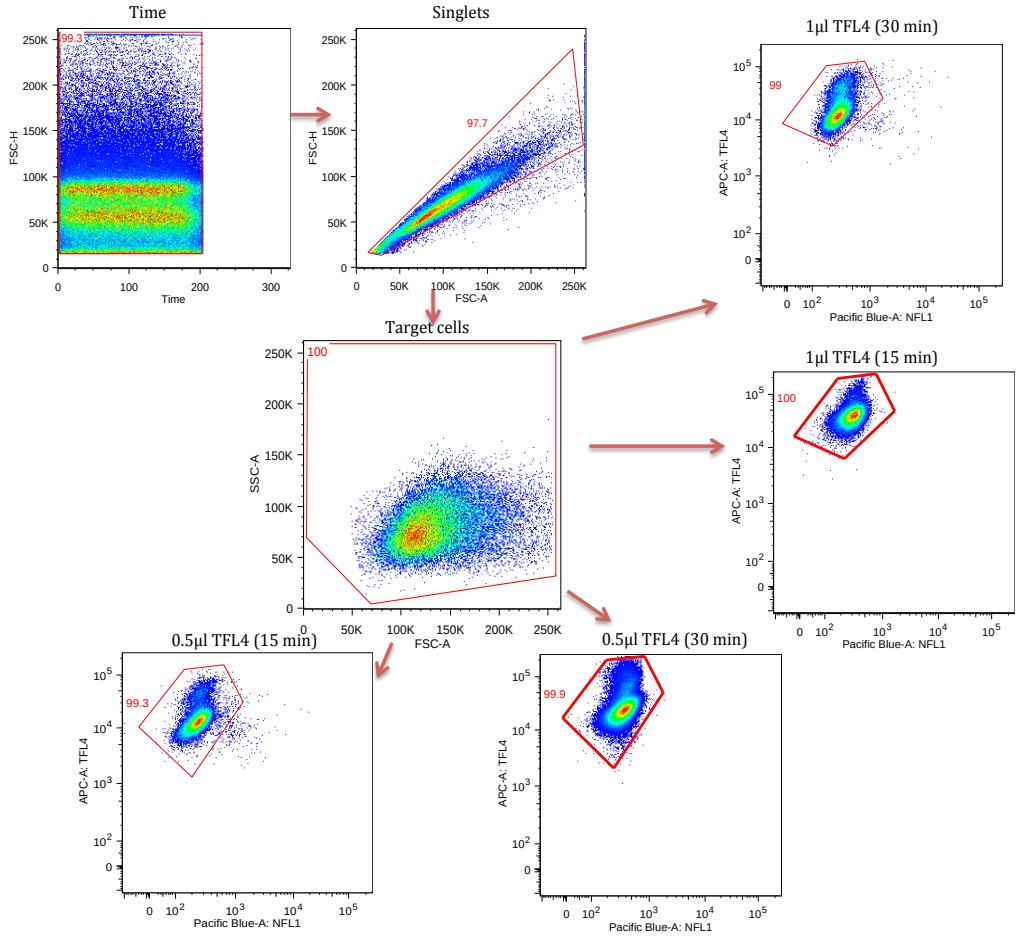

Figure 4.6. Optimisation of TFL4 staining of gp120-coated CEM.NKR$_{CCR5}$ cells. A time gate was set to exclude any technical irregularities, followed by a singlets gate to exclude doublet cells. Viable CEM.NKR$_{CCR5}$ cells were gated by combining staining for TFL4 and NFL1 (viability) marker signals. A total of 100 000 events was captured. Gating and analysis was performed using Flowjo.

4.2.3.3. Optimisation of effector to target ratios

It was necessary to optimise the effector to target ratio to ensure acceptable background and noise signal ratios for the differing substrates used in the GranToxilux and PanToxilux assays. To do this, the ratio of effectors:targets ranging from 5:1 to 30:1 were investigated (Figure 4.7). In both the GranToxilux and PanToxilux assays, 30:1 effector:target ratio gave the lowest background fluorescence of 0.96% and 1.59% respectively, compared to the other ratios tested (Figure 4.7B). Morever, this ratio has been reported to allow sensitive detection of ADCC responses in HIV-1 infected individuals in previous studies (Pollara et al., 2011).

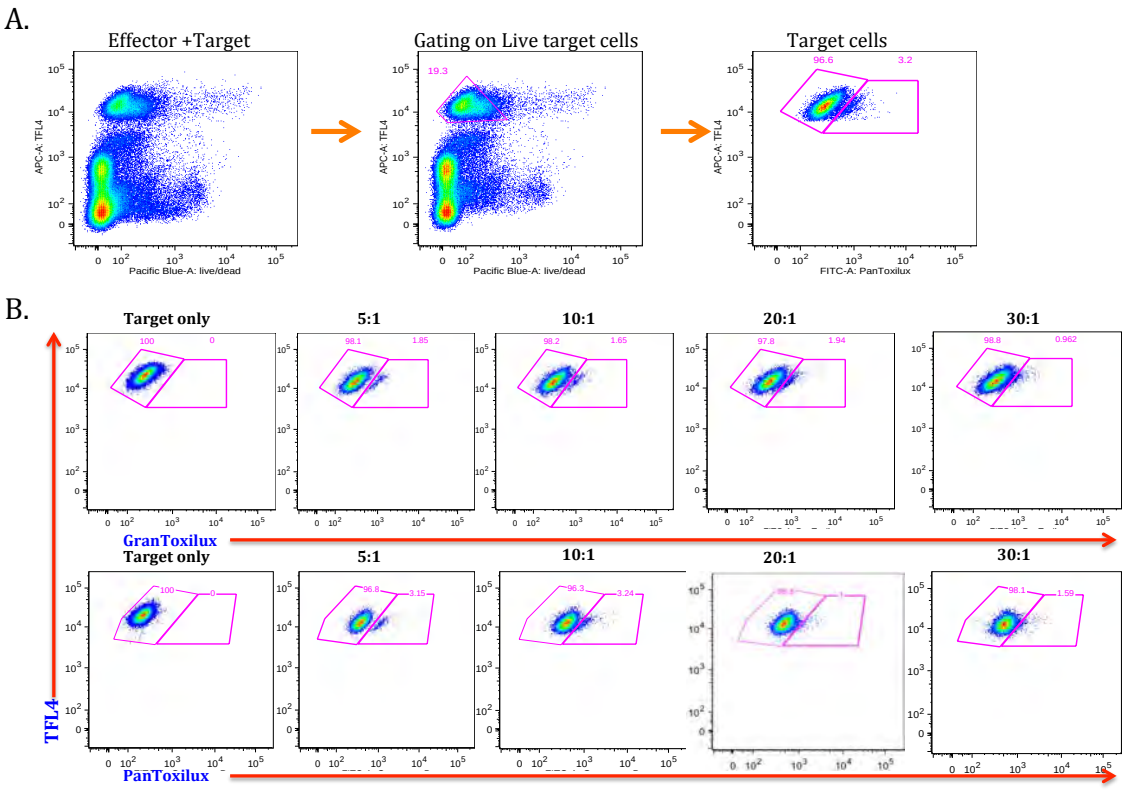

Figure 4.7. Optimisation of effector:target ratios of the GranToxilux and PanToxilux assays. Approximately 500 000 events were captured and analyzed using Flowjo. (A) From the combined effector and target cell population in plot one, viable target cells were gated out in plot two, using TFL4 and NFL1 signals. Plot three is gating on the target cells by combining TFL4 and FITC signals to look at granzyme B and caspase activity. (B) The first row is the GranToxilux assay using different effector to target ratios (5:1-30:1) in addition to the granzyme B substrate. The second row is the PanToxilux assay using different effector to target ratios (5:1-30:1), in addition to the granzyme B and caspases substrate.

4.2.3.4. Optimisation of HIV-positive plasma dilutions

To optimise the concentration of HIV-positive plasma to use as a source of HIV-specific antibodies, plasma from two chronically HIV-infected women (NY040 and NY094; Table 4.1) were used. A series of 10-fold HIV-positive plasma dilutions was carried out using the same HIV-negative NK cell donor (donor F, section 3.3.3; Chapter 3) to determine the optimum plasma dilution to use in these assays. Titratable granzyme B activity in the GranToxilux assay was observed across the different dilutions for both the HIV-positive samples NY010 (ranging from 1.77-14%) and NY094 (ranging from 3.49-16.50%) (Figure 4.8). The maximum granzyme B activity was observed at a 1:1000 plasma dilution in

both donors (Figure 4.8B). HIV-negative plasma was included as a negative control and there was a low background granzyme B. All samples were used at a 1:1000 plasma dilution in the final assays.

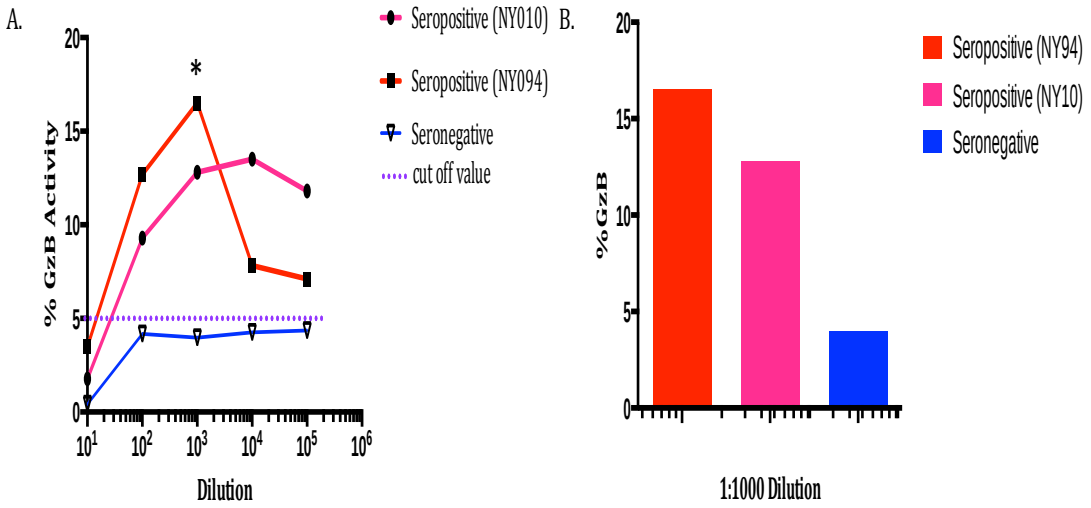

Figure 4.8. Optimisation of HIV-positive plasma dilutions for use in the GranToxilux and PanToxilux ADCC assays. (A) HIV seropositive plasma (red NY094 and pink lines NY010) and seronegative plasma (blue line) samples were used at a ten fold serial dilution starting at 1:10 to 1:100000. The optimal dilution selected (*) was 1:1000 plasma dilution. The background noise was determined as any value below 5% granzyme B activity (cut off value). (B) Histogram showing granzyme B activity of the seropositive samples and the seronegative sample at 1:1000 dilution. For this experiment, a 30:1 effector to target ratio was used, and approximately 200 000 events were captured and analyzed using Flowjo.

4.2.4. Final protocol for the GranToxilux and PanToxilux ADCC assay

Following this series of optimisations and titrations, the following protocol yielded the most optimal conditions for the GranToxilux and PanToxilux assays. Figure 4.9 summarises the major steps and optimisations. For all further experiments, CEM.NKR_{CCR5} cells were coated with 5µg/ml recombinant gp120 (optimised in section 4.2.3.1) and stained with TFL4 for 15 min (optimised in section 4.2.3.2). The CEM. NKR_{CCR5} cells were incubated with donor F PBMCs (as a source of NK cells), at an effector:target ratio of 30:1 (optimised in section section 4.2.3.3), in the presence of.1:1000 dilution of plasma from HIV-infected individuals (optimised in section 4.2.3.4).

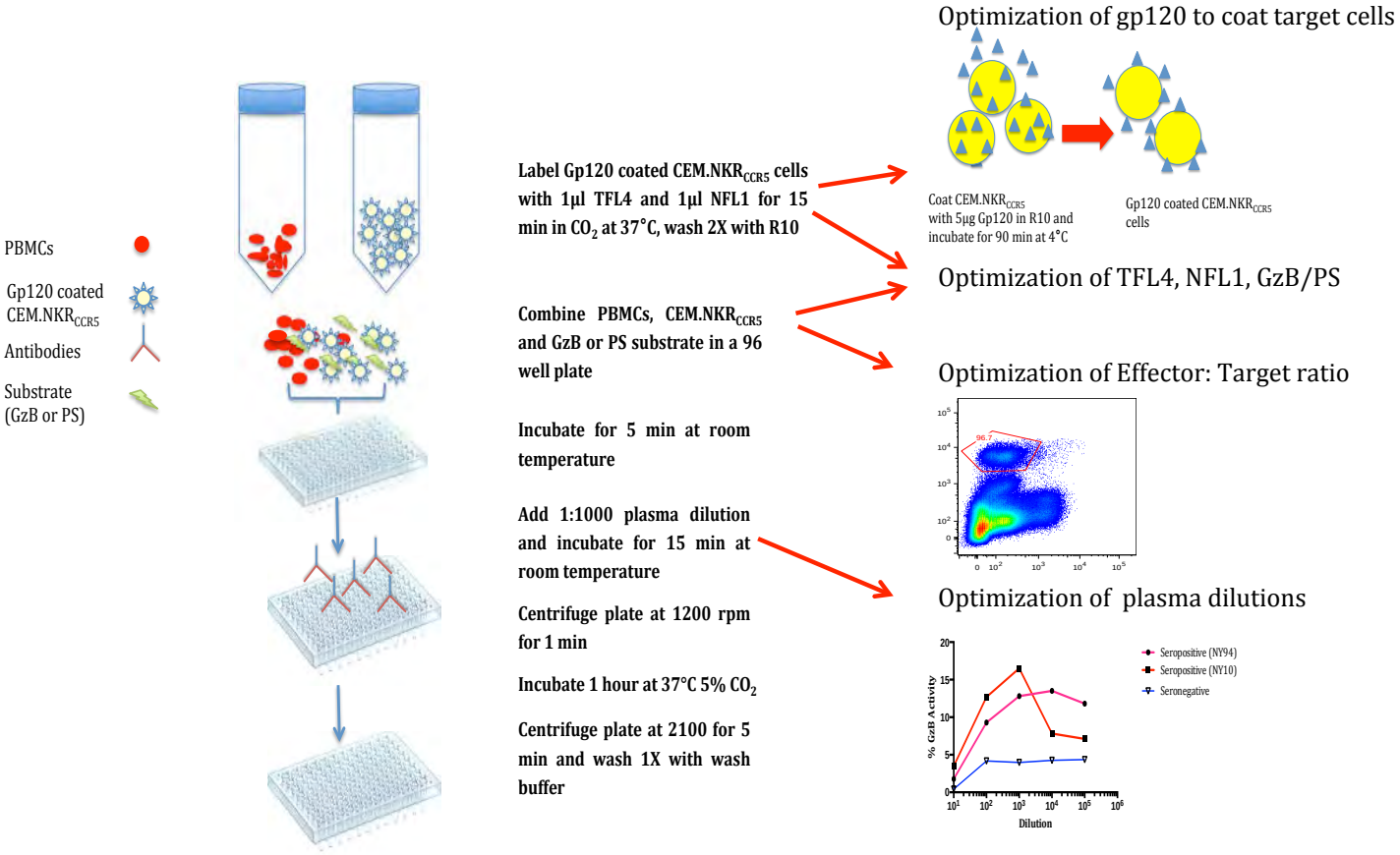

Figure 4.9. Overview of the GranToxilux and PanToxilux assays indicating all the steps optimised in this study. The CEM.NKR$_{CCR5}$ cells were first coated with the optimised amount of gp120 on the day of the assay before being used in both the GranToxilux and PanToxilux assays. The first step was optimising gp120 to coat the cells, followed by optimisation of the cell markers including substrates for GranToxilux (GzB) and PanToxilux (PS) assays, thirdly optimisation of the effector:target ratio and lastly optimisation of plasma dilutions.

Figure 4.10 shows a representative figure of the GranToxilux assay showing the gating strategy used. CEM.NKR$_{CCR5}$ cells (target cells alone) labeled with TFL4 and NFL1 were used to identify the viable cells which were TFL4 positive but NFL1 negative. Out of the viable CEM.NKR$_{CCR5}$ cells, granzyme B positive cells were identified. The results are expressed as % granzyme B (percentage of CEM.NKR$_{CCR5}$ cells positive for proteolytically active granzyme B) for the rest of the study.

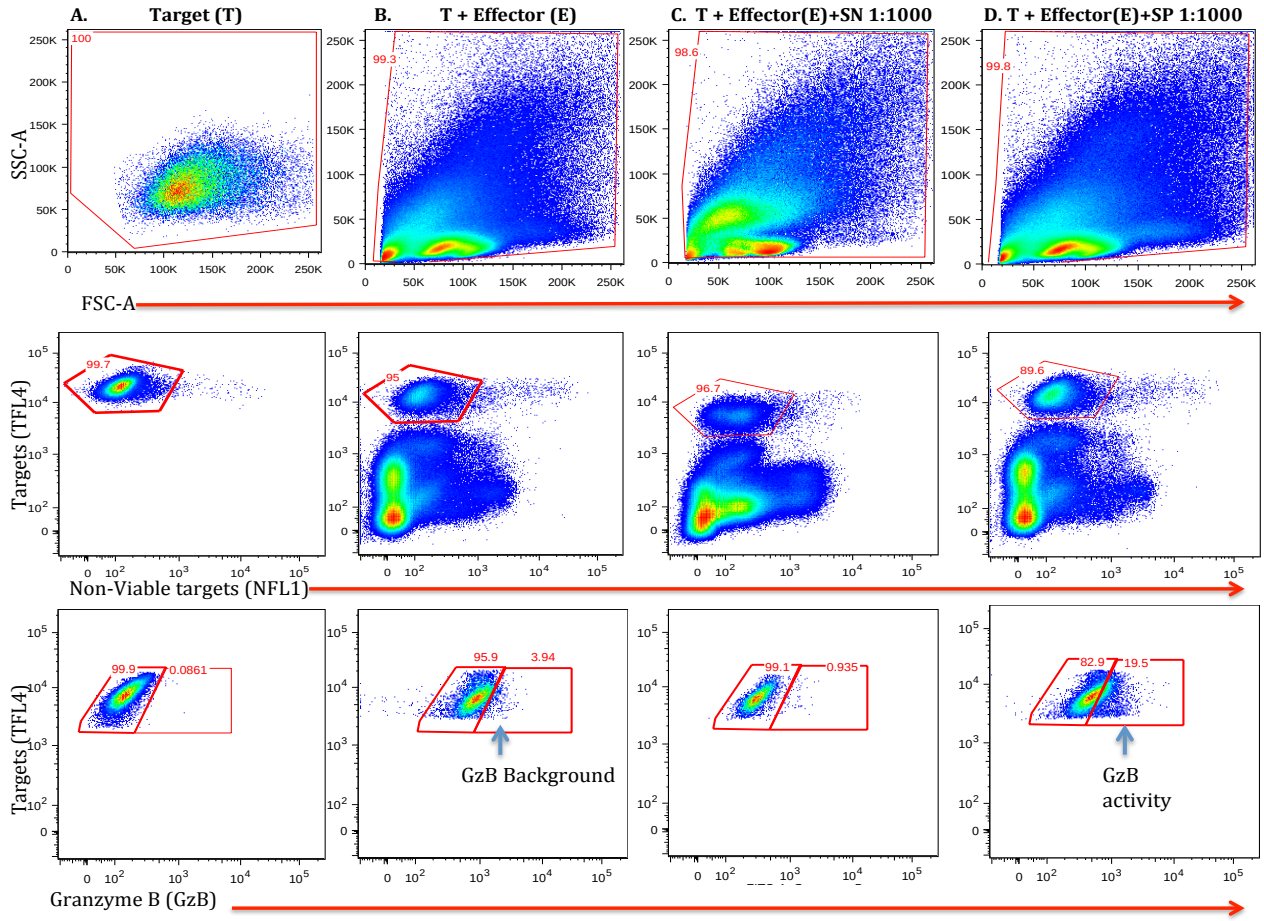

Figure 4.10. Representative plots showing the gating strategy used for the GranToxilux assay. (A) Target cells were gated on using SSC and FSC plots. Next, the background noise of GzB substrate (FITC) was evaluated using viable CEM.NKR$_{CCR5}$ (TFL4+NFL1-) and PBMCs without plasma (B). A seronegative plasma sample at a 1:1000 dilution (C) was used to set the final background noise with plasma (NY094). (D) A representative HIV-positive plasma sample at a 1:1000 dilution. Approximately 500 000 events were captured for each assay. Gating and analysis was performed using Flowjo.

Figure 4.11 shows a representative figure of the PanToxilux assay showing the gating strategy used. Similarly to the GranToxilux assay, the first gate was set on CEM.NKR$_{CCR5}$ cells using the forward and side scatter plot. Secondly, combining TFL4 and NFL1 signals gated out the viable CEM.NKR$_{CCR5}$ cells. Thirdly, granzyme B and caspase activity was measured in the viable CEM.NKR$_{CCR5}$ cells by combining TFL4 and FITC signals.

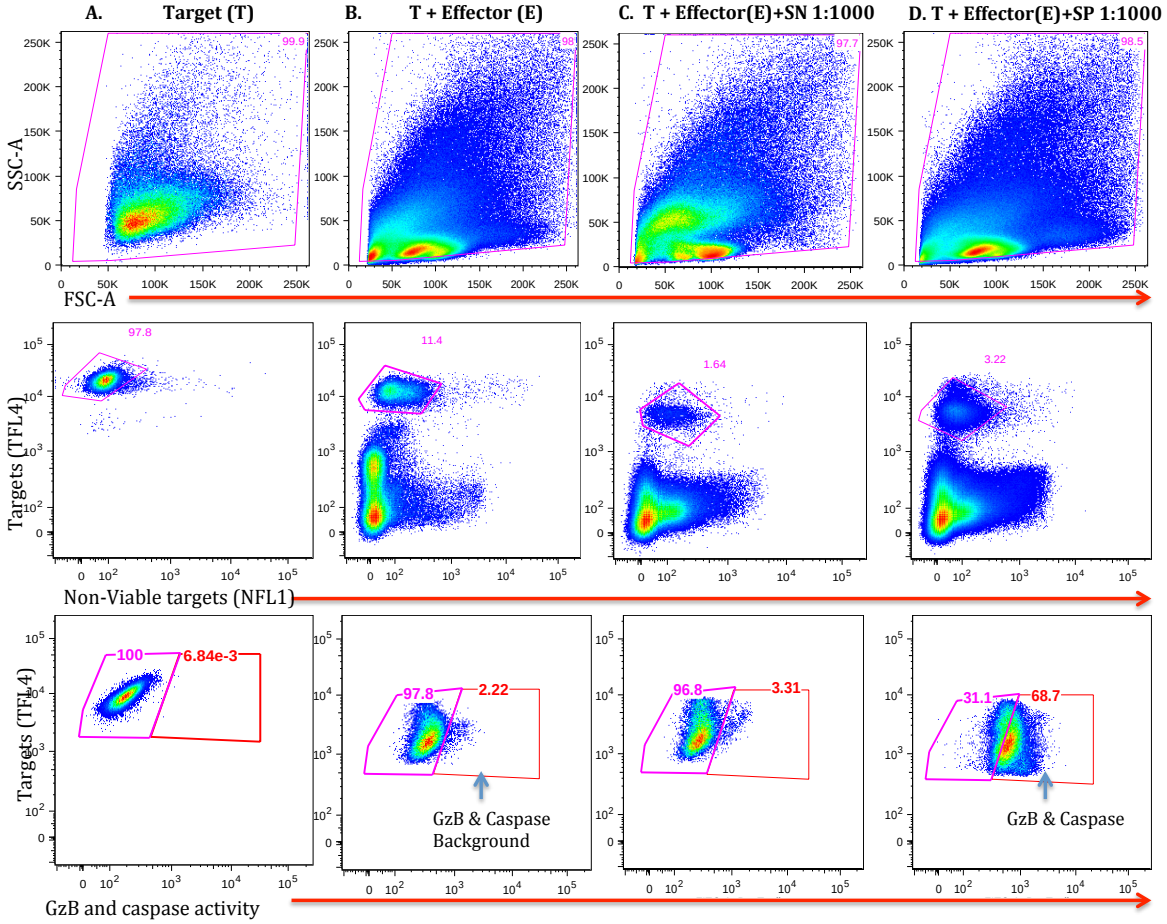

Figure 4.11. Representative plot showing the gating strategy used for the PanToxilux assay. (A) Target cells were gated on using SSC and FSC plots. Next the background noise of PS substrate (FITC) was evaluated using viable CEM.NKR$_{CCR5}$ (TFL4+NFL1-) and PBMCs without plasma (B). A seronegative plasma sample at a 1:1000 dilution (C) was used to set the final background noise with plasma. (D) A representative HIV-positive plasma sample (NY094) at a 1:1000 dilution. Approximately 500 000 events were captured. Gating and analysis was performed using Flowjo.

4.2.5. Comparison between GranToxilux and PanToxilux assays for measuring ADCC

The ability of plasma from the HIV-positive donors (Table 4.1) to mediate ADCC against CEM.NKR$_{CCR5}$ target cells was compared to plasma from HIV-negative donors using both the GranToxilux and PanToxilux assays (Figure 4.12). Using the GranToxilux assay to measure NK-cell mediated ADCC from the 9 HIV-positive plasma donors, the frequency of granzyme B+ target cells ranged from 3.53 to 42%. In contrast, the frequency of granzyme B+ target cells resulting from HIV-negative plasma samples ranged from 0.10 to 1.38%. Plasma from HIV-positive donors mediated significantly higher ADCC killing in the GranToxilux assay than the HIV-negative donors ($p=0.0028$). Using the PanToxilux assay to measure NK-cell mediated ADCC from the 9 HIV-positive donors, the frequency of target cells staining positive for granzyme B and caspase activity ranged from 7.5 to 66.5% (Figure 4.12). The amount of granzyme B and caspase activity induced by plasma from HIV-negative individuals ranged from 1 to 6%. Plasma from HIV-positive individuals mediated significantly higher ADCC killing than HIV-negative controls ($p=0.0004$) in the PanToxilux assay. While the magnitude of ADCC activity measured in plasma from HIV-infected individuals was largely similar between the GranToxilux and PanToxilux assays, the background level of ADCC detected in plasma from HIV-negative individuals was significantly higher in the PanToxilux than the GranToxilux assay ($p=0.0043$; Figure 4.12A), suggesting that the GranToxilux assay was superior to the PanToxilux assay by virtue of low background.

The Bland-Altman test was used to compare HIV-specific ADCC activity measured in matched plasma samples using the GranToxilux and PanToxilux assays (Figure 4.12C). The average bias between the two assays was -2, indicating that these two assays were largely in agreement and that there was no significant differences between these methods in measuring ADCC in the HIV-infected individuals. Of the 9 HIV-positive plasma samples used in this study, 2/9 showed noticable differences in ADCC activity measured using the two assays. Plasma from donor NY094 (dark blue dot; Figure 4.12C) resulted in 16% granzyme B activity in the GranToxilux assay compared to 66% granzyme B and caspase activity detected using the PanToxilux assay. Plasma from

donor NY234 (lime dot; Figure 4.12C) resulted in 42% granzyme B activity in the GranToxilux assay compared to 12% detected by the PanToxilux assay.

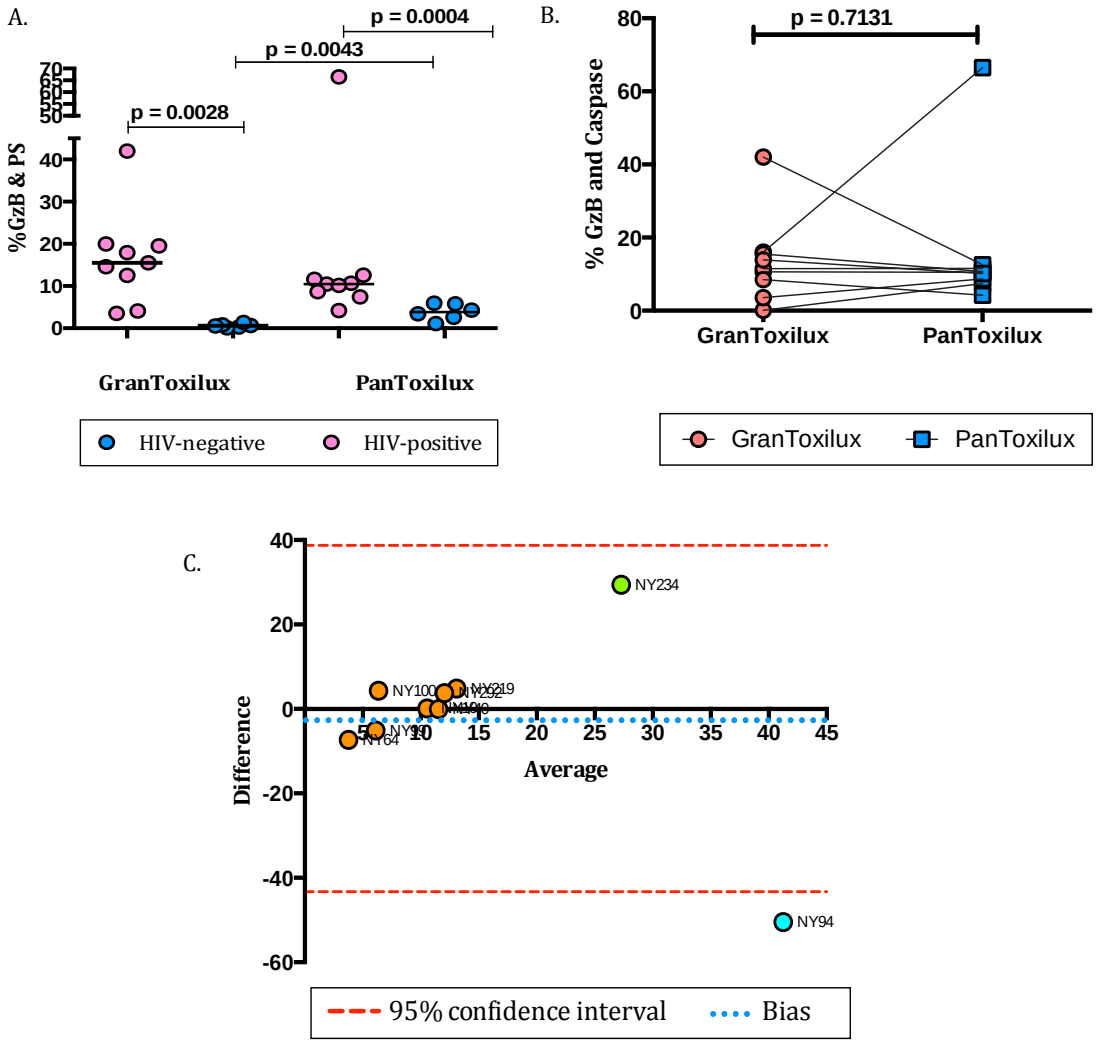

Figure 4.12. Comparison between the GranToxilux and PanToxilux assays for detecting ADCC activity in HIV-positive plasma. (A) HIV-positive (pink dots) and HIV-negative (blue dots) plasma samples were assessed for their ability to mediate ADCC, measured using either the GranToxilux or PanToxilux assays. Non-parametric Mann Whitney U test was used to compare unmatched HIV- and HIV+ serum, and a p-value of ≤0.05 was considered to be significant. Each data point represents a single individual. (B) In a matched pair analysis, the Wilxocon paired test was used to compare the magnitude of ADCC measured from HIV-positive plasma samples with the GranToxilux or PanToxilux assays. (C) Measurement of agreement between the GranToxilux and PanToxilux assays for measuring ADCC activity in plasma samples from HIV-positive individuals using the Bland-Altman test. The bias value (blue line) and 95% limits of agreement (red line) interval was calculated as a measure of assay agreement.

4.2.6. Relationship between ADCC activity, antibody titres and HIV clinical status

Previously, studies have reported that HIV-specific ADCC activity was associated with clinical status of HIV-infected individuals, including a positive association with $CD4^+$ T cell counts and a negative association with plasma viral loads (Ahmad et al., 2001; Johansson et al., 2011; Smalls-Mantey et al., 2012). In this study, HIV-specific ADCC activity measured by the GranToxilux and PanToxilux assays were compared with CD4+ T cell counts and plasma viral loads in the 9 HIV-positive individuals. ADCC activity did not correlate with either CD4+ T cell counts (Rho=0.28 p=0.46 for GranToxilux assay; Rho=0.20 p=0.6 for PanToxilux assay) or plasma viral loads (Rho=0.08 p=0.8 for GranToxilux assay; Rho=0.16 p=0.66 for PanToxilux assay).

High antibody titres have been reported in long-term non-progressors during HIV infection (Okulicz, 2012; Wren et al., 2013). Despite the HIV-infected individuals in this study being healthy despite being infected for >5 years with broad reactivity to most HIV proteins (measured by western blot), no correlation was found between ADCC activity and titres of gp120 antibodies (Rho=0.08 p=0.8 for GranToxilux and Rho=0.15 p=0.7 for PanToxilux assay).

4.3. Discussion

In this Chapter, two high-throughput commercial assays for measuring ADCC activity, the GranToxilux and PanToxilux assays were optimised and compared. The GranToxilux assay detects intracellular granzyme B activity (Packard and Komoriya, 2008; Pollara et al., 2011) while the PanToxilux assay detects both granzyme B and upstream caspase activity delivered by NK cells into the target cells (Packard and Komoriya, 2008; Packard et al., 2007). While both the GranToxilux and PanToxilux ADCC assays were useful in detecting HIV-specific ADCC activity in plasma from chronically HIV-infected individuals, the higher background ADCC activity detected by the PanToxilux assay in the HIV-negative plasma samples suggests that the GranToxilux assay may be more useful for the purposes of measuring HIV-specific activity.

The pro-apoptotic protease granzyme B is a potent inducer of caspase-dependent and caspase independent forms of target cell apoptosis (Anthony et al., 2010). Adding caspase detection could increase the PanToxilux assays sensitivity, since it detects both NK cell released granzyme B and target cell activated caspase activity. While both upstream and downstream caspases are activated by granzyme B to initiate apoptosis (Afonina et al., 2010; Anthony et al., 2010), the PanToxilux assay only detects upstream caspase activity. Interestingly, using the PanToxilux assay in this Chapter to detect ADCC activity (which measures both caspase and granzyme B activity) was not significantly different from measuring granzyme B alone using the GranToxilux assay. Since the PanToxilux assay detects only upstream but not downstream caspase activity, it might be that more downstream caspases were activated to initiate target cell apoptosis during ADCC, or that a caspase-independent pathway might have been the major pathway activated during ADCC activity in this study.

HIV-positive plasma donors in this study recognised all of the HIV proteins included on the western blot strip. HIV gp160, a precursor glycoprotein later processed into gp120 and gp41, was the most dominant antigen recognised in all donors, while gp120 was the least dominant antigen recognised. Furthermore, the HIV-positive plasma donors used had binding IgG antibodies against HIV envelope gp120 (assessed by ELISA). Most HIV

epitopes targeted by ADCC antibodies are within gp120 and gp41 (Bonsignori et al., 2012; Ferrari et al., 2011; Madhavi et al., 2013), and ADCC is mediated by IgG antibodies, particularly IgG1 and IgG3 (Bruhns et al., 2009; Haynes et al., 2011; Wren et al., 2013). The CD16 receptor on the surface of NK cells recognise the Fc region of these antibodies bound on the surface of a target cell expressing HIV antigens (Cox et al., 1999; Seidel et al., 2013). The antibody effector functions can be affected by different factors including Fc glycosylation. The exact subclass within the IgG isotype was not assessed further, which is one of the limitations of this study. Furthermore, antibody Fc glycosylation, which influences the ability of the antibodies to mediate ADCC was not investigated.

HIV-specific ADCC activity measured using the GranToxilux and PanToxilux assays did not correlate with clinical status (CD4 T cell counts or viral loads) of the HIV-positive plasma donors used in this study. However, the number of donors evaluated in this study was very small and these convenient donors would most likely be classified as long-term non-progressors or HIV controllers. Similar to this study, Smalls-Mantey et al. (2012), using the GranToxilux assay, did not observe any association between HIV plasma viral load and ADCC activity in sera from HIV-positive individuals. However, ADCC activity has been associated with total IgG binding during HIV infection (Smalls-Mantey et al., 2012). This is in contrast to a prior study which found a positive association between HIV-specific ADCC activity and viral load in long term non-progressors, and that long-term non-progressors had significantly lower ADCC activity compared to viremic individuals (Ahmad et al., 2001). However, this study used the chromium release assay and not the GranToxilux assay. A study by Sun et al. (2011) reported a positive correlation between NK cell mediated ADCC activity and SIV-specific antibody titers in non-human primates.

Choice of target cell for the ADCC assay is an important consideration because target selection provides useful information to determine immunogenecity and protective quality of antigens detected by the immune system. The target cells used in this Chapter were CEM.NKR$_{CCR5}$ cells, a CD4^{+} T cell line resistant to NK cell killing mediated cytotoxicity receptors (Trkola et al., 1999). Pollara et al. (2011) compared gp120-coated

CEM.NKR$_{CCR5}$ cells, CEM.NKR$_{CCR5}$ cells infected with A1953 strain of HIV, CEM.NKR$_{CCR5}$ cells infected with infectious molecular clones encoding HIV subtype B, or HIV-infected CD4+ T cells for GranToxilux assay. They concluded that CEM.NKR$_{CCR5}$ cells coated with gp120 or infected with A1953 virus were the most reliable target cell platforms to detect ADCC responses. In this study, HIV subtype C (predominant in Sub-Saharan Africa) recombinant gp120 was chosen to coat the CEM.NKR$_{CCR5}$ cells because most HIV-specific ADCC antibodies described in literature are against the gp120 protein (Ahmad et al., 2001; Ferrari et al., 2011; Pegu et al., 2013; Trkola et al., 1996). Although not reflecting a natural HIV infection in which HIV-infected CD4+ T cells are used as targets, this system using gp120-coating CEM.NKR$_{CCR5}$ cells as targets provides a robust system to compare the GranToxilux and PanToxilux assays. Using CEM.NKR$_{CCR5}$ cells as targets instead of donor CD4+ T cells as targets avoids issues around CD4+ T cell donor variability and using gp120-coating ensured a more even spread of HIV antigen to bind with HIV-specific antibodies than HIV infection, where not all of the target cells may become infected or express HIV antigens on their cell surface simultaneously (Pollara et al., 2011). Therefore, this Chapter focused on optimisation of gp120 coated CEM.NKR$_{CCR5}$ cells to measure HIV-specific ADCC activity.

In this study, the PanToxilux assay yielded higher levels of background ADCC activity from HIV-negative plasma donors than the GranToxilux assay, although the level of specific activity was similar. This higher level of background ADCC activity from the PanToxilux assay might be due to this assay detecting both granzyme B and upstream caspase activity compared to the GranToxilux assay which measures only granzyme B activity (Packard and Komoriya, 2008). Other studies have reported background noise of ~20% in some rapid and fluorometric antibody-dependent cellular cytotoxicity assays (Gómez-Román et al., 2006; Richard et al., 2014). Background noise of ~8% has been reported in HIV-negative samples using the GranToxilux assay (Pollara et al., 2011), which is in line with or slightly lower than the levels reported in this study. To my knowledge, there is currently no study published measuring ADCC activity during HIV infection using the PanToxilux assay, so the PanToxilux assay background can only be compared to studies which used the GranToxilux assay to measure ADCC activity during HIV infection.

In conclusion, I have optimised two high-throughput assays and compared their ability to measure HIV-specific ADCC activity. The GranToxilux assay was found to be better because it had similar specificity to the PanToxilux assay in detecting HIV-specific ADCC activity, but yielded significantly lower background or non-specific ADCC activity.

CHAPTER 5

Discussion and Conclusion

5.1. Discussion

The ability to define the effectiveness of ADCC responses has been hampered by traditional methods which are labour intensive and time consuming, make use of radioactive labelling and are not easily used for high throughput screening (Chung et al., 2008). There is no clear consensus on the best ADCC assay to use that correlates most closely with improved outcomes for HIV infection, since different assays measure overlapping functions of ADCC antibodies. More recent high-throughput methods to measure ADCC activity during HIV infection have either focused on measuring properties of the effector NK cell population (Alter et al., 2004; Gómez-Román et al., 2006) or the target cell populations (Ferrari et al., 2011; Lambotte et al., 2013; Pollara et al., 2011; Tomaras et al., 2013). This study optimised two high-throughput assays, the GranToxilux and PanToxilux, to measure NK cell direct killing and ADCC activity during HIV infection. The GranToxilux assay has been utilised before measuring HIV-specific ADCC (Ferrari et al., 2011; Lambotte et al., 2013; Pollara et al., 2011; Tomaras et al., 2013), however, to my knowledge, there is no published study using the PanToxilux assay to measure HIV-specific ADCC.

Chapter 3 focused on selection of an HIV-negative NK cell donor for measuring both direct killing and ADCC activity; and subsequent optimisation and comparison of the GranToxilux and PanToxilux assays to measure direct NK killing of the tumour cell line K562. NK cells from the selected universal donor were phenotypically and functionally characterised and shown to be predominantly $CD56^{Dim}$ NK cells, with only a minor population of $CD56^{Bright}$ and CD16+ CD56- NK cells. The $CD56^{Dim}$ NK cells were shown to degranulate (CD107a+) more than the other two subsets and produce more IFN-γ following polyclonal stimulation. Using this NK cell donor, findings from Chapter 3 suggest that the PanToxilux assay was more sensitive at detecting NK-cell direct killing than the GranToxilux assay, yielding direct killing activity that was significantly higher; and that there was poor agreement between the assays for measuring NK-cell direct killing.

Chapter 4 focused on measurement of ADCC activity, using the GranToxilux and PanToxilux assays, mediated by plasma from HIV-positive individuals against gp120-coated CEM.NKR$_{CCR5}$ target cells. Both the GranToxilux and PanToxilux assays had similar sensitivity in detecting ADCC activity using HIV-positive plasma. However, lower background ADCC activity was measured from HIV-negative plasma samples using the GranToxilux assay compared to the Pantoxilux assay. Despite differences between these assays in background, both performed quiet similarly at detecting HIV-specific NK-cell mediated ADCC killing in this study and were shown to be in agreement.

5.2. Proposed model for the differences in performance of these assays

NK cells can mediate cytotoxicity through different receptors and different pathways. NCRs on NK cells have been reported to play a major role in NK cell direct killing (De Maria et al., 2003; Garcia-Iglesias et al., 2009; Mavilio et al., 2003), while the CD16 receptor mediate ADCC by binding to the Fc region of the antibodies (He et al., 2013; Johansson et al., 2011; Mandelboim et al., 1999). This study found that the GranToxilux and PanToxilux assays differed in sensitivity to measure NK cell direct killing of K562 cells, but were largely similar at measuring HIV-specific ADCC activity against gp120-coated CEM.NK$_{CCR5}$ target cells. The disparate finding in sensitivity might be because of the differences in NK cell direct killing of tumor cell compared to NK cell ADCC killing mechanism.

During direct killing, granzyme B released by degranulating NK cells might activate the caspase-dependent pathway to induce tumour target cell apoptosis. Therefore, the detectation of both granzyme B and upstream caspases by the PanToxilux assay might make it more sensitive compared to the GranToxilux assay which only detects granzyme B. In contrast, during ADCC, the released granzyme B might alternatively activate apoptosis through a caspase-dependent pathway or a caspase-independent manner which preferentially activates more downstream caspases not detected by the PanToxilux assay (which measures only upstream caspase activity). Since direct NK-cell killing does not require activation through antibodies, caspases may be activated

quickly and detected by the PanToxilux compared to ADCC. Furthermore, the interaction of K562 cells with the NK cells inhibitory and activating receptors may lead to a stronger cumulative activating signal that may stimulate the release of IFN-γ by NK cells. This may induce surface expression of the FAS-L receptors on K562 cells leading to elevated caspase production and therefore enhanced sensitivity of the PanToxilux assay. Alternatively, the differences in performance between the GranToxilux and PanToxilux assay may reflect differences in the target cells used. CEM target cells used in the ADCC assay may not activate upstream caspases as efficiently or with the same kinetics as K562 cells used in the direct killing assay. This proposed model is summarised in Figure 5.1.

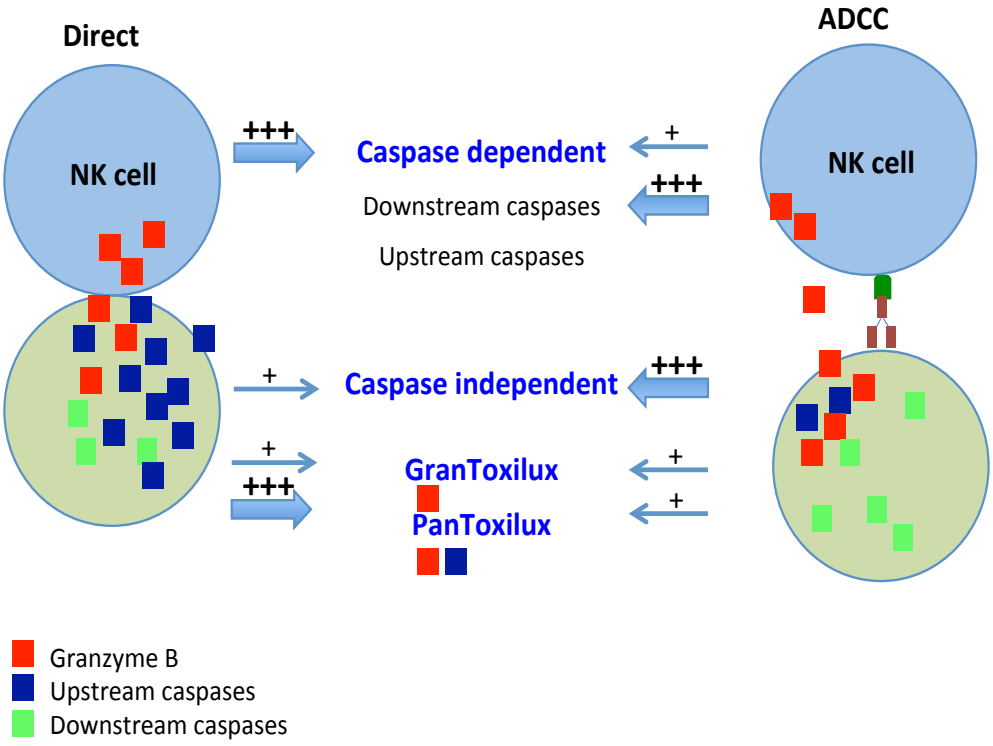

Figure 5.1. Proposed model to explain differences in the sensitivity of the GranToxilux and PanToxilux assay to detect direct killing by NK cells versus ADCC-mediated killing. During direct killing, granzyme B might strongly (+++) activate the caspase dependent pathway rather than the caspase independent pathway. Since the PanToxilux assay detects both granzyme B (red square) and upstream caspase (blue square) activity, its sensitivity is heightened (+++) to detect direct killing compared to the GranToxilux detecting granzyme B only (+). During ADCC, more downstream caspases (+++) might be involved compared to upstream caspase activity (+), or, granzyme B strongly activates the caspase independent pathway (+++). This results in similar sensitivity of the PanToxilux to the GranToxilux assay, since not much upstream caspase are activated, and therefore both of them only detecting granzyme B equally.

5.3. Potential limitations of this study

PBMCs were used as the source of effector NK cells and not purified NK cells. In addition to having about 15% NK cells, PBMCs could also contain 20% neutrophils and 15% monocytes which have also been reported to mediate ADCC during HIV infection (Smalls-Mantey et al., 2013), and might have contributed to the ADCC activity measured in this study. Selection of the universal NK cell donor was based on NK cell direct killing of K562 following polyclonal stimulation with PMA/ionomycin or PHA, but the mechanism by which NK cells kill K562 cells may differ from the mechanism they use for ADCC. Inhibitory receptors on NK cells recognise tumour cells lacking HLA class I (missing self; Long 2002), which then interacts with activating receptors to activate granzyme B and caspase activity, while during ADCC, granzyme B and caspase activity is activated by the cross-linking of the FcγRIIIa activating receptor. So it is possible that the ability of NK cells to directly kill K562 tumour cells does not reflect their potency to kill antigen-coated target cells in an ADCC assay. It may have been better to use a broader evaluation of NK cell activity in selection of the universal donor, such as evaluating NK cell performance against HIV-coated CEM.NKR$_{CCR5}$ target cells or their ability to degranulate in response to HIV antigens. In addition, antibodies with known good ADCC activity such as the well-characterized A32 monoclonal antibody should have been used to screen the panel of NK cell donors for ADCC activity. Donor to donor variation in NK cell activity are likely to influence the results, as the amount of granzyme B and caspase produced by a chosen NK cell donor is dependent on the ability of NK cells to be activated, inhibited, to bind antibodies and to effeciently release cytolytic granules to kill target cells (Alpert et al., 2012; Davis et al., 2011). These donor NK cells studied in this dissertation were not phenotyped for the activating and inhibiting receptors, and the net result of activating and inhibitory receptor engagement are likely to also influence NK cell ability to mediate ADCC. Moreover, the frequency of NK cells was not assessed and the FcγRIIIa receptor was not genotyped for polymorphisms that could influence ADCC activity (Wren et al., 2013b).

Although gp120-coated CEM.NKR$_{CCR5}$ target cells have been reported to be reliable target cells for measuring ADCC activity (Pollara et al., 2011), use of gp120 alone instead of virally-infected cells or coating with other HIV antigens was a possible limitation in

this study. Some ADCC epitopes are found on gp41 as well as on other HIV proteins, therefore antibodies that target epitopes other than the ones on gp120 may have been missed. HIV-specific antibodies from plasma of HIV-positive individuals were quantified using gp120 ELISA and western blot analysis, both of which measured IgG titres. IgG1 and IgG3 have been described as the most common IgG isotype to mediate ADCC via strong CD16 interactions (Chung et al., 2008). During HIV infection, anti-Env plasma antibodies are predominantly IgG1 subclass, whereas anti-Env IgG3 is the second most predominant IgG subclass and had been shown to decline in individuals infected with HIV for more than five years (Yates et al., 2011). The amount of IgG subclasses was not quantified in this study. Furthermore, antibody functions can be affected by other factors, such as polymorphisms which increases IgG affinity to the CD16 receptor, which were not evaluated in this study (Bruhns et al., 2009; Boyd et al., 1996; Shinkawa et al., 2003). In previous studies using the GranToxilux assay to measure HIV-specific ADCC activity, HIVIG immunoglobulin has been used as a positive HIV-specific antibody control (Bonsignori et al., 2012; Ferrari et al., 2011; Lambotte et al., 2013). Alternatively, the HIV monoclonal antibody A32 has also been reported to mediate potent ADCC activity and has been used as a positive control (Ferrari et al., 2011). There was no positive HIV-specific antibody control used in this study with known properties or performance in ADCC assays.

5.4. Conclusion

The GranToxilux and PanToxilux high-throughput flow cytometry based ADCC assays were optimised and compared to measure direct NK cell killing and HIV-specific ADCC activity. While the PanToxilux assay was more sensitive at measuring direct killing than the GranToxilux assay, both assays were similar in detecting ADCC activity in plasma of HIV-infected individuals. However, lower background activity was measured by the GranToxilux assay using HIV-negative control plasma than the PanToxilux assay. This study suggests that both the GranToxilux and PanToxilux assays represent simple, rapid and reliable flow cytometry based high-throughput assays to study HIV-1 gp120 specific ADCC responses using gp120-coated CEM.NKR$_{CCR5}$ cells, although the GranToxilux assay out-performed the PanToxilux assay in its ability to measure HIV-specific ADCC activity.

In conclusion, ADCC in vivo is enormously complex and very few assays can provide an accurate reflection of the combined features of an individual's unique target cell, antibody and effector cell interactions that give an overall snapshot of their all-encompassing ADCC capability.

REFERENCES

Aasa-chapman, M.M.I., Holuigue, S., Aubin, K., Wong, M., Jones, N.A., Cornforth, D., Newton, P., Williams, I., Aasa-chapman, M.I., Pellegrino, P., Borrow, P., 2005. Detection of Antibody-Dependent Complement-Mediated Inactivation of both Autologous and Heterologous Virus in Primary Human Immunodeficiency Virus Type 1 Infection Detection of Antibody-Dependent Complement-Mediated Inactivation of both Autologous and Het. J. Virol. 75, 2823–2830.

Ackerman, M.E., Dugast, A.-S., Alter, G., 2012. Emerging concepts on the role of innate immunity in the prevention and control of HIV infection. Annu. Rev. Med. 63, 113–130.

Ackerman, M.E., Dugast, A.-S., McAndrew, E.G., Tsoukas, S., Licht, A.F., Irvine, D.J., Alter, G., 2013. Enhanced phagocytic activity of HIV-specific antibodies correlates with natural production of immunoglobulins with skewed affinity for FcγR2a and FcγR2b. J. Virol. 87, 5468–5476.

Afonina, I.S., Cullen, S.P., Martin, S.J., 2010. Cytotoxic and non-cytotoxic roles of the CTL/NK protease granzyme B. Immunol. Rev. 235, 105–116.

Ahmad, R., Sindhu, S.T., Toma, E., Morisset, R., Vincelette, J., Menezes, J., Ahmad, A., 2001. Evidence for a correlation between antibody-dependent cellular cytotoxicity-mediating anti-HIV-1 antibodies and prognostic predictors of HIV infection. J. Clin. Immunol. 21, 227–233.

Alpert, M.D., Heyer, L.N., Williams, D.E.J., Harvey, J.D., Greenough, T., Allhorn, M., Evans, D.T., 2012. A novel assay for antibody-dependent cell-mediated cytotoxicity against HIV-1- or SIV-infected cells reveals incomplete overlap with antibodies measured by neutralization and binding assays. J. Virol. 86, 12039–12052.

Alter, G., Malenfant, J.M., Altfeld, M., 2004. CD107a as a functional marker for the identification of natural killer cell activity. J. Immunol. Methods 294, 15–22.

Alter, G., Moody, M.A., 2010. The humoral response to HIV-1: new insights, renewed focus. J. Infect. Dis. 202, 315–322.

Altfeld, M., Fadda, L., Frleta, D., Bhardwaj, N., 2011. DCs and NK cells: critical effectors in the immune response to HIV-1. Nat. Rev. Immunol. 11, 176–186.

Anthony, D. a, Andrews, D.M., Watt, S. V, Trapani, J. a, Smyth, M.J., 2010. Functional dissection of the granzyme family: cell death and inflammation. Immunol. Rev. 235, 73–92.

Archary, D., Rong, R., Gordon, M.L., Boliar, S., Madiga, M., Gray, E.S., Dugast, A., Hermanus, T., Goulder, P.J.R., Hoosen, M., 2013. Characterization of anti-HIV-1 neutralizing and binding antibodies in chronic HIV-1 subtype C infection. Virology. 433, 410–420.

Baba, M., Miyake, H., Okamoto, M., Iizawa, Y., Okonogi, K., 2000. Establishment of a CCR5-expressing T-lymphoblastoid cell line highly susceptible to R5 HIV type 1. AIDS Res. Hum. Retroviruses 16, 935–941.

Baran, J., Kowalczyk, D., Oz, M., Zembala, M., 2001. Three-Color Flow Cytometry Detection of Intracellular Cytokines in Peripheral Blood Mononuclear Cells : Comparative Analysis of Phorbol Myristate Acetate-Ionomycin and Phytohemagglutinin Stimulation Three-Color Flow Cytometry Detection of Intracellular Cy. Clin. Vaccine Immunol. 7, 303–313.

Bayigga, L., Nabatanzi, R., Sekiziyivu, P.N., Mayanja-Kizza, H., Kamya, M.R., Kambugu, A., Olobo, J., Kiragga, A., Kirimunda, S., Joloba, M., Nakanjako, D., 2014. High CD56++CD16- natural killer (NK) cells among suboptimal immune responders after four years of suppressive antiretroviral therapy in an African adult HIV treatment cohort. BMC Immunol. 15, 2.

Bergmeier, L. a., Lehner, T., 2006. Innate and Adaptive Mucosal Immunity in Protection against HIV Infection. Adv. Dent. Res. 19, 21–28.

Biron, C. a, 2012. Yet another role for natural killer cells: cytotoxicity in immune regulation and viral persistence. Proc. Natl. Acad. Sci. U. S. A. 109, 1814–1815.

Björkström, N.K., Ljunggren, H.-G., Sandberg, J.K., 2010. CD56 negative NK cells: origin, function, and role in chronic viral disease. Trends Immunol. 31, 401–406.

Bland, J.M., Altman, D.G., 1999. Statistical Methods in Medical Research. Stat. Methods Med. Res. 8, 135.

Bluman, E.M., Bartynski, K.J., Avalos, B.R., Caligiuri, M. a, 1996. Human natural killer cells produce abundant macrophage inflammatory protein-1 alpha in response to monocyte-derived cytokines. J. Clin. Invest. 97, 2722–2727.

Bonsignori, M., Pollara, J., Moody, M.A., Alpert, M.D., Chen, X., Hwang, K.-K., Gilbert, P.B., Huang, Y., Gurley, T.C., Kozink, D.M., Marshall, D.J., Whitesides, J.F., Tsao, C.-Y., Kaewkungwal, J., Nitayaphan, S., Pitisuttithum, P., Rerks-Ngarm, S., Kim, J.H., Michael, N.L., Tomaras, G.D., Montefiori, D.C., Lewis, G.K., DeVico, A., Evans, D.T., Ferrari, G., Liao, H.-X., Haynes, B.F., 2012. Antibody-dependent cellular cytotoxicity-mediating antibodies from an HIV-1 vaccine efficacy trial target multiple epitopes and preferentially use the VH1 gene family. J. Virol. 86, 11521–11532.

Bots, M., Medema, J.P., 2006. Granzymes at a glance. J. Cell Sci. 119, 5011–5014.

Boulet, S., Song, R., Kamya, P., Bruneau, J., Shoukry, N.H., Tsoukas, C.M., Bernard, N.F., 2010. HIV Protective KIR3DL1 and HLA-B Genotypes Influence NK Cell Function Following Stimulation with HLA-Devoid Cells. J. Immunol. 184, 2057–2064.

Boyd, P.N., Lines, A.C., Patel, A.K., 1996. The effect of the removal of siliac acid, galactose and total carbohydrate and the functional activity of Campath-1H. Mol. Immunol. 32, 1311–1318.

Brenner, B.G., Dascal, a, Margolese, R.G., Wainberg, M. a, 1989. Natural killer cell function in patients with acquired immunodeficiency syndrome and related diseases. J. Leukoc. Biol. 46, 75–83.

Briggs, J. a G., Kräusslich, H.-G., 2011. The molecular architecture of HIV. J. Mol. Biol. 410, 491–500.

Briggs, J. a G., Wilk, T., Welker, R., Kräusslich, H.-G., Fuller, S.D., 2003. Structural organization of authentic, mature HIV-1 virions and cores. EMBO J. 22, 1707–1715.

Broussas, M., Broyer, L., Goetsch, L., 2013. Glycosylation Engineering of Biopharmaceuticals. Methods in Molecular Biology. 988, 305–317.

Brown, B.K., Wieczorek, L., Kijak, G., Lombardi, K., Currier, J., Wesberry, M., Kappes, J.C., Ngauy, V., Marovich, M., Michael, N., Ochsenbauer, C., Montefiori, D.C., Polonis, V.R., 2012. The role of natural killer (NK) cells and NK cell receptor polymorphisms in the assessment of HIV-1 neutralization. PLoS One 7, e29454.

Bruhns, P., Iannascoli, B., England, P., Mancardi, D.A., Fernandez, N., Jorieux, S., 2009. Specificity and affinity of human Fc □ receptors and their polymorphic variants for human IgG subclasses. Blood 113, 3716–3725.

Bryceson, Y.T., Chiang, S.C.C., Darmanin, S., Fauriat, C., Schlums, H., Theorell, J., Wood, S.M., 2011. Molecular mechanisms of natural killer cell activation. J. Innate Immun. 3, 216–226.

Calame, K.L., 2001. Plasma cells: finding new light at the end of B cell development. Nat. Immunol. 2, 1103–1108.

Caligiuri, M. a, 2008. Human natural killer cells. Blood 112, 461–469.

Campbell-yesufu, O.T., Gandhi, R.T., 2011. Update on Human Immunodeficiency Virus (HIV) -2 Infection. Clin. Infect. Dis. 52, 780–787.

Carlson, L.-A., Briggs, J. a G., Glass, B., Riches, J.D., Simon, M.N., Johnson, M.C., Müller, B., Grünewald, K., Kräusslich, H.-G., 2008. Three-dimensional analysis of budding sites and released virus suggests a revised model for HIV-1 morphogenesis. Cell Host Microbe 4, 592–599.

Carson, B.W.E., Giri, J.G., Lindemann, M.J., Linett, M.L., Ahdieh, M., Paxton, R., Anderson, D., Eisenmann, J., Grabstein, K., Caligiuri, M.A., 1994. Interleukln (IL) 15 Is a Novel

Cytokine That Activates Human Natural Killer Cells via Components of the IL-2 Receptor. J. Exp. Methods. 180, 1395-1403.

Catalfamo, M., Wilhelm, C., Tcheung, L., Proschan, M., Friesen, T., Park, J.-H., Adelsberger, J., Baseler, M., Maldarelli, F., Davey, R., Roby, G., Rehm, C., Lane, C., 2011. CD4 and CD8 T cell immune activation during chronic HIV infection: roles of homeostasis, HIV, type I IFN, and IL-7. J. Immunol. 186, 2106–2116.

Cheema, Z.F., Santillano, D.R., Wade, S.B., Newman, J.M., Miranda, R.C., 2004. cell-surface Fas / Apo-1 suicide receptor expression in proliferating modifies estrogen control of cell-cycle proteins. BMC Neurosci. 21, 1–21.

Chung, A., Rollman, E., Johansson, S., Kent, S.J., Stratov, I., 2008. The utility of ADCC responses in HIV infection. Curr. HIV Res. 6, 515–519.

Chung, A.W., Alter, G., 2014. Dissecting the antibody constant region protective immune parameters in HIV infection. Future Virol. 9, 397–414.

Chung, A.W., Isitman, G., Navis, M., Kramski, M., Center, R.J., Kent, S.J., Stratov, I., 2011. Immune escape from HIV-specific antibody-dependent cellular cytotoxicity (ADCC) pressure. Proc. Natl. Acad. Sci. U. S. A. 108, 7505–7510.

Chung, A.W., Rollman, E., Center, R.J., Kent, S.J., Stratov, I., Stephen, J., 2009. Rapid degranulation of NK cells following activation by HIV-specific antibodies. J. Immunol. 182, 1202–1210.

Cohen, M.S., Gay, C.L., Busch, M.P., Hecht, F.M., 2010. The detection of acute HIV infection. J. Infect. Dis. 202 Suppl , S270–277.

Cooper, M. a, Fehniger, T. a, Caligiuri, M. a, 2001. The biology of human natural killer-cell subsets. Trends Immunol. 22, 633–640.

Cox, J.H., Garner, R.P., Redfield, R.R., Aronson, N.E., Davis, C., Ruiz, N., Birx, D.L., 1999. Antibody-dependent cellular cytotoxicity in HIV type 1-infected patients receiving VaxSyn, a recombinant gp160 envelope vaccine. AIDS Res. Hum. Retroviruses 15, 847–854.

Davis, Z.B., Ward, J.P., Barker, E., 2011. Preparation and use of HIV-1 infected primary CD4+ T-cells as target cells in natural killer cell cytotoxic assays. J. Vis. Exp. 1–7.

De Maria, A., Fogli, M., Costa, P., Murdaca, G., Puppo, F., Mavilio, D., Moretta, A., Moretta, L., 2003. The impaired NK cell cytolytic function in viremic HIV-1 infection is associated with a reduced surface expression of natural cytotoxicity receptors (NKp46, NKp30 and NKp44). Eur. J. Immunol. 33, 2410–2418.

Deeks, S.G., Phillips, A.N., 2009. HIV infection, antiretroviral treatment, ageing, and non-AIDS related morbidity. BMJ. 338, 288-292.

Deeks, S.G., Schweighardt, B., Wrin, T., Galovich, J., Hoh, R., Sinclair, E., Hunt, P., McCune, J.M., Martin, J.N., Petropoulos, C.J., Hecht, F.M., 2006. Neutralizing antibody responses against autologous and heterologous viruses in acute versus chronic human immunodeficiency virus (HIV) infection: evidence for a constraint on the ability of HIV to completely evade neutralizing antibody responses. J. Virol. 80, 6155–6164.

Doria-rose, N.A., Connors, M., 2010. Antibody Secreting B-cells in HIV Infection. Curr. Opin. HIV AIDS 4, 426–430.

Egger, M., May, M., Chêne, G., Phillips, A.N., Ledergerber, B., Dabis, F., Costagliola, D., D'Arminio Monforte, A., de Wolf, F., Reiss, P., Lundgren, J.D., Justice, A.C., Staszewski, S., Leport, C., Hogg, R.S., Sabin, C. a, Gill, M.J., Salzberger, B., Sterne, J. a C., 2002. Prognosis of HIV-1-infected patients starting highly active antiretroviral therapy: a collaborative analysis of prospective studies. Lancet 360, 119–129.

Elmore, S., 2007. Apoptosis: a review of programmed cell death. Toxicol. Pathol. 35, 495–516.

F. Okulicz, J., 2012. Elite Controllers and Long-term Nonprogressors: Models for HIV Vaccine Development? J. AIDS Clin. Res. 03, 1–4.

Fauriat, C., Long, E.O., Ljunggren, H.-G., Bryceson, Y.T., 2010. Regulation of human NK-cell cytokine and chemokine production by target cell recognition. Blood 115, 2167–2176.

Ferrari, G., Pollara, J., Kozink, D., Harms, T., Drinker, M., Freel, S., Moody, M.A., Alam, S.M., Tomaras, G.D., Ochsenbauer, C., Kappes, J.C., Shaw, G.M., Hoxie, J. a, Robinson, J.E., Haynes, B.F., Munir, S., John, C., James, E., 2011. An HIV-1 gp120 envelope human monoclonal antibody that recognizes a C1 conformational epitope mediates potent antibody-dependent cellular cytotoxicity (ADCC) activity and defines a common ADCC epitope in human HIV-1 serum. J. Virol. 85, 7029–7036.

Fiebig, E.W., Wright, D.J., Rawal, B.D., Garrett, P.E., Schumacher, R.T., Peddada, L., Heldebrant, C., Smith, R., Conrad, A., Kleinman, S.H., Busch, M.P., 2003. Dynamics of HIV viremia and antibody seroconversion in plasma donors: implications for diagnosis and staging of primary HIV infection. AIDS 17, 1871–1879.

Frackman, B.S., Kobs, G., Simpson, D., Storts, D., Corporation, P., 1998. Betaine and DMSO : Enhancing Agents for PCR. 65, 27.

Frankel, a D., Young, J. a, 1998. HIV-1: fifteen proteins and an RNA. Annu. Rev. Biochem. 67, 1–25.

Friedrich, B.M., Dziuba, N., Li, G., Endsley, M. a, Murray, J.L., Ferguson, M.R., 2011. Host factors mediating HIV-1 replication. Virus Res. 161, 101–114.

Forthal, D. N., Landucci, G., Gorny, M. K., Zolla-Pazner, S., & Robinson, W. E.,1995. Functional activities of 20 human immunodeficiency virus type 1 (HIV-1)-specific

human monoclonal antibodies. AIDS Research and Human Retroviruses, 11(9), 1095–1099.

Funke, J., Dürr, R., Dietrich, U., Koch, J., 2011. Natural Killer Cells in HIV-1 Infection : A Double-Edged Sword. AIDS Rev. 13, 67–76.

Gallo, R.C., Montagnier, L., 2003. The discovery of HIV as the cause of AIDS. N. Engl. J. Med. 349, 2283–2285.

Garcia-Iglesias, T., Del Toro-Arreola, A., Albarran-Somoza, B., Del Toro-Arreola, S., Sanchez-Hernandez, P.E., Ramirez-Dueñas, M.G., Balderas-Peña, L.M.A., Bravo-Cuellar, A., Ortiz-Lazareno, P.C., Daneri-Navarro, A., 2009. Low NKp30, NKp46 and NKG2D expression and reduced cytotoxic activity on NK cells in cervical cancer and precursor lesions. BMC Cancer 9, 186.

Garoff, H., Hewson, R., Opstelten, D.E., 1998. Virus Maturation by Budding Virus Maturation by Budding. Microbiol. Mol. Biol. Rev. 62, 1171-1190.

Geiger, T., Wehner, A., Schaab, C., Cox, J., Mann, M., 2012. Comparative proteomic analysis of eleven common cell lines reveals ubiquitous but varying expression of most proteins. Mol. Cell. Proteomics 11, M111.014050.

Gervaix, a, West, D., Leoni, L.M., Richman, D.D., Wong-Staal, F., Corbeil, J., 1997. A new reporter cell line to monitor HIV infection and drug susceptibility in vitro. Proc. Natl. Acad. Sci. U. S. A. 94, 4653–4658.

Glasner, A., Ghadially, H., Gur, C., Stanietsky, N., Tsukerman, P., Enk, J., Mandelboim, O., 2012. Recognition and prevention of tumor metastasis by the NK receptor NKp46/NCR1. J. Immunol. 188, 2509–2515.

Gómez-Román, V.R., Florese, R.H., Patterson, L.J., Peng, B., Venzon, D., Aldrich, K., Robert-Guroff, M., 2006. A simplified method for the rapid fluorometric assessment of antibody-dependent cell-mediated cytotoxicity. J. Immunol. Methods 308, 53–67.

Gottardo, R., Bailer, R.T., Korber, B.T., Gnanakaran, S., Phillips, J., Shen, X., Tomaras, G.D., Turk, E., Imholte, G., Eckler, L., Wenschuh, H., Zerweck, J., Greene, K., Gao, H., Berman, P.W., Francis, D., Sinangil, F., Lee, C., Nitayaphan, S., Rerks-Ngarm, S., Kaewkungwal, J., Pitisuttithum, P., Tartaglia, J., Robb, M.L., Michael, N.L., Kim, J.H., Zolla-Pazner, S., Haynes, B.F., Mascola, J.R., Self, S., Gilbert, P., Montefiori, D.C., 2013. Plasma IgG to linear epitopes in the V2 and V3 regions of HIV-1 gp120 correlate with a reduced risk of infection in the RV144 vaccine efficacy trial. PLoS One 8, e75665.

Gray, E.S., Taylor, N., Wycuff, D., Moore, P.L., Tomaras, G.D., Wibmer, C.K., Puren, A., DeCamp, A., Gilbert, P.B., Wood, B., Montefiori, D.C., Binley, J.M., Shaw, G.M., Haynes, B.F., Mascola, J.R., Morris, L., 2009. Antibody specificities associated with neutralization breadth in plasma from human immunodeficiency virus type 1 subtype C-infected blood donors. J. Virol. 83, 8925–8937.

Guan, Y., Pazgier, M., Sajadi, M. M., Kamin-Lewis, R., Al-Darmarki, S., Flinko, R., Lewis, G. K. (2013). Diverse specificity and effector function among human antibodies to HIV-1 envelope glycoprotein epitopes exposed by CD4 binding. Proc. Natl. Acad. Sci. U. S. A., *110*(1), E69–78.

Greene, W.C., 2007. A history of AIDS: looking back to see ahead. Eur. J. Immunol. 37 Suppl 1, S94–102.

Harrich, D., Hooker, B., 2002. Mechanistic aspects of HIV-1 reverse transcription initiation. Rev. Med. Virol. 12, 31–45.

Harris, A., Borgnia, M.J., Shi, D., Bartesaghi, A., He, H., Pejchal, R., Kang, Y.K., Depetris, R., Marozsan, A.J., Sanders, R.W., Klasse, P.J., Milne, J.L.S., Wilson, I. a, Olson, W.C., Moore, J.P., Subramaniam, S., 2011. Trimeric HIV-1 glycoprotein gp140 immunogens and native HIV-1 envelope glycoproteins display the same closed and open quaternary molecular architectures. Proc. Natl. Acad. Sci. U. S. A. 108, 11440–11445.

Hatjiharissi, E., Xu, L., Santos, D.D., Hunter, Z.R., Ciccarelli, B.T., Verselis, S., Modica, M., Cao, Y., Manning, R.J., Leleu, X., Dimmock, E.A., Kortsaris, A., Mitsiades, C., Anderson, K.C., Fox, E.A., Treon, S.P., 2007. Increased natural killer cell expression of CD16 , augmented binding and ADCC activity to rituximab among individuals expressing the Fc RIIIa-158 V / V and V / F polymorphism. Blood 110, 2561–2564.

Haynes, B.F., Gilbert, P.B., McElrath, M.J., Zolla-Pazner, S., Tomaras, G.D., Alam, S.M., Evans, D.T., Montefiori, D.C., Decamp, A., Huang, Y., Rao, M., Billings, E., Karasavvas, N., Bailer, R.T., Soderberg, K.A., Andrews, C., Berman, P.W., Frahm, N., Rosa, S.C. De, Alpert, M.D., Yates, N.L., Shen, X., Koup, R.A., 2012. Immune-Correlates Analysis of an HIV-1 Vaccine Efficacy Trial Barton. N. Engl. J. Med. 14,1275–1286.

Haynes, B.F., Moody, M.A., Liao, H.-X., Verkoczy, L., Tomaras, G.D., 2011. B cell responses to HIV-1 infection and vaccination: pathways to preventing infection. Trends Mol. Med. 17, 108–116.

He, B., Qiao, X., Klasse, P.J., Chiu, A., Chadburn, A., Knowles, D.M., Moore, J.P., Cerutti, A., 2006. HIV-1 Envelope Triggers Polyclonal Ig Class Switch Recombination through a CD40-Independent Mechanism Involving BAFF and C-Type Lectin Receptors. J. Immunol. 176, 3931–3941.

Hezareh, M., Hessell, A. J., Jensen, R. C., van de Winkel, J. G., & Parren, P. W. (2001). Effector function activities of a panel of mutants of a broadly neutralizing antibody against human immunodeficiency virus type 1. Journal of Virology, *75*(24), 12161–12168.

He, X., Li, D., Luo, Z., Liang, H., Peng, H., Zhao, Y., Wang, N., Liu, D., Qin, C., Wei, Q., Yan, H., Shao, Y., 2013. Compromised NK cell-mediated antibody-dependent cellular cytotoxicity in chronic SIV/SHIV infection. PLoS One 8, e56309.

Hong, H.S., Rajakumar, P. a, Billingsley, J.M., Reeves, R.K., Johnson, R.P., 2013. No monkey business: why studying NK cells in non-human primates pays off. Front. Immunol. 4, 32.

Hoves, S., Trapani, J. a, Voskoboinik, I., 2010. The battlefield of perforin/granzyme cell death pathways. J. Leukoc. Biol. 87, 237–243.

Hubert, P., Amigorena, S., 2012. Antibody-dependent cell cytotoxicity in monoclonal antibody-mediated tumor immunotherapy. Oncoimmunology. 1, 103–105.

Hudspeth, K., Silva-Santos, B., Mavilio, D., 2013. Natural cytotoxicity receptors: broader expression patterns and functions in innate and adaptive immune cells. Front. Immunol. 4, 69.

Huth, T.K., Brenu, E.W., Nguyen, T., Hardcastle, S.L., Johnston, S., Ramos, S., Staines, D.R., Sonya, M., 2014. Characterization of natural killer cell phenotypes in chronic fatigue syndrome/myalgic encephalomyelitis. Clin. Cell. Immunol. 5, 223.

Hwang, I., Zhang, T., Scott, J.M., Kim, A.A.R., Lee, T., Kakarla, T., Sunwoo, J.B., Kim, S., 2012. Identification of human NK cells that are deficient for signaling adaptor FcRγ and specialized for antibody-dependent immune functions. Int. Immunol. 24, 793–802.

Iannello, A., Debbeche, O., Samarani, S., Ahmad, A., 2008. Antiviral NK cell responses in HIV infection: II. viral strategies for evasion and lessons for immunotherapy and vaccination. J. Leukoc. Biol. 84, 27–49.

Isitman, G., Chung, A.W., Navis, M., Kent, S.J., Stratov, I., 2011. Pol as a target for antibody dependent cellular cytotoxicity responses in HIV-1 infection. Virology 412, 110–116.

Isitman, G., Stratov, I., Kent, S.J., 2012. Antibody-Dependent Cellular Cytotoxicity and NK Cell-Driven Immune Escape in HIV Infection: Implications for HIV Vaccine Development. Adv. Virol. 2012, 637208.

Jia, M., Li, D., He, X., Zhao, Y., Peng, H., Ma, P., Hong, K., Liang, H., Shao, Y., 2013. Impaired natural killer cell-induced antibody-dependent cell-mediated cytotoxicity is associated with human immunodeficiency virus-1 disease progression. Clin. Exp. Immunol. 171, 107–116.

Jiang, Y., Zhou, F., Tian, Y., Zhang, Z., Kuang, R., Liu, J., Han, X., Hu, Q., Xu, J., Shang, H., 2013. Higher NK Cell IFN-γ Production is Associated with Delayed HIV Disease Progression in LTNPs. J. Clin. Immunol. 10, 1007.

Johansson, S.E., Rollman, E., Chung, A.W., Center, R.J., Hejdeman, B., Stratov, I., Hinkula, J., Wahren, B., Kärre, K., Kent, S.J., Berg, L., 2011. NK cell function and antibodies mediating ADCC in HIV-1-infected viremic and controller patients. Viral Immunol. 24, 359–368.

Jost, S., Altfeld, M., 2012. Evasion from NK cell-mediated immune responses by HIV-1. Microbes Infect. 14, 904–915.

Jost, S., Altfeld, M., 2013. Control of human viral infections by natural killer cells. Annu. Rev. Immunol. 31, 163–194.

Karasavvas, N., Billings, E., Rao, M., Williams, C., Zolla-Pazner, S., Bailer, R.T., Koup, R. a, Madnote, S., Arworn, D., Shen, X., Tomaras, G.D., Currier, J.R., Jiang, M., Magaret, C., Andrews, C., Gottardo, R., Gilbert, P., Cardozo, T.J., Rerks-Ngarm, S., Nitayaphan, S., Pitisuttithum, P., Kaewkungwal, J., Paris, R., Greene, K., Gao, H., Gurunathan, S., Tartaglia, J., Sinangil, F., Korber, B.T., Montefiori, D.C., Mascola, J.R., Robb, M.L., Haynes, B.F., Ngauy, V., Michael, N.L., Kim, J.H., de Souza, M.S., 2012. The Thai Phase III HIV Type 1 Vaccine trial (RV144) regimen induces antibodies that target conserved regions within the V2 loop of gp120. AIDS Res. Hum. Retroviruses 28, 1444–1457.

Karim, Q.A., Sibeko, S., Baxter, C., Abdool Karim, Q., 2010. Preventing HIV infection in women: a global health imperative. Clin. Infect. Dis. 50 Suppl 3, S122–129.

Karnasuta, C., Paris, R.M., Cox, J.H., Nitayaphan, S., Pitisuttithum, P., Thongcharoen, P., Brown, A.E., Gurunathan, S., Tartaglia, J., Heyward, W.L., McNeil, J.G., Birx, D.L., de Souza, M.S., 2005. Antibody-dependent cell-mediated cytotoxic responses in participants enrolled in a phase I/II ALVAC-HIV/AIDSVAX B/E prime-boost HIV-1 vaccine trial in Thailand. Vaccine 23, 2522–2529.

Kasturi, S.P., Skountzou, I., Albrecht, R.A., Koutsonanos, D., Hua, T., Nakaya, H., Ravindran, R., Stewart, S., Alam, M., Kwissa, M., Villinger, F., Murthy, N., Steel, J., Jacob, J., Hogan, R.J., García-sastre, A., Compans, R., 2011. responses with innate immunity 470, 543–547.

Kaufmann, T., Strasser, a, Jost, P.J., 2012. Fas death receptor signalling: roles of Bid and XIAP. Cell Death Differ. 19, 42–50.

Keele, B.F., Estes, J.D., 2011. Barriers to mucosal transmission of immunodeficiency viruses. Blood 118, 839–846.

Kinchington, P.R., Hendricks, R.L., 2008. Noncytotoxic Lytic Granule – Mediated Reactivation from Neuronal Latency. Science. 25314, 268–271.

Kirchhoff, F., 2010. Immune evasion and counteraction of restriction factors by HIV-1 and other primate lentiviruses. Cell Host Microbe 8, 55–67.

Koch, J., Steinle, A., Watzl, C., Mandelboim, O., 2013. Activating natural cytotoxicity receptors of natural killer cells in cancer and infection. Trends Immunol. 34, 182–191.

Koeffler, P., Golde, D.W., 1980. Human myeloid leukemia cells. Blood 56, 344–350.

Kogan, M., Rappaport, J., 2011. HIV-1 accessory protein Vpr: relevance in the pathogenesis of HIV and potential for therapeutic intervention. Retrovirology 8, 25.

König, R., Zhou, W., 2004. Signal Transduction in T Helper Cells : CD4 Coreceptors Exert Complex Regulatory Effects on T Cell Activation and Function. Curr. Issues Mol. Biol. 6, 1–16.

Krzewski, K., Gil-Krzewska, A., Nguyen, V., Peruzzi, G., Coligan, J.E., 2013. LAMP1/CD107a is required for efficient perforin delivery to lytic granules and NK-cell cytotoxicity. Blood. 121, 4672-4683.

Kute, T., Stehle Jr, J.R., Ornelles, D., Walker, N., Delbono, O., Vaughn, J.P., 2012. Understanding key assay parameters that affect measurements of trastuzumab-mediated ADCC against Her2 positive breast cancer cells. Oncoimmunology 1, 810–821.

Kwong, P.D., Mascola, J.R., Nabel, G.J., 2013. Broadly neutralizing antibodies and the search for an HIV-1 vaccine: the end of the beginning. Nat. Rev. Immunol. 13, 693–701.

Kwong, P.D., Wyatt, R., Robinson, J., Sweet, R.W., Sodroski, J., Hendrickson, W. a, 1998. Structure of an HIV gp120 envelope glycoprotein in complex with the CD4 receptor and a neutralizing human antibody. Nature 393, 648–59.

Lambotte, O., Pollara, J., Boufassa, F., Moog, C., Venet, A., Haynes, B.F., Delfraissy, J.-F., Saez-Cirion, A., Ferrari, G., 2013. High antibody-dependent cellular cytotoxicity responses are correlated with strong CD8 T cell viral suppressive activity but not with B57 status in HIV-1 elite controllers. PLoS One 8, e74855.

Lane, H.C., 2010. Pathogenesis of HIV infection: total CD4+ T-cell pool, immune activation, and inflammation. Top. HIV Med. 18, 2–6.

Lanier, L.L., 2003. Natural killer cell receptor signaling. Curr. Opin. Immunol. 15, 308–314.

Lanier, L.L., Phillips, J.H., Hackett, J., Tutt, M., Kumar, V., 1986. Natural killer cells: definition of a cell type rather than a function. J. Immunol. 137, 2735–2739.

Larson, B., Dhawan, S., Wadwani, S., Pierre, N., Martinez, S., Degorce, F., Banks, P., 2011. Novel , Antibody-Dependent Cell-Mediated Cytotoxicity (ADCC) Assays 48041312.

Leng, Q., Borkow, G., Weisman, Z., 2001. Immune activation correlates better than HIV plasma viral load with CD4 T-cell decline during HIV infection. J. Acquir. Immune Defic. Syndr. 27, 389-397.

Li, Y., O'Dell, S., Wilson, R., Wu, X., Schmidt, S.D., Hogerkorp, C.-M., Louder, M.K., Longo, N.S., Poulsen, C., Guenaga, J., Chakrabarti, B.K., Doria-Rose, N., Roederer, M., Connors, M., Mascola, J.R., Wyatt, R.T., 2012. HIV-1 neutralizing antibodies display

dual recognition of the primary and coreceptor binding sites and preferential binding to fully cleaved envelope glycoproteins. J. Virol. 86, 11231–11241.

Liao, H.-X., Chen, X., Munshaw, S., Zhang, R., Marshall, D.J., Vandergrift, N., Whitesides, J.F., Lu, X., Yu, J.-S., Hwang, K.-K., Gao, F., Markowitz, M., Heath, S.L., Bar, K.J., Goepfert, P. a, Montefiori, D.C., Shaw, G.C., Alam, S.M., Margolis, D.M., Denny, T.N., Boyd, S.D., Marshal, E., Egholm, M., Simen, B.B., Hanczaruk, B., Fire, A.Z., Voss, G., Kelsoe, G., Tomaras, G.D., Moody, M.A., Kepler, T.B., Haynes, B.F., 2011. Initial antibodies binding to HIV-1 gp41 in acutely infected subjects are polyreactive and highly mutated. J. Exp. Med. 208, 2237–2249.

Lichtfuss, G.F., Meehan, A.C., Cheng, W.-J., Cameron, P.U., Lewin, S.R., Crowe, S.M., Jaworowski, A., 2011. HIV inhibits early signal transduction events triggered by CD16 cross-linking on NK cells, which are important for antibody-dependent cellular cytotoxicity. J. Leukoc. Biol. 89, 149–158.

Liu, X., Li, P., Widlak, P., Zou, H., Luo, X., Garrard, W.T., Wang, X., 1998. The 40-kDa subunit of DNA fragmentation factor induces DNA fragmentation and chromatin condensation during apoptosis. Proc. Natl. Acad. Sci. U. S. A. 95, 8461–8466.

Ljunggren, K., Broliden, P., Morfeldt-Manson, L., Jondal, M., Wahren, B., 1988. IgG subclass response to HIV in relation to antibody-dependent cellular cytotoxicity at different clinical stages. Clin. Exp. Immunol. 73, 343–347.

Llano, A., Est, J.A., 2005. Chemokines and other cytokines in human immunodeficiency virus type 1 (HIV-1) infection. Immunologia 24, 246–260.

Lopez-verge, S., Milush, J.M., Pandey, S., York, V.A., Arakawa-hoyt, J., Pircher, H., Norris, P.J., Nixon, D.F., Lanier, L.L., 2010. CD57 defines a functionally distinct population of mature NK cells in the human CD56 dim CD16 ¿ NK-cell subset. Immunobiology 116, 3865–3874.

Long, O.E., 2002. Tumor cell recognition by natural killer cells. Cancer Biology. 12, 57-61.

Lyerly, H.K.I.M., Reed, D.L., Matthews, T.J., Langlois, A.J., Ahearne, P.A., Petteway, S.R., Weinhold, K.J., 1987. Anti-GP 120 Antibodies from HIV Seropositive Individuals Mediate Broadly Reactive. AIDS Res. Hum. Retroviruses 3, 409–422.

Madhavi, V., Navis, M., Chung, A.W., Isitman, G., Wren, L.H., Rose, R. De, Kent, S.J., Stratov, I., 2013. Role for granulocytes in expressing HIV-1 peptide epitopes Activation of NK cells by HIV-specific ADCC antibodies. Hum. vaccines Immunother. 1–9.

Malim, M.H., Emerman, M., 2008. HIV-1 accessory proteins--ensuring viral survival in a hostile environment. Cell Host Microbe 3, 388–398.

Mandelboim, O., Malik, P., Davis, D.M., Jo, C.H., Boyson, J.E., Strominger, J.L., 1999. Human CD16 as a lysis receptor mediating direct natural killer cell cytotoxicity. Proc. Natl. Acad. Sci. U. S. A. 96, 5640–5644.

Marin, M., Rose, K.M., Kozak, S.L., Kabat, D., 2003. HIV-1 Vif protein binds the editing enzyme APOBEC3G and induces its degradation. Nat. Med. 9, 1398–1403.

Mascola, J.R., Haynes, B.F., 2013. HIV-1 neutralizing antibodies: understanding nature's pathways. Immunol. Rev. 254, 225–244.

Mata, M.M., Mahmood, F., Sowell, R.T., Baum, L.L., 2014. Effects of cryopreservation on effector cells for antibody dependent cell-mediated cytotoxicity (ADCC) and natural killer (NK) cell activity in (51)Cr-release and CD107a assays. J. Immunol. Methods 406, 1–9.

Mavilio, D., Benjamin, J., Daucher, M., Lombardo, G., Kottilil, S., Planta, M. a, Marcenaro, E., Bottino, C., Moretta, L., Moretta, A., Fauci, A.S., 2003. Natural killer cells in HIV-1 infection: dichotomous effects of viremia on inhibitory and activating receptors and their functional correlates. Proc. Natl. Acad. Sci. U. S. A. 100, 15011–15016.

Mavilio, D., Lombardo, G., Benjamin, J., Kim, D., Follman, D., Marcenaro, E., Shea, M.A.O., Kinter, A., Kovacs, C., Moretta, A., Fauci, A.S., 2005. cells : A highly dysfunctional NK subset expanded in HIV-infected viremic individuals. Proc. Natl. Acad. Sci. U. S. A. 102, 2886-2891.

McMichael, A.J., Borrow, P., Tomaras, G.D., Goonetilleke, N., Haynes, B.F., 2010. The immune response during acute HIV-1 infection: clues for vaccine development. Nat. Rev. Immunol. 10, 11–23.

Melar, M., Ott, D.E., Hope, T.J., 2007. Physiological levels of virion-associated human immunodeficiency virus type 1 envelope induce coreceptor-dependent calcium flux. J. Virol. 81, 1773–1785.

Mikell, I., Sather, D.N., Kalams, S. a, Altfeld, M., Alter, G., Stamatatos, L., 2011. Characteristics of the earliest cross-neutralizing antibody response to HIV-1. PLoS Pathog. 7, e1001251.

Mlisana, K., Werner, L., Garrett, N.J., McKinnon, L.R., Van Loggerenberg, F., Passmore, J.S., Gray, C.M., Morris, L., Williamson, C., 2014. Rapid disease progression in HIV-1 subtype C infected South African women Accepted. Clin. Infect. Adv. access 1–26.

Mogensen, T.H., Melchjorsen, J., Larsen, C.S., Paludan, S.R., 2010. Innate immune recognition and activation during HIV infection. Retrovirology 1–19.

Montefiori, D.C., Morris, L., Ferrari, G., Mascola, J.R., Manuscript, A., 2011. Neutralizing and other antiviral antibodies in HIV-1 infection and vaccination. Curr. Opin. HIV AIDS 2, 169–176.

Moog, C., Fleury, H.J., Pellegrin, I., Kirn, a, Aubertin, a M., 1997. Autologous and heterologous neutralizing antibody responses following initial seroconversion in human immunodeficiency virus type 1-infected individuals. J. Virol. 71, 3734–3741.

Moore, P.L., Gray, E.S., Choge, I. a, Ranchobe, N., Mlisana, K., Abdool Karim, S.S., Williamson, C., Morris, L., 2008. The c3-v4 region is a major target of autologous neutralizing antibodies in human immunodeficiency virus type 1 subtype C infection. J. Virol. 82, 1860–1869.

Moore, P.L., Gray, E.S., Wibmer, C.K., Bhiman, J.N., Nonyane, M., Sheward, D.J., Hermanus, T., Bajimaya, S., Tumba, N.L., Abrahams, M.-R., Lambson, B.E., Ranchobe, N., Ping, L., Ngandu, N., Abdool Karim, Q., Abdool Karim, S.S., Swanstrom, R.I., Seaman, M.S., Williamson, C., Morris, L., 2012. Evolution of an HIV glycan-dependent broadly neutralizing antibody epitope through immune escape. Nat. Med. 18, 1688–1692.

Morice, W.G., 2007. The immunophenotypic attributes of NK cells and NK-cell lineage lymphoproliferative disorders. Am. J. Clin. Pathol. 127, 881–886.

Muster, T., Steindl, F., Purtscher, M., Trkola, A., Klima, A., Himmler, G., Ruker, F., Katinger, H., 1993. A Conserved Neutralizing Epitope on gp4l of Human Immunodeficiency Virus Type 1. J. Virol. 67, 6642–6647.

Muthukumar Balasubramaniam and Eric O. Freed, 2012. New Insights into HIV Assembly and Trafficking. Physiology 26, 236–251.

Naranbhai, V., Altfeld, M., Karim, S.S.A., Ndung'u, T., Karim, Q.A., Carr, W.H., 2013. Changes in Natural Killer cell activation and function during primary HIV-1 Infection. PLoS One 8, e53251.

Naumann, S., Reutzel, D., Speicher, M., Decker, H.J., 2001. Complete karyotype characterization of the K562 cell line by combined application of G-banding, multiplex-fluorescence in situ hybridization, fluorescence in situ hybridization, and comparative genomic hybridization. Leuk. Res. 25, 313–322.

Niwa, R., Natsume, A., Uehara, A., Wakitani, M., Iida, S., Uchida, K., Satoh, M., Shitara, K., 2005. IgG subclass-independent improvement of antibody-dependent cellular cytotoxicity by fucose removal from Asn297-linked oligosaccharides. J. Immunol. Methods 306, 151–160.

Okulicz, J.F., Marconi, V.C., Landrum, M.L., Wegner, S., Weintrob, A., Ganesan, A., Hale, B., Crum-Cianflone, N., Delmar, J., Barthel, V., Quinnan, G., Agan, B.K., Dolan, M.J., 2009. Clinical outcomes of elite controllers, viremic controllers, and long-term nonprogressors in the US Department of Defense HIV natural history study. J. Infect. Dis. 200, 1714–1723.

Overbaugh, J., Morris, L., 2012. The Antibody Response against HIV-1. Cold Spring Harb. Perspect. Med. 2, a007039.

Packard, B.Z., Komoriya, A., 2008. Intracellular protease activation in apoptosis and cell-mediated cytotoxicity characterized by cell-permeable fluorogenic protease substrates. Cell Res. 18, 238–247.

Packard, B.Z., Telford, W.G., Komoriya, a., Henkart, P. a., 2007. Granzyme B Activity in Target Cells Detects Attack by Cytotoxic Lymphocytes. J. Immunol. 179, 3812–3820.

Pan, Q., Hammarström, L., 2000. Molecular basis of IgG subclass deficiency. Immunol. Rev. 178, 99–110.

Pantaleo, G., Graziosi, C., Demarest, J.F., Butini, L., Montroni, M., Fox, C.H., Orenstein, J.M., Kotler, D.P., Fauci, A.S., 1993. HIV infection is active and progressive in lymphoid tissue during the clinically latent stage of disease. Nature. 362, 355-358.

Parsons, M.S., Boulet, S., Song, R., Bruneau, J., Shoukry, N.H., Routy, J., Tsoukas, C.M., Bernard, N.F., 2010. Mind the Gap: Lack of Association between KIR3DL1*004/HLA-Bw4–Induced Natural Killer Cell Function and Protection from HIV Infection. J. Infect. Dis. 202, S356–S360.

Parsons, M.S., Wren, L., Isitman, G., Navis, M., Stratov, I., Bernard, N.F., Kent, S.J., 2012. HIV infection abrogates the functional advantage of natural killer cells educated through KIR3DL1/HLA-Bw4 interactions to mediate anti-HIV antibody-dependent cellular cytotoxicity. J. Virol. 86, 4488–4495.

Pegu, P., Vaccari, M., Gordon, S., Keele, B.F., Doster, M., Guan, Y., Ferrari, G., Pal, R., Ferrari, M.G., Whitney, S., Hudacik, L., Billings, E., Rao, M., Montefiori, D., Tomaras, G., Alam, S.M., Fenizia, C., Lifson, J.D., Stablein, D., Tartaglia, J., Michael, N., Kim, J., Venzon, D., Franchini, G., 2013. Antibodies with high avidity to the gp120 envelope protein in protection from simian immunodeficiency virus SIV(mac251) acquisition in an immunization regimen that mimics the RV-144 Thai trial. J. Natl. Cancer Inst. 87, 1708–1719.

Penack, O., Gentilini, C., Fischer, L., Asemissen, a M., Scheibenbogen, C., Thiel, E., Uharek, L., 2005. CD56dimCD16neg cells are responsible for natural cytotoxicity against tumor targets. Leukemia 19, 835–840.

Pilgrim, A.K., Pantaleo, G., Cohen, O.J., Fink, L.M., Zhou, J.Y.T., Bolognesi, D.P., Fauci, A.S., Montefiori, D.C., 1996. Neutralizing Antibody Responses to Human Immunodeficiency Virus Type 1 in Primary Infection and Long-Term – Nonprogressive Infection. J. Infect. Dis. 924–932.

Poli, A., Michel, T., Thérésine, M., Andrès, E., Hentges, F., Zimmer, J., 2009. CD56bright natural killer (NK) cells: an important NK cell subset. Immunology 126, 458–465.

Pollara, J., Bonsignori, M., Moody, M.A., Pazgier, M., Haynes, B.F., Ferrari, G., 2013a. Epitope Specificity of Human Immunodeficiency Virus-1 Antibody Dependent Cellular Cytotoxicity [ADCC] Responses Ab-Fab Ab-Fc HIV-1. Curr. HIV Res. 378–387.

Pollara, J., Hart, L., Brewer, F., Pickeral, J., Packard, B.Z., Hoxie, J. a, Komoriya, A., Ochsenbauer, C., Kappes, J.C., Roederer, M., Huang, Y., Weinhold, K.J., Tomaras, G.D., Haynes, B.F., Montefiori, D.C., Ferrari, G., 2011. High-throughput quantitative

analysis of HIV-1 and SIV-specific ADCC-mediating antibody responses. Cytometry. A 79, 603–612.

Pollard, V.W., Malim, M.H., 1998. THE HIV-1 REV PROTEIN Overview of the Retroviral Life Cycle. Annu. Rev. Microbiol. 491–532.

Rauf, A., Khatri, M., Murgia, M. V., Saif, Y.M., 2012. Fas/FasL and perforin–granzyme pathways mediated T cell cytotoxic responses in infectious bursal disease virus infected chickens. Results Immunol. 2, 112–119.

Ray, K., Gupta, S.M., Bala, M., Muralidhar, S., Kumar, J., 2006. CD4/CD8 lymphocyte counts in healthy, HIV-positive individuals & AIDS patients. Indian J. Med. Res. 124, 319–330.

Rerks-Ngarm, S., Pitisuttithum, P., Nitayaphan, S., Kaewkungwal, J., Chiu, J., Paris, R.M., Souza, M. De, Adams, E., Benenson, M., Gurunathan, S., Tartaglia, J., Mcneil, J.G., Francis, D.P., Stablein, D., Birx, D.L., 2009. Vaccination with ALVAC and AIDSVAX to Prevent HIV-1 Infection in Thailand. N. Engl. J. Med. 361, 2209–2220.

Richard, J., Veillette, M., Batraville, L.-A., Coutu, M., Chapleau, J.-P., Bonsignori, M., Bernard, N., Tremblay, C., Roger, M., Kaufmann, D.E., Finzi, A., 2014. Flow cytometry-based assay to study HIV-1 gp120 specific antibody-dependent cellular cytotoxicity responses. J. Virol. Methods 208, 107–114.

Romee, R., Foley, B., Lenvik, T., Wang, Y., Zhang, B., Ankarlo, D., Luo, X., Cooley, S., Verneris, M., Walcheck, B., Miller, J., 2013. NK cell CD16 surface expression and function is regulated by a disintegrin and metalloprotease-17 (ADAM17). Blood 121, 3599–3608.

Sanders, R.W., Venturi, M., Schiffner, L., Kalyanaraman, R., Katinger, H., Lloyd, K.O., Kwong, P.D., Moore, J.P., 2002. The mannose-dependent epitope for neutralizing antibody 2G12 on human immunodeficiency virus type 1 glycoprotein gp120. J. Virol. 76, 7293–7305.

Sansoni, P., Cossarizza, a, Brianti, V., Fagnoni, F., Snelli, G., Monti, D., Marcato, a, Passeri, G., Ortolani, C., Forti, E., 1993. Lymphocyte subsets and natural killer cell activity in healthy old people and centenarians. Blood 82, 2767–2773.

Sarnquist, C.C., Rahangdale, L., Maldonado, Y., 2013. Reproductive health and family planning needs among HIV-infected women in Sub-Saharan Africa. Curr. HIV Res. 11, 160–168.

Schubert, U., Antón, L.C., Bacík, I., Cox, J.H., Bour, S., Bennink, J.R., Orlowski, M., Strebel, K., Yewdell, J.W., Bac, I., 1998. CD4 Glycoprotein Degradation Induced by Human Immunodeficiency Virus Type 1 Vpu Protein Requires the Function of Proteasomes and the Ubiquitin-Conjugating Pathway CD4 Glycoprotein Degradation Induced by Human Immunodeficiency Virus Type 1 Vpu Protein Requ. J. Virol. 72, 2280-2288.

Screpanti, V., Wallin, R.P. a., Ljunggren, H.-G., Grandien, a., 2001. A Central Role for Death Receptor-Mediated Apoptosis in the Rejection of Tumors by NK Cells. J. Immunol. 167, 2068–2073.

Seidel, U.J.E., Schlegel, P., Lang, P., 2013. Natural killer cell mediated antibody-dependent cellular cytotoxicity in tumor immunotherapy with therapeutic antibodies. Front. Immunol. 4, 76.

Shannon, K., Leiter, K., Phaladze, N., Hlanze, Z., Tsai, A.C., Heisler, M., Iacopino, V., Weiser, S.D., 2012. Gender inequity norms are associated with increased male-perpetrated rape and sexual risks for HIV infection in Botswana and Swaziland. PLoS One 7, e28739.

Sharif-Askari, E., Alam, a, Rhéaume, E., Beresford, P.J., Scotto, C., Sharma, K., Lee, D., DeWolf, W.E., Nuttall, M.E., Lieberman, J., Sékaly, R.P., 2001. Direct cleavage of the human DNA fragmentation factor-45 by granzyme B induces caspase-activated DNase release and DNA fragmentation. EMBO J. 20, 3101–3113.

Sharp, P.M., Hahn, B.H., Swanstrom, R., Coffin, J., Walker, B., Mcmichael, A., Wilen, C.B., Tilton, J.C., Doms, R.W., Craigie, R., Bushman, F.D., Connell, R.J.O., Kim, J.H., Shaw, G.M., Hunter, E., 2011. Origins of HIV and the AIDS pandemic. Cold Spring Harb. Perspect. Med. 1, a006841.

Shinkawa, T., Nakamura, K., Yamane, N., Shoji-Hosaka, E., Kanda, Y., Sakurada, M., Uchida, K., Anazawa, H., Satoh, M., Yamasaki, M., Hanai, N., Shitara, K., 2003. The absence of fucose but not the presence of galactose or bisecting N-acetylglucosamine of human IgG1 complex-type oligosaccharides shows the critical role of enhancing antibody-dependent cellular cytotoxicity. J. Biol. Chem. 278, 3466–3473.

Sierra, S., Kupfer, B., Kaiser, R., 2005. Basics of the virology of HIV-1 and its replication. J. Clin. Virol. 34, 233–244.

Sips, M., Sciaranghella, G., Diefenbach, T., Dugast, a-S., Berger, C.T., Liu, Q., Kwon, D., Ghebremichael, M., Estes, J.D., Carrington, M., Martin, J.N., Deeks, S.G., Hunt, P.W., Alter, G., 2012. Altered distribution of mucosal NK cells during HIV infection. Mucosal Immunol. 5, 30–40.

Smalls-Mantey, A., Doria-Rose, N., Klein, R., Patamawenu, A., Migueles, S. a, Ko, S.-Y., Hallahan, C.W., Wong, H., Liu, B., You, L., Scheid, J., Kappes, J.C., Ochsenbauer, C., Nabel, G.J., Mascola, J.R., Connors, M., 2012. Antibody-dependent cellular cytotoxicity against primary HIV-infected CD4+ T cells is directly associated with the magnitude of surface IgG binding. J. Virol. 86, 8672–8680.

Smalls-Mantey, A., Connors, M., Sattentau, Q.J., 2013. Comparative efficiency of HIV-1 infected T cell killing by NK cells, monocytes and neutrophils. Plos One. 8, e74858.

Trapani, T.A., Smy, J., 2002. Functional significance of the perforin/granzyme cell death pathway. Nat. Rev. Immunol. 2, 735–747.

Smyth, M.J., Cretney, E., Kelly, J.M., Westwood, J. a, Street, S.E. a, Yagita, H., Takeda, K., van Dommelen, S.L.H., Degli-Esposti, M. a, Hayakawa, Y., 2005. Activation of NK cell cytotoxicity. Mol. Immunol. 42, 501–510.

Srisurapanon, S., Louisirirotchanakul, S., Sumransurp, K., Ratanasrithong, M., Chuenchitra, T., Jintakatkorn, S., Wasi, C., 2005. Binding antibody to neutralizing epitope gp41 in HIV-1 subtype CRF 01_AE infection related to stage of disease. Southeast Asian J. Trop. Med. Public Health 36, 221–227.

Sterjovski, J., Churchill, M.J., Roche, M., Ellett, A., Farrugia, W., Wesselingh, S.L., Cunningham, A.L., Ramsland, P. a, Gorry, P.R., 2011. CD4-binding site alterations in CCR5-using HIV-1 envelopes influencing gp120-CD4 interactions and fusogenicity. Virology. 410, 418–428.

Stiegler, G., Kunert, R., Purtscher, M., Wolbank, S., Voglauer, R., Steindl, F., Katinger, H., 2001. A potent cross-clade neutralizing human monoclonal antibody against a novel epitope on gp41 of human immunodeficiency virus type 1. AIDS Res. Hum. Retroviruses. 17, 1757–1765.

Stoermer, K. a, Morrison, T.E., 2011. Complement and viral pathogenesis. Virology. 411, 362–373.

Stratov, I., Chung, A., Kent, S.J., 2008. Robust NK cell-mediated human immunodeficiency virus (HIV)-specific antibody-dependent responses in HIV-infected subjects. J. Virol. 82, 5450–5459.

Su, B., Moog, C., 2014. Which Antibody Functions are Important for an HIV Vaccine? Front. Immunol. 5, 289.

Suhasini, M., Reddy, T.R., 2009. Cellular proteins and HIV-1 Rev function. Curr. HIV Res. 7, 91–100.

The South African Antiretroviral Treatment Guidelines, 2013. [Online:http://www.sahivsoc.org/upload/documents/2013%20ART%20Guidelines-˘-Short%20Combined%20FINAL%20draft%20guidelines%2014%20March%202013.pdf

Thobakgale, C.F., Fadda, L., Lane, K., Toth, I., Pereyra, F., Bazner, S., Ndung'u, T., Walker, B.D., Rosenberg, E.S., Alter, G., Carrington, M., Allen, T.M., Altfeld, M., 2012. Frequent and strong antibody-mediated natural killer cell activation in response to HIV-1 Env in individuals with chronic HIV-1 infection. J. Virol. 86, 6986–6993.

Thomas, D. a, Du, C., Xu, M., Wang, X., Ley, T.J., 2000. DFF45/ICAD can be directly processed by granzyme B during the induction of apoptosis. Immunity 12, 621–632.

Tiemessen, C.T., Shalekoff, S., Meddows-Taylor, S., Schramm, D.B., Papathanasopoulos, M. a, Gray, G.E., Sherman, G.G., Coovadia, A.H., Kuhn, L., 2009. Cutting Edge: Unusual NK cell responses to HIV-1 peptides are associated with protection against maternal-infant transmission of HIV-1. J. Immunol. 182, 5914–5918.

Timmons, B.W., Cieslak, T., 2008. Human natural killer cell subsets and acute exercise: a brief review. Exerc. Immunol. Rev. 14, 8–23.

Tomaras, G.D., Ferrari, G., Shen, X., Alam, S.M., Liao, H.-X., Pollara, J., Bonsignori, M., Moody, M.A., Fong, Y., Chen, X., Poling, B., Nicholson, C.O., Zhang, R., Lu, X., Parks, R., Kaewkungwal, J., Nitayaphan, S., Pitisuttithum, P., Rerks-Ngarm, S., Gilbert, P.B., Kim, J.H., Michael, N.L., Montefiori, D.C., Haynes, B.F., 2013. Vaccine-induced plasma IgA specific for the C1 region of the HIV-1 envelope blocks binding and effector function of IgG. Proc. Natl. Acad. Sci. U. S. A. 110, 9019–9024.

Tomaras, G.D., Yates, N.L., Liu, P., Qin, L., Fouda, G.G., Chavez, L.L., Decamp, A.C., Parks, R.J., Ashley, V.C., Lucas, J.T., Cohen, M., Eron, J., Hicks, C.B., Liao, H.-X., Self, S.G., Landucci, G., Forthal, D.N., Weinhold, K.J., Keele, B.F., Hahn, B.H., Greenberg, M.L., Morris, L., Karim, S.S.A., Blattner, W. a, Montefiori, D.C., Shaw, G.M., Perelson, A.S., Haynes, B.F., 2008. Initial B-cell responses to transmitted human immunodeficiency virus type 1: virion-binding immunoglobulin M (IgM) and IgG antibodies followed by plasma anti-gp41 antibodies with ineffective control of initial viremia. J. Virol. 82, 12449–12463.

Trapani, J. a, Sutton, V.R., 2003. Granzyme B: pro-apoptotic, antiviral and antitumor functions. Curr. Opin. Immunol. 15, 533–543.

Trkola, a, Matthews, J., Gordon, C., Ketas, T., Moore, J.P., 1999. A cell line-based neutralization assay for primary human immunodeficiency virus type 1 isolates that use either the CCR5 or the CXCR4 coreceptor. J. Virol. 73, 8966–8974.

Trkola, A., Purtscher, M., Muster, T., Ballaun, C., Buchacher, A., Sullivan, N., Srinivasan, K., Sodroski, J., Moore, J.P., Katinger, H., 1996. Human monoclonal antibody 2G12 defines a distinctive neutralization epitope on the gp120 glycoprotein of human immunodeficiency virus type 1. J. Virol. 70, 1100–1108.

Valiante, N.M., Lienert, K., Shilling, H.G., Smits, B.J., Parham, P., 1997. Killer cell receptors: keeping pace with MHC class I evolution. Immunol. Rev. 155, 155–164.

Van Domselaar, R., Bovenschen, N., 2011. Cell death-independent functions of granzymes: hit viruses where it hurts. Rev. Med. Virol. 21, 301–314.

Veillette, M., Désormeaux, A., Medjahed, H., Gharsallah, N.-E., Coutu, M., Baalwa, J., Guan, Y., Lewis, G., Ferrari, G., Hahn, B.H., Haynes, B.F., Robinson, J.E., Kaufmann, D.E., Bonsignori, M., Sodroski, J., Finzi, A., 2014. Interaction with cellular CD4 exposes HIV-1 envelope epitopes targeted by antibody-dependent cell-mediated cytotoxicity. J. Virol. 88, 2633–2644.

Vivier, E., Nunès, J. a, Vély, F., 2004. Natural killer cell signaling pathways. Science. 306, 1517–1519.

Vivier, E., Raulet, D.H., Moretta, A., Caligiuri, M. a, Zitvogel, L., Lanier, L.L., Yokoyama, W.M., Ugolini, S., 2011. Innate or adaptive immunity? The example of natural killer cells. Science (80-.). 331, 44–49.

Walzer, T., Dalod, M., Robbins, S.H., Zitvogel, L., Vivier, E., 2005. Review article Natural-killer cells and dendritic cells : " l ' union fait la force " Blood 106, 2252–2258.

Ward, J.P., Bonaparte, M.I., Barker, E., 2004. HLA-C and HLA-E reduce antibody-dependent natural killer cell-mediated cytotoxicity of HIV-infected primary T cell blasts. AIDS 18, 1769–1779.

Weber, J., 2001. The pathogenesis of HIV-1 infection. Br. Med. Bull. 58, 61–72.

Wei, X., Decker, J.M., Wang, S., Hui, H., Kappes, J.C., Wu, X., Salazar-Gonzalez, J.F., Salazar, M.G., Kilby, J.M., Saag, M.S., Komarova, N.L., Nowak, M. a, Hahn, B.H., Kwong, P.D., Shaw, G.M., 2003. Antibody neutralization and escape by HIV-1. Nature 422, 307–312.

WHO, 2008. Towards Universal access.

Wilen, C.B., Tilton, J.C., Doms, R.W., 2012. HIV: cell binding and entry. Cold Spring Harb. Perspect. Med. 2, 1-13.

Williams, L., 2007. Dysfunctional natural killer cells, in vivo, are governed by HIV viremia regardless of whether the infected individual is on antiretroviral therapy. AIDS. 21, 2355–2367.

Woof, J.M., Burton, D.R., 2004. Human antibody-Fc receptor interactions illuminated by crystal structures. Nat Rev Immunol 4, 89–99.

UNAIDS, 2011. Faster. Smarter. Better.

UNAIDS, 2013. Global Report.

Wren, L., Parsons, M.S., Isitman, G., Center, R.J., Kelleher, A.D., Stratov, I., Bernard, N.F., Kent, S.J., 2012. Influence of cytokines on HIV-specific antibody-dependent cellular cytotoxicity activation profile of natural killer cells. PLoS One 7, e38580.

Wren, L.H., Chung, A.W., Isitman, G., Kelleher, A.D., Parsons, M.S., Amin, J., Cooper, D. a, Stratov, I., Navis, M., Kent, S.J., 2013a. Specific antibody-dependent cellular cytotoxicity responses associated with slow progression of HIV infection. J. Immunol. 138, 116–23.

Wren, L.H., Stratov, I., Kent, S.J., Parsons, M.S., 2013b. Obstacles to ideal anti-HIV antibody-dependent cellular cytotoxicity responses. Vaccine 31, 5506–5517.

Wyatt, R., Moore, J., Accola, M., Desjardin, E., Robinson, J., Wyatt, R., Moore, J., Accola, M., Desjardin, E., Robinson, J., Sodroski, J., 1995. Involvement of the V1 / V2 variable loop structure in the exposure of human immunodeficiency virus type 1 gp120 epitopes induced by receptor binding . Involvement of the V1 / V2 Variable Loop Structure in the Exposure of Human Immunodeficiency Virus Type. Journal of Virology 69, 5723-5733.

Xiang, S., Pacheco, B., Bowder, D., Yuan, W., Sodroski, J., Shi-hua Xiang, Beatriz Pacheco, Dane Bowder, Wen Yuan, J., Sodroski, 2014. Characterization of a Dual-tropic Human Immunodeficiency Virus (HIV-1) Strain Derived from the Prototypical X4 Isolate HXBc2. Virology 438, 5–13.

Yates, N.L., Lucas, J.T., Nolen, T.L., Vandergrift, N.A., Soderberg, K.A., Seaton, K.E., Denny, T.N., Haynes, B.F., Cohen, M.S., Tomaras, G.D., 2011. Multiple HIV-1 specific IgG3 responses decline during acute HIV-1: implications for detection of incident HIV infection. AIDS 25, 2089-2097.

Zaritskaya, L., Shurin, M.R., Sayers, T.J., Malyguine, A.M., 2010. New flow cytometric assays for monitoring cell-mediated cytotoxicity. Science 9, 601–616.

Zhang, M.-Y., Yuan, T., Li, J., Rosa Borges, A., Watkins, J.D., Guenaga, J., Yang, Z., Wang, Y., Wilson, R., Li, Y., Polonis, V.R., Pincus, S.H., Ruprecht, R.M., Dimitrov, D.S., 2012. Identification and characterization of a broadly cross-reactive HIV-1 human monoclonal antibody that binds to both gp120 and gp41. PLoS One 7, e44241.

Appendix I

Table A1.1. Laboratory reagents prepared for this study

Reagent	**Composition**	**Supplier**
Fetal Bovine Serum (FBS; 100 ml)	-	Invitrogen
RPMI-1640 Medium.(1X)	200 mM L-glutamine, 25 mM HEPES, pH indicator	Invitrogen
Phosphate Buffer Saline (PBS; 1X)	0.138M NaCl, 0.0027M KCl (pH 7.2)	Invitrogen
Penicillin/ Streptomycin (100 ml)	100 units/ml penicillin,100µg streptomycin	Invitrogen
R1	1 % FBS in RPMI	
R10	10 % FBS in RPMI	
R20	20 % FBS in RPMI	

Appendix II

A2.1. CD107a flow cytometry

A.2.1.1. Titrating antibodies

Titration for all antibodies included in the CD107a degranulation panel were carried out to ensure the volumes used in each experiment allowed for optimal separation between the positive and negative populations, and also to exclude maximum background fluorescence possible. Titrating the antibodies by 6 fold dilutions allowed determination of each antibody saturation titre (volume of antibody that allows complete staining of the particular cellular marker in a sample). Pseudo-colour plots were generated to determine the degree of separation and amount of fluorescence with each antibody volume (Figure A2.1).

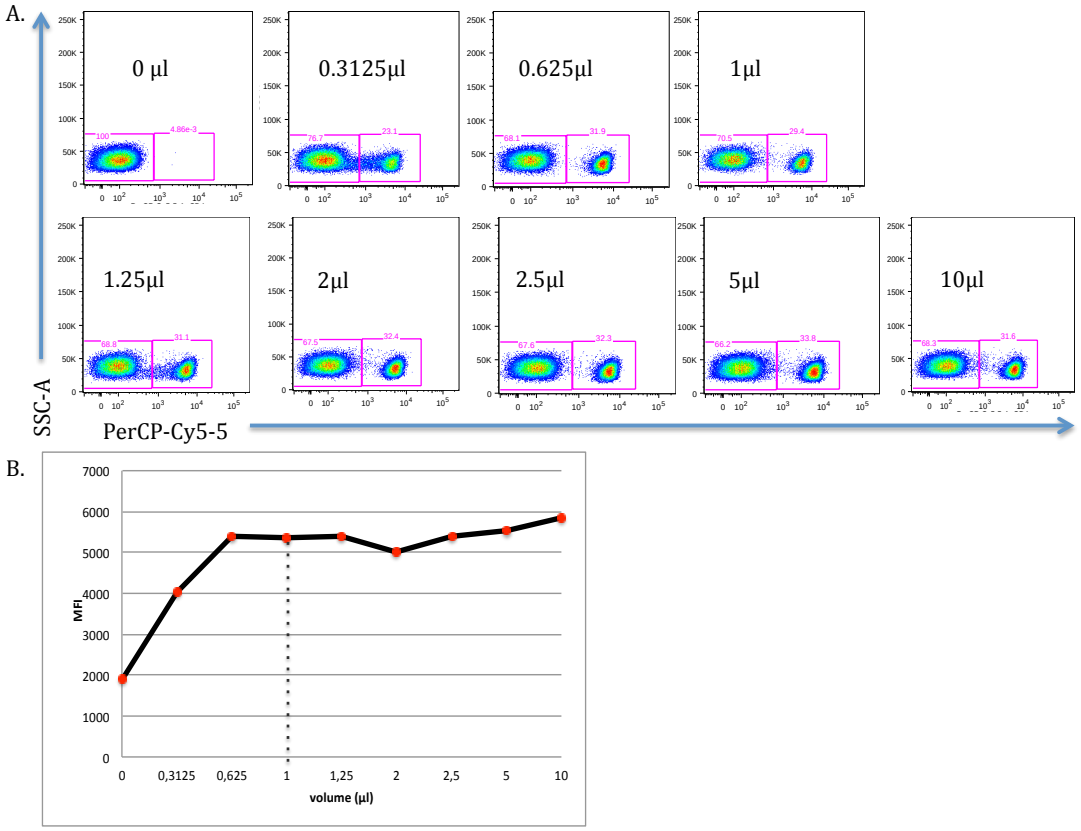

Figure A2.1. CD4-PerCP-Cy5-5 antibody titration. (A) Pseudo-colour plots with gates showing the position of the positive and negative populations and the separation between the two. (B) Graph of CD4 median fluorescence intensity at different antibody concentrations. One µl (dotted line) was chosen as the optimal volume for the CD4 antibody.

A.2.1.2. Fluorescence Minus One (FMO) controls

To set the gates accurately, FMO controls for all the antibodies were included in each experiment. FMO controls provide a means to measure the effect of spillover from populations in other dye dimensions in the channel of interest. To prepare the FMO tubes, 1x10^6 PBMCs were stained with all antibodies excluding one individual antibody (Figure A2.2).

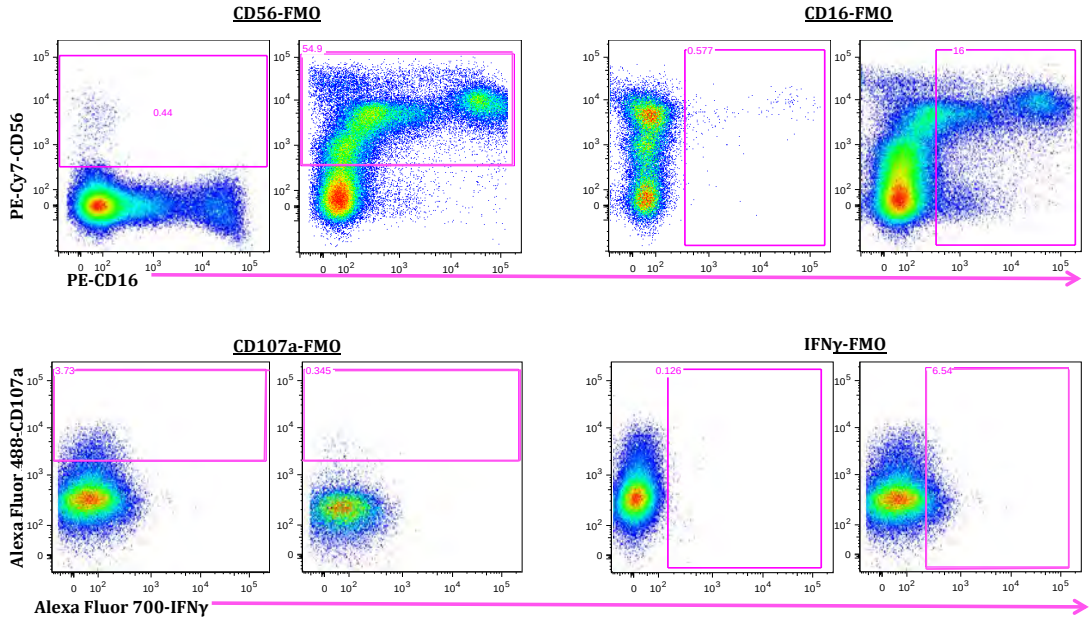

Figure A2.2. Example of FMO controls for the NK cell markers. All plots were first gated on singlets, live cells, lymphocytes and CD3- cells. Each antibody FMO plot on the left has a corresponding pseudo-colour plot on the right that have been gated on a fully stained PBMC sample.

Appendix III

A3.1. GranToxilux and PanToxilux assays

A3.1.1. Optimising the flow cytometry settings for APC, PacBlue and FITC channels

After optimising the concentration of TFL4 for staining CEM.NKR$_{CCR5}$ cells, an experiment combining CEM.NKR$_{CCR5}$ only and PBMCs only was carried out to position the populations at the right Pacblue and FITC channels. The PBMCs were positioned in the lower left quadrant on the Pacblue and FITC channels (10^1-10^3), and the CEM.NKR$_{CCR5}$ cells stained with TFL4 were positioned in the upper left quadrant on the Pacblue and FITC channels (10^1-10^3) (Figure A3.1).

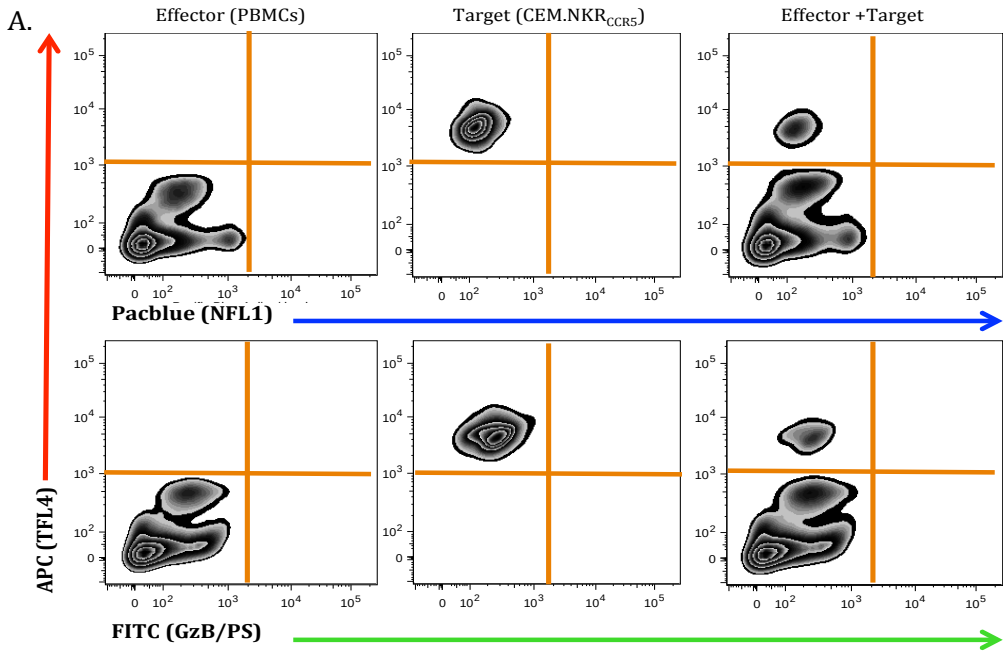

Figure A3.1. Positioning PBMCs and CEM.NKR$_{CCR5}$ in the right APC, Pacblue and FITC quadrants on the flow plots. (A) The first column shows PBMCs only, the second column shows, CEM.NKR$_{CCR5}$ cells only, and the third column shows a combination of effector and target cells. The first row shows PBMCs and CEM.NKR$_{CCR5}$ cells positioned on the APC and Pacblue channels. The second row shows positioned PBMCs and CEM.NKR$_{CCR5}$ cells using the APC and FITC channels.